Novel process of biochemical ammonia removal from air streams using a zeolite (clinoptilolite) filter system.

Sebastian Vitzthum von Eckstaedt

Dipl.-Ing. agr

This thesis is presented for the degree of Doctor of Philosophy, Murdoch University, Western Australia, January 2012

DECLARATION

I declare that this thesis is my own account of my research and contains as its main content work, which has not previously been submitted for a degree at any tertiary education institution.

Sebastian Vitzthum von Eckstaedt

“If I have seen a little further

it is by standing on the shoulders of giants”

- *Isaac Newton*

To my Turboschatz

who guides me to new limits

ABSTRACT

Ammonia (NH_3) in air is of major health and environmental concern, i.e. contribution to the greenhouse effect when NH_3 is converted to nitrous oxide (N_2O) in the atmosphere. Another important concern for ammonia in the atmosphere, is the possible conversion to secondary fine particulate matter in the presence of SO_x or NO_x. The main sources of NH_3 in air are waste and food processing industries as well as animal livestock production. The increase in environmental litigation, coupled with rising environmental awareness and a focus on quality of life, has resulted in an increase in the investigation and implementation of new technologies for the treatment of ammonia. In addition, existing methods are cost intensive, unreliable or complex and difficult to control.

In this research, a novel biochemical ammonia removing process has been developed and operated for 300 days. This process involves a sequence of biological, physical and chemical processes initiated by the dissolution of the introduced ammonia into the water of the filter system to make the ammonium available for biological degradation (nitrification). A spontaneous reaction of the intermediate nitrification product, nitrite, and ammonium to nitrogen takes place as soon as both compounds are present. This reaction is known to be catalysed by zeolite (clinoptilolite).

Water from the discharged moisture of the filter system was condensed on top of the reactor by employing a novel moisture control mechanism. The clean condensate percolated by gravity through the reactor bed and forced the

accumulated compounds to the bottom of the reactor. This led to a gradient distribution of compounds across the reactor depth with the highest concentrations at the bottom (140 mM ammonium, 1 M nitrite and 350 mM nitrate), favouring the chemical reaction of $NH_4^+ + NO_2^- \rightarrow N_2 + 2\ H_2O$. The low concentration (4 mM ammonium, 22 mM nitrite and 15 mM nitrate) at the top allowed simultaneous biological nitrification. The developed moisture control also ensured sufficient moisture content for biological activity in the reactor bed without leachate production.

Chemical reactions were supported and enhanced by the chosen filter medium clinoptilolite due to its unique characteristics such as (i) ion exchange capabilities, (ii) resistance to biodegradation and (iii) affinity to catalyse chemical reactions. A variety of online gas analyses (NH_3, N_2O and NO_x), as well as detailed reactor depth profiles (NH_4^+, NO_2^-, NO_3^-, pH and other cations (Na, K, Ca and Mg)) gained a thorough understanding of the system. Conducted DNA analysis indicated the presence of ammonia and nitrite oxidizing bacteria and was taken in combination with the accumulation of nitrite and nitrate, as proof that nitrification must have occurred.

The novel technology developed in this research enables the conversion of high concentrations of ammonium to N_2 in a single reactor under permanent aerobic conditions contrasting other treatment processes available today, e.g. Anaerobic Ammonium Oxidation (ANAMMOX).

ACKNOWLEDGMENTS

First I would like to express my gratitude to my principle supervisor, Prof. Goen Ho, for his advice, scientific input and guidance during my study. Thanks to Goen sufficient money could be acquired for developing, constructing and operating the experiments required for my thesis. Goen's access to a vast social and scientific network was very helpful to overcome some challenges during my Ph.D. time.

I wish to thank my associate supervisor Dr. Wipa Charles for support and helpful discussions. Wipa was always in the lab when she was needed and contributed many valuable thoughts and ideas. Thanks also to my associate supervisor Dr. Ralf Cord-Ruwisch for many (constructive) discussions and the provision of lab space.

A special thank you goes to Dr. Sebastian Bochmann, who never gave up explaining chemical basics to one of "the inventors of the green sulphur". I would like to thank my colleagues Suwat Suwannoppadol, Lee Walker, Liang Cheng and Vincent Clement for ongoing scientific and cultural exchange of knowledge. I also take the opportunity to say thank you to Suwat, Emily, Dmitry and Sebastian whom joined for social interactions at the Murdoch pub.

I gratefully acknowledge Environmental Biotechnology Cooperative Research Centre (EBCRC) for a full Ph.D. stipend, associated consumable costs and financial support to attend the EcoForum 2009 conference in Sydney (Australia).

Further, I acknowledge Murdoch University for the payment of my scholarship and further financial support throughout the project.

For fun at the composting facility and philosophising all night long at one of our conferences I would like to thank Steve Roberts (SMRC) whose door was always open to talk about work and fishing. I also thank the SMRC staff for their help.

Furthermore, I would like to thank Roland Hähnel and Graham Hoskins for their constructive comments and unwavering engagement on this Ph.D. thesis, which was a tremendous help. A special thank you goes also to Oliver Heyme for helping to solve tricky computer questions and Mathias Kolbe for the help in visualisation. I would also like to thank my entire friends who have helped in providing a life besides the Ph.D.

A very warm thanks goes to my family for their support from the other end of the world. They were always there, always supportive, always willing to help and laid the foundation for my achievements.

Last, but certainly not least a massive thanks to my beloved wife Christiane. She gave me the strength and power to finish. My Turboschatz has been there at all times and rewarded me with a smile or a kiss.

Sebastian Vitzthum von Eckstaedt

Perth, January 28, 2012

The work presented in this thesis was primarily designed, experimentally executed and interpreted by Sebastian Vitzthum von Eckstaedt. The individual manuscripts were also prepared by Sebastian Vitzthum von Eckstaedt. Contributions by co-authors are described below.

CHAPTER 2

Sebastian Vitzthum von Eckstaedt, Goen Ho and Wipa Charles contributed intellectually to the experimental design and concept. Literature review and gathering of ideas was achieved by Sebastian Vitzthum von Eckstaedt. Experiments were conducted and analyzed by Sebastian Vitzthum von Eckstaedt. Sebastian Vitzthum von Eckstaedt performed data processing and visualization. Sebastian Vitzthum von Eckstaedt, Ralf Cord-Ruwisch, Wipa Charles and Goen Ho interpreted the results and provided intellectual input through discussions. Sebastian Vitzthum von Eckstaedt wrote the paper and Goen Ho contributed to the writing of the paper.

CHAPTER 3

Sebastian Vitzthum von Eckstaedt invented the moisture controlled (reflux) filter system. Goen Ho and Wipa Charles provided intellectual input through discussions. Ralf Cord-Ruwisch made lab space available to conduct and develop the experiment. Sebastian Vitzthum von Eckstaedt worked on the set

up of the experimental rig, especially constructing the framework and assembling the hardware. The first author carried out electronic wiring and software development. Sebastian Vitzthum von Eckstaedt designed the sampling procedures and methods with the help of Goen Ho and Wipa Charles. Sebastian Vitzthum von Eckstaedt operated, maintained and adjusted the experiment, performed manual sampling, analyzed samples and did data processing and visualization. Sebastian Vitzthum von Eckstaedt wrote that paper. Goen Ho and Wipa Charles contributed to the writing of the article.

CHAPTER 4

Sebastian Vitzthum von Eckstaedt designed and conducted the experiments with assistance from Goen Ho and Wipa Charles. Sampling, sample analysis, data processing and visualization were carried out by Sebastian Vitzthum von Eckstaedt. Wipa Charles provided intellectual input at all times. Sebastian Vitzthum von Eckstaedt wrote this paper and Goen Ho contributed to the writing of this article. Ralf Cord-Ruwisch made lab space available to conduct and develop the experiments and contributed to the results and method section of that paper.

SECONDARY PUBLICATIONS

G. Ho, R. Cord-Ruwisch, W. Charles, and S. Vitzthum von Eckstaedt, "Odour control presentation to industry partner SMRC," Southern Metropolitan Regional Council (SMRC), Perth: 2008

S. Vitzthum von Eckstaedt, G. Ho, W. Charles, and R. Cord-Ruwisch, "Odour control biotechnology," presented at the EcoForum conference 2009, Sydney, 2009.

CONTENTS

LIST OF FIGURES

LIST OF TABLES

ABBREVIATIONS

Abbreviation	Meaning
amoA	ammonia monooxygenase
ANAMMOX	anaerobic ammonium oxidation
AOB	ammonium oxidizing bacteria
APHA	American Public Health Association
DI	deionised
DNA	deoxyribonucleic acid
dNTP	deoxyribonucleotide triphosphate
D/ T	dilution-to-threshold value
dt	delta time
e.g.	for example
EDS	energy dispersive spectroscopy
EMMA	enhanced multi materials analyzer
FID	Flame ionisation detector
FA	free ammonia
Fig	figure
FNA	free nitrous acid
GC	gas chromatograph
HPLC	high-performance liquid chromatography
i.d.	inner diameter
ID	Identification
k	Abel constant
MS	Mass spectrometry
nosZ	nitrate reductase
PCR	polymerase chain reaction
ps	saturation vapour pressure
(r^2)	coefficient of determination
SPME	solid phase microextraction

SND	simultaneous nitrification denitrification
T	temperature
TA Luft	German Technical Instructions for Clean Air
TBRT	true empty bed residence time
TCD	thermo conductivity detector
TPD	temperature programmed desorption
U	unit
UV	ultraviolet
VDC	volts direct current
wc	water content
X-ray	Roentgen radiation
zosZ	nitrous oxide reductase

UNITS

Units	Full Name
%	percent
°C	grad celcius
cm	centimeter
cm^3	cubic centimeter
g	gram
h	hour
kg	kilogram
L	liter
m	meter
M	molar
m^2	square meter
m^3	cubic meter
mg	milligram
mL	milliliter
mm	millimeter
mM	millimolar
mmol	millimol
ms	millisecond
nm	nanometer
Pa	pascal
pmol	picomol
ppm	parts per million
ppmv	parts per million volume
rpm	rotations per minute
sec	second
sL	standard liter
V	volt

µg	microgram
µL	microliter
µm	micrometer
µM	micromolar
µmol	micromol

TERMS AND DEFINITIONS

Absorbate Compound or substrate dissolved in the absorbent.

Absorbent Is the agent in which the absorbate dissolves in.

Absorption Absorption is the accumulation and sorption of gas or liquid in liquid. In this case gas molecules accumulated into the liquid and are evenly distributed within the liquid. Absorption is also the penetration of a substance into the body of another. One distinguishes between physical, chemical or biochemical absorption.

Adaptation Adaptation is the acclimatization or adjustment to a certain environment.

Adsorption Of adsorption one speaks when a gas or liquid accumulates or sorbs on a solid surface forming a molecular or atomic film. Therefore, adsorption is the taking up of one substance on the surface of another. This includes ion exchange as a specific form of adsorption. In this thesis, ammonia may be adsorbed but not exchanged, while ammonium is exchanged but not

	adsorbed.
Biofilm	A biofilm is a layer microorganisms attached to a surface.
Biofilter specific odour	Odour directly resulting from the biofilter media.
Bioscrubber	A biological waste gas treatment process in which the water-soluble compound (absorbate) dissolves in water (absorbent) and becomes available as a nutrient source for microorganisms attached within the bioscrubber.
Buffer effect	Capacity of a system to balance the impact of variable gas loads or concentrations.
Clean gas	Odour free and treated waste gas.
Degradation efficiency	Is the efficiency of biological or chemical degradation of compounds accomplished by microorganisms or chemical reactions.
Desorption	Desorption means the reverse/ opposite process of sorption.
Detectagas	Is a trademarked name owned by BOC Limited (http://www.trademarkify.com.au/trademark/963089?i=DETECTAGAS-

	BOC_Limited_ACN_Avenue_NORTH_RYDE_NSW_2113_AUSTRALIA). Detectagases are gases and gas mixtures for the calibration of instruments including field instrumentation for atmospheric and environmental monitoring
Dilution number	The volume ratio of clean gas to waste gas determined by the participants of an odour panel to bring the odour to its threshold value (olfactometry).
Enclosure	A structure fully enclosing a building, which offers complete waste gas collection and its treatment.
Filter material	Provides surface area and can be nutrient source for microorganisms. In addition it can act as a load buffer and adsorbent. Furthermore, it also helps to homogenize the waste gas and distribute water trickling through it.
Greenhouse gas	Any gas, which contributes to the greenhouse effect.
Inoculation	The introduction, attachment or fixation of microorganisms onto a filter material.
Ion exchange	The reversible exchange of ions between a solid material (such as filter material) and solution.
Mechanical-	Facility to treat the biodegradable fraction of municipal solid

biological treatment facility (MBTF)	waste and other waste streams by biological, mechanical, physical or a combination of those processes.
Moisture content	a) Water content in air depending on temperature and atmospheric pressure [mL m^{-3} or µL L^{-1}] b) Amount of water surrounding the filter material [g g^{-1} zeolite].
Odour threshold	The lowest concentration at which 50% or greater of panellists could detect an odour.
Odorant	Gaseous compound that triggers an odour sensation.
Olfactometer	Device to dilute waste gas with clean gas for the presentation to participants of an odour panel.
Olfactometry	Science of smell and odour.
Porosity	a) Pores, pockets, cavities and channels within a solid particle (zeolite) forming microscopic spaces. b) Channels and pathways formed between the individual filter material particles providing macroscopic inter particle spaces.
Raw gas	Untreated waste gas.

Regeneration	Process where a physical or chemical state is restored to its original state. One distinguishes between biological and chemical regeneration.
Sorption	The term sorption encompasses both adsorption and absorption processes and is the attachment of one or more chemical compounds on a solid surface (adsorption) or in a liquid (absorption).
Waste gas	Gas stream containing solid, liquid or gaseous emissions generated by treatment processes.

Introduction

1.1 Odour

From an evolutionary perspective the sense of smell is an information channel for receiving signals required for survival which are carried by gaseous volatile compounds via the breath [1]. This causes the need of precise selectivity and distinction to decode these environmental signals under any circumstance. Odour or smell properties result in the ability to distinguish between an odour active and odourless gas, to determine the extreme variation of odour responsiveness, the adaption by long-term exposure and the capability to differentiate between a pleasant and nuisance odour. Neutralization or creation of a new smell can occur, when one odour masks another odour. The introduction of different odours is often not additive, but rather, causes unexpected odour experiences.

In environmental science, odours are generally described as unacceptable, annoying or unpleasant. These unpleasant odours can arise from certain industrial processes, adversely affecting workers and even residents downwind of the industry. The most common sources of industrial odour arise from sewage treatment plants and other waste treatment facilities, e.g. composting facilities and landfills [2, 3]. Odorous compounds can also be released from refineries [4], animal rendering plants [5], and chemical industry processes [6], which can lead to resentment by the general public, and may lead to lawsuits. Nuisance lawsuits which describe general decline in community or neighbourhood quality of life, include legal terminology such as:

1. Personal distress, unpleasantness and annoyance,
2. Loss of enjoyment of personal property, and/ or
3. Diminished property value or rental value.

Intensive livestock farmers are increasingly confronted with prosecutions from nearby residents. In 2009 Vansickly et al. [7]reported three nuisance cases caused by livestock producers which went to trial in 2008 in Iowa. Other authors refer to conflicts with hog producers [8] but also cases are reported for other agricultural industries such as cattle production [9].

The rising number of nuisance lawsuits recorded in the USA also indicates an increase in populations experiencing non-specific symptoms such as headaches, nausea, reflex nausea, gastrointestinal distress, fatigue, eye irritation, throat irritation, shortness of breath, runny nose, sleep disturbance, inability to concentrate, classical stress response. However, the health effect

component to the individual is seldom reported. Non-specific symptoms have been experienced in populations next to industrial and agricultural sites, waste water treatment plants, and hazardous waste facilities [10]. However, it is still unclear whether these non-specific symptoms are directly or indirectly related to the odour exposure. For example, is a headache due to a physiological change caused by the presence of a chemical odorant, or is it because the citizen is “simply annoyed” [11]. Surveys rather document that individuals complain about a general discomfort which they relate to chemical odours, i.e. 10 % of the residents of a nearby waste treatment plant reported that odours had made them sick [12]. Health effects caused by pesticides used on a potato farm revealed that while health effects were not related to nearness of population to the fields, odour perception was strongly related to the number of symptoms reported, the length of occurrence of the symptoms, and the severity of the symptoms [13].

Another study assessed both the physical and mental health of residents near a large-scale swine livestock. The results indicated that the neighbours of the agricultural facility reported higher rates of symptoms including respiratory problems, nausea, headaches, and irritated eyes, nose and throat [14]. The medical community acknowledges that certain non-specific symptoms have causes that cannot be explained using conventional medical or toxicological theories. Multidisciplinary research that is studying animal and human physiological and neurological responses to odorants will lead to new understanding of the ‘gray line’ between odour nuisance and health effects [11].

All of the mentioned cases above make regulations and actions necessary.

1.1 Regulations

The regulations of air pollutants in general are very different across the globe ranging from non-existent, e.g. in undeveloped countries, to highly regulated, e.g. in Germany. Policies and guidelines like the TA Luft (German Technical Instructions for Clean Air) [15] prevent dangerous environmental impacts caused by air pollution and also help to protect the general public and the neighbourhood, achieving a high protection of the environment altogether. Australian councils have the power to handle public nuisance declared in Act 1993 [16]. In section 3 of the Act 1993 (Interpretation) a pollutant is defined as any solid, liquid or gas (or combination thereof) including waste, smoke, dust, fumes and odour [16]. In section 4 (Responsibility for pollution) it is defined, that the occupier or person in charge of the vehicle or place emitting the emission, discharge and or deposition is responsible for the pollution. Section 82 (Causing environmental nuisance) subsection 1 “A person who causes an environmental nuisance by polluting the environment intentionally or recklessly and with the knowledge that an environmental nuisance will or might result is guilty of an offence.” In subsection 2 “A person who by polluting the environment causes an environmental nuisance is guilty of an offence.” In section 10 (Objects of Act), subsection 1 b (i) of the Act 1993 it is written: “to ensure that all reasonable and practicable measures are taken to protect, restore and enhance the quality of the environment having regard to the principles of ecologically sustainable development, and

(i) to prevent, reduce, minimize and, where practicable, eliminate harm to the environment”.

Summarizing it can be said that the Act 1993 defines odour as a pollutant and the institution releasing the pollutants is responsible to minimize, reduce and prevent the impact and therefore the environmental nuisance.

1.2 Odour detection and evaluation

1.2.1 Olfactometry (Human odour evaluation)

The elusiveness of smell or odour characterisation by chemical and physical methods complicates their detection and evaluation [17]. Olfactometry is state of art in odour detection utilising the human nose as a sensor [17]. It is known as the science of smell with the aim to evaluate and detect odorous compounds. It is defined as “the controlled presentation of odour for the observation of the resulting human sensation” [18]. The reaction of a single person or panel participant on a certain odour impulse is thereby measured [19].

An example for a single person odour evaluation technique is provided by St. Croix Sensory, Inc. The Nasal Ranger is an infield olfactometer for measuring and quantifying odour strength in ambient air. The portable device (Fig. 1-1) enables the user to determine ambient odour dilution-to-threshold (D/ T) values. A calibrated series of discrete dilutions generates a mixture of odorous and carbon filtered ambient air. The D/ T ratio is a measure of the number of dilutions needed to make the odorous in ambient air just “non-detectable”.

Fig. 1-1: Nasal range olfactometer [20]

A more conventional method employs an odour panel where a number of participants determine the D/ T value. The number of panellists (Fig. 1-2) and the sample size (minimum number of panellists) is usually adjusted to meet the accuracy requirements imposed by the objective of the test. This is essential to determine the spread of the confidence interval, e.g. German guidelines recommend that not less than eight panellists need to be employed [21]. The selected panellists are chosen in relation to their ability (health, tendency to guess, decisiveness) to determining odour [18]. The odour detection sensitivity of the panellist (position of his/ her individual odour threshold) is not a selection criterion [21].

Fig. 1-2: Odour panel [22]

1.1.1 Compound specific odour detection (Machine olfactometry)

Several attempts have been undertaken in the last few decades to use electronic equipment to determine gas composition and evaluate odour nuisance based on these results. ‘Electronic noses’ for example belong to those devices. The year 1982 is known as the beginning of the development of technological-sensorial measurement equipment which are able to technically imitate the sense of smell [23]. In an electronic nose, chemosensory arrays were combined with electronic data processing and pattern recognition. Persaud and colleagues [23] report that this device can reproducibly discriminate between a variety of odour. Its properties show that discrimination in an olfactory system could be achieved without the use of highly specific receptors. Modern software development and material science improvements

are important aspects of the development of electronic noses which consist of five elements:

1. A sensor array which is exposed to the volatiles;
2. Conversion of the sensor signals to a readable format;
3. Software analysis of the data to produce characteristic outputs related to the odour encountered;
4. Clean-out mechanism to remove the carry-over from previous samples; and
5. Correction for electronic signal drift.

The sensor output signals are interpreted via a variety of methods such as pattern recognition algorithms, principal component analysis, discriminate function analysis, cluster analysis and artificial neural networks to discriminate between samples [24].

Another approach is to apply commonly used separation techniques such as gas chromatography (GC) to separate a gas sample into its chemical compounds or compound groups. Subsequent detectors (e.g. mass spectrometer (MS) [25] or flame ionisation detector (FID) [26]) identify the compounds and its amount in the gas mix. There are different sample injection methods available depending or influenced by the type of sample, sample size and sampling method. Evacuated stainless steel chambers and a container of synthetic gas tight material (Tedlar bags) are commonly used for whole air samples but are very limited in sampling volume. In contrast, adsorption and absorption techniques i.e. solid phase microextraction (SPME) and sampling with adsorbent tubes are used to concentrate the sample but can be highly

selective. The adsorbent is thereby exposed to an odour or gas for a period of time. Desorption of the accumulated compounds is initiated via specific properties of the analytical instrument (thermo or chemical).

All these mechanical measurements fail in terms of presenting an odour result rather than a list of chemical compounds. Simultaneous GC-MS Olfactometry is a method to separate the individual components of odorous mixtures and combining the perception of the human nose with MS (Fig. 1-3). The gas stream is thereby separated into a “human nose” stream and a MS stream. Simultaneous analysis by the MS allows the odorous molecules to be identified using sophisticated chemical library software. The author questioned the reliability of that method, since the human odour sensation also depends on the amount and exposure time and GC are only capable to separate gas and analyse certain (small) amounts of gas.

Modern and portable equipment such as portable GC and FTIR allow in field and laboratory online monitoring. Online monitoring (especially in laboratory setups) and automated data acquisition allows accurate mass balance calculations. The limitation of these techniques is the moisture sensibility of the equipment. Dry gas streams can be achieved by various physical or chemical methods such as activated carbon [27], silica gel [28, 29] or potassium hydroxide (KOH) pellets [30]. A disadvantage of this method is that compounds of interest also adsorb onto the used physical or chemical dryer method and thereby requiring additional analytical techniques [31-35].

Fig. 1-3: Simultaneous GC-MS and olfactometry [36]

1.2 Overview of odour treatment

The process of odour formation, emission, transport and dispersion, exposure to the individuals and resulting nuisance in the exposed environment is very complex [37]. A significant odour free environment can only be established by either not producing any odour or by treating the pollutions at the emission source. Prevention should be always the first choice. Reductions in odour emissions can also be made by considering seasonal conditions. For example, limited use of pesticides and nutrients based on weather conditions for the agricultural industry. The application of slurry is only recommended on windless days, away from settlements (observing prevailing wind direction), or on cool and less sunny weather conditions to minimize evaporation. The risk of odour

emissions from other industries such as compost facilities, wastewater treatment plants, food processing or chemical industries are permanent. These industry sectors cover or encase the odour source to reduce gaseous emissions. This has the advantage that the odour release can be controlled by sucking or pumping the gas into a treatment system [38]. The success of controlled odour removal is only given when most, if not all odour components can be converted into odourless compounds. A number of odour removal systems are known and widely used. An overview is given in Fig. 1-4.

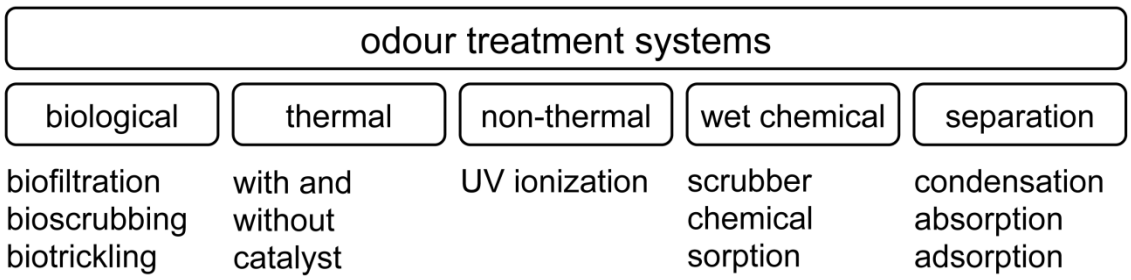

Fig. 1-4: Overview of odour treatment processes

All the mentioned treatment systems have disadvantages. Some are expensive (thermal treatments [39, 40]), producing high concentrated end products which need further treatment or must be disposed by wet chemical and separation treatments [41-43] or fail because of a combination of the above reasons [44, 45].

In common biofiltration for example, the pollutant (odour) is first absorbed into the water phase of the biofilter. That water is essential for microbial life but contains the risk of producing leachate when too much water is present. Moisture control is therefore a key issue in biofiltration similar to the choice of the filter material. Organic filter materials such as compost [46], pine bark [47],

pruning waste [48] and combinations [49] of those provide additional nutrient source but are also biodegradable causing blockages and channelling in the filter system. Organic filter materials are readily available and less costly than inorganic filter materials. Inorganic filter materials like ceramics [50, 51], plastics [51, 52] or foams [6] have the advantage of high stability and persistence but microorganisms attachment is often difficult since all nutrients need to be supplied.

In addition, in countries like Germany, biological treatment systems alone are not sufficient to reach the targeted threshold anymore [17]. For these reasons the attempt to develop a novel biochemical biofilter system for odour removal is necessary.

1.3 Ammonia – an odour model compound

As mentioned above, odour is a complex chemical composition with unique and unpredictable characteristics. To test a novel biofilter system it is therefore essential to choose model compounds to reduce the complexity and to clearly allocate cause and effect in the system. In this thesis ammonia was chosen as the model compound.

On the 5th of July 2011 an article presented on the German news website “www.tagesschau.de” [53] reported about “biting ammonia” in piggeries. This showed that (a) ammonia is still a present problem and (b) confirmed that we had chosen the correct model compound for our research four years ago. Ammonia (NH_3) is one of the most common odorous gases emitted by petrochemical industry, food processing, paper manufacturing, waste water

treatment plants (measured at concentrations as high as 1023 ppm_v [54]), composting facilities (reported up to 394 ppm_v [55]) and livestock farms (detected at a range of 10 – 60 ppm_v [56]). The colourless, corrosive and toxic gas has a strong, offensive and repellent odour with an olfactory threshold of detection of 0.16 µmol L^{-1} (4 ppm_v) [57] and 2.05 µmol L^{-1} (50 ppm_v) [58]. Reasons for the two different thresholds are unclear. However, different sensitive perception and training of the panellists as well as variations in gas volume and gas flow rate can result in dissimilar detection threshold. Exposure to 50 – 100 ppm_v NH_3 causes irritation to the mucous membranes, generating a burning sensation in the eyes, nose and throat [59]. At concentrations of 400 ppm_v the irritation is immediate, at 1500 ppm_v ammonia causes coughing and at 2500 ppm_v it is life-threatening [60]. Research has shown that animal health and animal productivity are also related to ammonia concentration in the livestock environment [61]. The increase in environmental litigation, coupled with a rising environmental awareness and a focus on quality of life has resulted in an increased number of proposed technologies and methods for ammonia treatment. Ammonia can also be converted to nitrous oxide (N_2O), which is a strong greenhouse gas [62] and is therefore a precursor of global warming. Another important concern for ammonia in the atmosphere, is the possible conversion to secondary fine particulate matter in the presence of SO_x or NO_x [63, 64].

In the German TA Luft [15] it is regulated that depending on the industry (fertilizer industry or facilities to dry waste) a maximum of 80 – 20 mg m^{-3} (4.7 – 1.2 µM) of ammonium are allowed to be emitted. Biofiltration is commonly used to remove ammonia from air streams. Nitrifying bacteria (*Nitrosomonas* and

Nitrobacter) are capable to convert NH_4^+ to nitrite and nitrate. The metabolites will accumulate under aerobic conditions, until the biofilter activity is inhibited due to high concentration. Flushing the metabolites out (by water irrigation), replacing the filter material or switching the filter to anaerobic conditions can prevent inhibition. The disadvantages of such actions are:

1. Production of leachate with high concentration of ammonium, nitrite and nitrate which needs treatment or disposal
2. Filter material replacement interrupts the filter operation, causes down time and additional costs
3. For a continuous ammonia treatment and filter regeneration (at least) two separate aerobic and anaerobic filter need to be available

Another but never implemented aerobic treatment method is the conversion of the accumulated NH_4^+ and NO_2^- by a spontaneous chemical reaction of NH_4NO_2 to N_2 and 2 H_2O (Equation 1-1). This reaction is known for more than 160 years [65] and takes place as soon as ammonium and nitrite are present in aqueous and non aqueous conditions [66].

$$NH_4^+ + NO_2^- \rightarrow N_2 + 2H_2O$$ **Equation 1-1**

Abel [67] describes the kinetics of the reaction as a third order reaction involving NH_4^+, HNO_2 and NO_2^- (Equation 1-2):

$$d(N_2)/dt = k[NH_4^+][NO_2^-][HNO_2]$$ **Equation 1-2**

Other authors [68] use a simpler 2nd order reaction (Equation 1-3):

$$d(N_2)/dt = k[NH_4^+][HNO_2]$$ **Equation 1-3**

Because Abel's model is more widely accepted [69] Equation 1-2 will be used in this work. The k constant was subject of discussion in a number of publications [68, 70] however in this study we use the k constant of $3.67*10^{-3}$ [unit less] at 25 °C [67] as it was originally postulated by Abel. It need to be noted, that the k constant was note checked in this research and was therefore accepted from the publication mentioned above. Interestingly this reaction is not only dependent on nitrite and ammonium concentration but also on the amount of free nitrous acid which means that the reaction will proceed faster at lower pH values with a maximum rate at around the pKa value (3.4) of the NO_2^- / HNO_2 equilibrium. By adding an acid as a catalyst the reaction in Equation 1-1 can be initiated at room temperature.

1.4 Zeolite

Zeolites belong to the group of solid acids [71, 72] and can be used as catalyst for the reaction in Equation 1-1 [69, 73]. Zeolite was first identified as a mineral group in 1756 by Baron A. F. Cronstedt, a Swedish mineralogist [74]. Zeolites are crystalline, porous 3 dimensional aluminosilicates of the alkali (Na and K) and alkaline earth (Ca) metals (Fig. 1-5).

Zeolites primary building structure of the silicate is a tetrahedron attached to four oxygen atoms around a silicon atom. Replacement of the silicon by aluminium results in an unbalanced charge. In this state the four oxygen atoms are still present (4 times 1^- charge), but the silicon (4^+ charge) is replaced by one single atom of aluminium (3^+ charge), resulting in a total negative charge of

one. The unbalanced charge will then be compensated by a cation. This cation is not strongly bound and is therefore readily exchanged (depending on selectivity and relative concentration) with cations in a surrounding solution (if

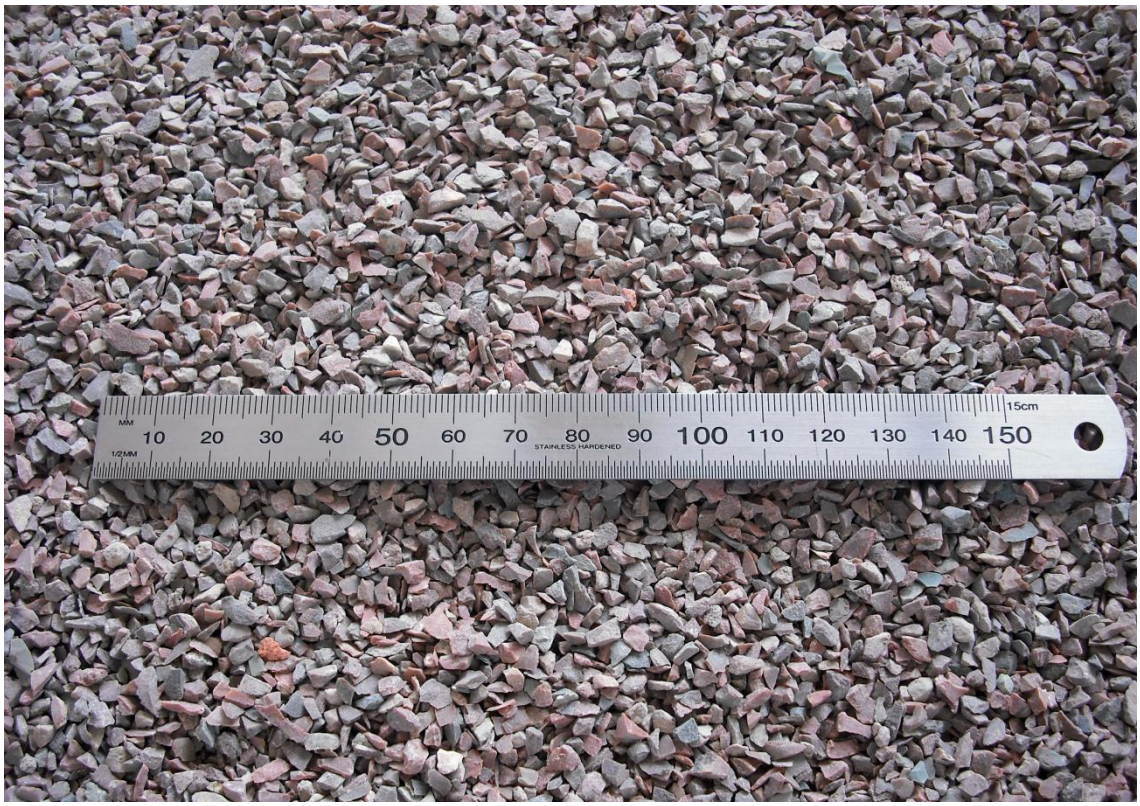

Fig. 1-5: Zeolite grain sieved to 2.4 – 4.0 mm

available). The exchangeable cations in zeolites are located in regularly arranged channels and cavities (Fig. 1-6), near molecular size, through which liquid can flow. Zeolites have therefore significantly higher cation exchange capacities than other aluminosilicates.

The ratio of aluminium and silicon atoms as well as the type and relative abundance of associated cations varies and results in a wide range of zeolites with different structures and characteristics. Almost all zeolites facilitate cation exchange. The degree of cation exchange and their positive discrimination

differs with type. Clinoptilolite, for example is a zeolite with known selective affinity for ammonium and potassium. That capability of selective cation exchanged is already applied in adsorption industries and waste treatment processes.

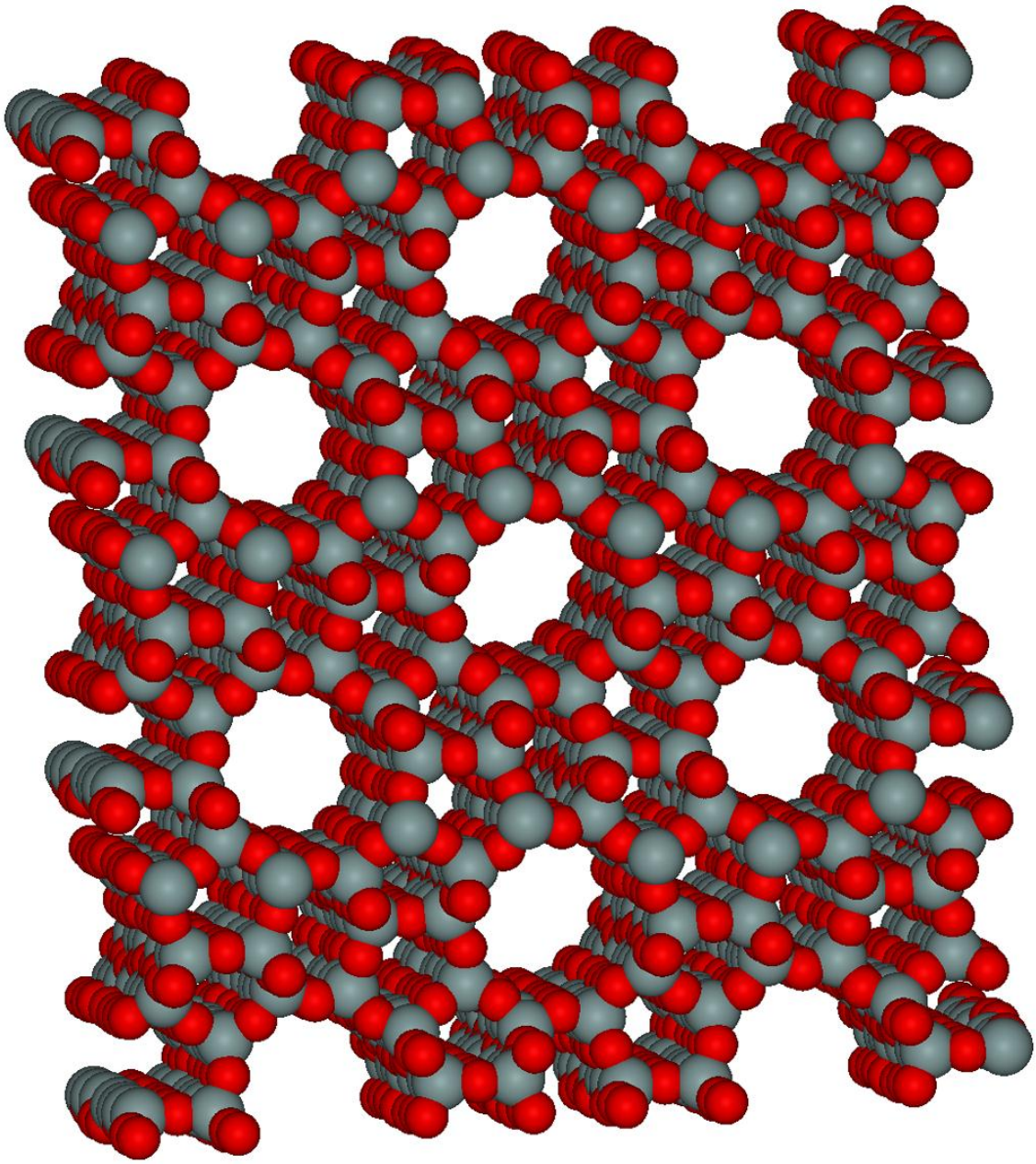

Fig. 1-6: Zeolite structure [75]

For example, clinoptilolite exposed to ammonium dissolved into solution triggers ion exchange until exhaustion of NH_4^+ from the solution or NH_4^+ saturation of the clinoptilolite. The adsorbing capacity is limited and regeneration steps are required in order to reuse or prolong adsorption capabilities. The most accepted and widely available methods for regeneration of NH_4^+ saturated clinoptilolite are (i) the chemical and (ii) the biological regeneration. The chemical regeneration is usually achieved by exposing the zeolite to a strong solution (KCl) causing cation exchange from this solution displacing the ammonium from the zeolite into solution [76]. This results in high ammonia/ ammonium concentration in the regenerate liquor. Biological regeneration involves microorganisms [76]. Ammonium oxidising bacteria (nitrifyers) are grown on the zeolite and under aerobic conditions; ammonium is oxidised to nitrite and nitrate. This results in high nitrate concentrations in the regenerated liquor. In wastewater treatment plants a subsequent anaerobic step is required for the denitrification of the regenerate liquor [76].

Regeneration of exchange capacity is generally carried out off-line because the nitrogen which has been removed is released back into solution, which normally cannot be tolerated in the effluent [76].

1.5 Objectives

This thesis presents a novel biofilter design with zeolite as an inert filter material acting as microorganism carrier and catalyst. The ammonium filter system works under aerobic conditions with a simultaneous regeneration of zeolite. The objectives of this study are:

I. The development and testing of a biofilter system for sustainable ammonia removal from air and conversion to nitrogen
II. The use of zeolite as an non-biodegradable filter material as biofilm carrier and catalyst
III. The natural development of biological and chemical microenvironments (layer) without pH or water adjustment
IV. The application of the reflux method to biofiltration in order to maintain moisture content within the biofilter and achieve layer formation and gradual distribution of ammonium, nitrite and nitrate to achieve areas with biological and chemical microenvironments
V. The development of a single filter system with spatial separation due to layer formation allowing simultaneous biological degradation of ammonium to nitrite and nitrate as well as the chemical reaction of ammonium nitrite catalysed by zeolite at room temperature
VI. Achieve a dry gas outlet of the biofilter to allow continuous online monitoring with moisture sensitive equipment
VII. The development of a biofilter system without leachate production and zero additional water supply to reduce water usage

This thesis describes the theoretical background and the development of the biofilter and shows and discusses the results of comprehensive test series. This thesis is composed of five chapters, whereof chapter one contains a general introduction, chapters two, three and four are written as publications, aiming for publication in peer-reviewed journals. The manuscripts have not been submitted yet because the content of this thesis is currently in the process of intellectual property (IP) approval. Chapter two describes the need and potential

as well as the theory of a novel biochemical ammonia filter system. Chapter three contains information about the design, automation and operation of the novel filter system. Chapter four presents detailed results and layer formation. The conclusions of the findings are presented in chapter five.

A novel way of biochemical ammonia removal:

Literature review and proof of concept

Sebastian Vitzthum von Eckstaedt, Goen Ho, Wipa Charles, Ralf Cord-Ruwisch

Abstract

A sufficiently reliable and sustainable method to remove ammonia from air streams has still not been found for biofiltration. The degradation of biofilter media, the accumulation of ammonium, nitrite and nitrate or the production of leachate causes biofilter failure and inefficiency. We present a novel concept on how future ammonia biofilter systems can be operated and designed. Zeolite (clinoptilolite) is recommended as a non-biodegradable filter material that also offers surfaces for nitrifying bacteria to flourish. In addition zeolite's capability to adsorb and thereby buffer ammonia loads as well as to catalyse the reaction of NH_4NO_2 to N_2 and 2 H_2O is of great benefit. In water, dissolved ammonium is first nitrified by nitrifying bacteria to nitrite. Ammonium and nitrite are then allowed to react, chemically catalysed by the zeolite. The feasibility of oxidising ammonia to nitrite by nitrifying bacteria is well established, but the subsequent chemical reaction of ammonia and nitrite has not been applied to a biofilter before. Experiments were carried out to demonstrate the feasibility of the reaction. We then present the feasibility of operating a single biochemical filter system to convert ammonia in an air stream biochemically to nitrogen gas.

Keywords: ammonia, biofilter, reaction with nitrite, zeolite

2.1 Introduction

Ammonia (NH_3) is one of the most common odorous gases that can be produced in today's societies; e.g. petrochemical industry, food processing, paper manufacturing, wastewater treatment plants (1023 ppm_v [54]), composting facilities (394 ppm_v [55]) and livestock farms (10 – 60 ppm_v [56]). The colourless, corrosive and toxic gas has a strong, offensive and repellent odour with an olfactory threshold of detection of approximately 0.16 µmol L^{-1} (4 ppm_v) [57] and 2.05 µmol L^{-1} (50 ppm_v) [58]. Reasons for the two different thresholds are unclear. However, different sensitive perception and training of the panellists as well as variations in gas volume and gas flow rate can result in dissimilar detection threshold. Exposure to 50 – 100 ppm_v NH_3 causes irritation to the mucous membranes, generating a burning sensation in the eyes, nose and throat [59]. At concentrations of 400 ppm_v the irritation is immediate, at 1500 ppm_v ammonia causes coughing and at 2500 ppm_v it is life-threatening [60]. Research has shown that animal health and animal productivity are also related to ammonia concentration in the livestock environment [61]. The increase in environmental litigation, coupled with a rising environmental awareness and a focus on quality of life has resulted in an increased number of proposed technologies and methods for ammonia treatment. In addition, if ammonia is not sufficiently removed from gas streams released into the atmosphere, it can be converted to nitrous oxide (N_2O), which is a powerful greenhouse gas [62].

A number of ammonia removal methods are known but all show disadvantages. Ammonia scrubbing for example, is an energy and/ or cost intensive process

which requires additional chemicals [77] or biological treatment. Scrubbing often results in large amounts of ammonium solution [78] that need to be disposed. Biofiltration is an alternative which can be operated at lower operational costs. It has been demonstrated in various studies to be an effective and reliable biological method to treat a wide range of pollutants [39].However, ammonia biofiltration involves the dissolution of ammonia gas in the water phase of the wet filter bed. Depending on temperature and pH the dissolved ammonia in solution is present as free ammonia (FA) or ammonium (NH_4^+). NH_4^+ can be biologically oxidized to nitrite (nitritification) and nitrate (nitratification) when a suitable biofilm has been allowed to develop. Both nitritification and nitratification are carried out by different microorganisms, *Nitrobacter* and *Nitrosomonas*, respectively [79]. Accumulation of the metabolites will cause inhibition and finally cause biofilter failure.

In contrast to the risk of biological inhibition, the well-established chemical reaction of ammonia and nitrite to nitrogen gas (N_2) in aqueous solutions (Equation 2-1) is favoured at high concentrations [65]. This decomposition is rapid near 100 °C and does not require a catalyst at that temperature [73].

$$\mathrm{NH_4^+ + NO_2^- \rightarrow N_2 + 2H_2O}$$ **Equation 2-1**

This chemical reaction needs a more detailed description. Following Million's findings [65] studies showed poor reproducibility until Abel et al. [67] demonstrated that in the presence of a supplementary acid, reproducible results for the production of N_2 can be achieved. The acid catalysed reaction of $NH_4NO_2 \rightarrow N_2 + 2\ H_2O$ was observed at significantly lower temperature (25 °C)

then without an acid. It was concluded that strong Brönsted acids interrelate with ammonium nitrite by lowering the activation energy of Equation 2-1.

Abel [67] describes the kinetics of the reaction as a third order reaction involving NH_4^+, HNO_2 and NO_2^- (Equation 2-2).

$$d(N_2)/dt = k[NH_4^+][NO_2^-][HNO_2] \qquad \textbf{Equation 2-2}$$

Other authors [68] use a simpler 2nd order reaction (Equation 2-3).

$$d(N_2)/dt = k[NH_4^+][HNO_2] \qquad \textbf{Equation 2-3}$$

Results presented by Li in 2006 [69] support and reinforce the findings by Abel [67] even in the absence of an aqueous phase and therefore Equation 2-2 will be used in this work. The appropriate k constant was subject of discussion in a number of publications [68, 70]. In this study we use the k constant of $3.67*10^{-3}$ [unit less] at 25 °C which was originally suggested by Abel [67]. The catalytic acid will be provided by the solid acid zeolite.

Zeolites are used as catalysts in many industries [52, 72, 73, 80-82]. Zeolites are naturally and widely occurring aluminosilicate minerals. They are composed of tectosilicates with isomorphous substitution of Al^{+3} for Si^{4+} and have a high ion exchange capacity [83]. Some of the quadrivalent silicon atoms are replaced by trivalent aluminium atoms resulting in an increase of the deficiency in positive charge. The charge is balanced by the presence of cations usually in the following order of decreasing amounts Na^+, NH_4^+, K^+, Mg^{2+}, Ca^{2+}. Zeolites are classified depending on their chemical structure and their ion exchange capabilities. In this study clinoptilolite (a type of zeolite) has been used since its

structure makes the mineral highly selective for K^+ and NH_4^+ and less selective for Na^+, Mg^{2+} and Ca^{2+} [84, 85]. Clinoptilolite can also adsorb molecules due to its large internal surface area. The adsorption area can be reached by a given molecule passing through their “pores” [86, 87]. Clinoptilolite is known to catalyse the NH_4 and NO_2^- to N_2 reaction [69, 88]. The acidity and characteristic pore structure of clinoptilolite appeared to be responsible for the increased performance. Some zeolites can be considered to be a solid (mineral) acids [87, 89]. Yeom and colleagues speculated that solid acids will protonate ammonium nitrite. They suggested that the reaction given in Equation 2-1 actually proceeds in two steps with protonated nitrosamine $[H_2NNOH]^+$ being an intermediate [88]. Yeom [88] conducted experiments to investigate the effect of solid acids and studied physical mixtures that consisted of the acid zeolite with ammonium nitrite covered powder [69]. It was found, that 80 % of the NH_4NO_2 was converted to N_2 + 2 H_2O within 13 h at room temperature (25 °C). That demonstrated that surface diffusion of acid protons and/ or ammonium nitrite is sufficient to enable the solid acid-catalysed reaction (Equation 2-1) to occur at a low temperature [69]. In addition, Sun and colleagues [90] demonstrated that the N_2 product contains respectively of one N from NH_3 and the other from NO_x.

The understanding of the effect of solid acidity on catalytic activity is also the subject of recent research [71]. For catalysis at room temperature, two pathways are widely accepted:

Pathway one shows cyclic double interaction between the ammonia and cationic zeolites. Cyclic double interaction have been reported in a study of the interaction of ammonia and protonic zeolites [91] and in a more recent

publication, Eckert et al. have [92] reported the same interaction between chloroform and Na–Y faujasite. Double interaction is probably accountable for the decomposition of ammonia as observed by TPD-MS and IR measurements [93]. The decomposition of ammonia within cationic zeolite can be corresponded to the decomposition of water molecules inside lanthanum faujasite zeolites reported by Das et al. [94]. Gilles et al. postulates that the electrostatic potential of multivalent cations as counterions causes the dissociation of the water molecules to release strong Brönsted acid [93]. Using temperature programmed desorption mass spectrometry (TPD MS) for analysis, Gilles and colleagues [93] monitored the appearance of four products (i) ammonia, (ii) amine groups, (iii) dihydrogen and (iv) dinitrogen. Products (i) and (ii) come from the ionization and decomposition of the ammonia molecules in the chamber of the spectrometer. This pathway cannot explain the presence of dihydrogen and the dinitrogen. The authors proposed that these elements were produced inside the zeolite cavities before desorption. Subsequently the possibility of decomposition of ammonia molecules in cationic zeolites resulting in N_2 and H_2 as products was suggested. Brandle [91]and his colleagues have summarised that process in the following equation (Equation 2-4), where Z represent the zeolite and B the molecule.

$$Z - OH \cdots B \rightarrow Z - O^{-} \cdots BH^{+}$$

Equation 2-4

Pathway two is based on the capability of di- or trivalent cations (M) to dissociate water molecules to produce the acidic species H^{+} and alkaline components such as MOH^{+} (divalent metal cations) or MOH^{2+} (trivalent metal cations) [95]. The dissociation of water by cations is well established and occurs

even at room temperatures [96]. A number of infrared studies concerning rare-earth or alkali-earth metal cation exchanged zeolites have demonstrated the existence of such species (MOH^+ or MOH^{2+}) [97-100]. The dissociative chemisorption of water is energetically preferred on zeolites with multipositive cations in their cavities [73]. Li et al. [73] also reports that the negative charge of zeolite is effectively localized on Al-centered oxygen tetrahedra in the rigid lattice, but the positive-charge carriers are ions located in the cavities. Only the positive-charge carriers are mobile. Electrostatic interactions of mono-positive ions, such as Na^+ are at optimum when the positive ions are located close to the negative-charge carriers. However, for multipositive ions (e.g. Ca^{2+} and Mg^{2+}) a separate position for the positive charged carrier must be found [73]. That is necessary because multipositive ions cannot simultaneously be a close neighbour to each of the two or three immobile negative charges that it compensates. In this situation the electrostatic energy of the system will be reduced by materials that dissipate the (n+) charge of the positive ion into n(1+) charges that can seek positions near an Al-centered tetrahedron of the zeolite [103]. An example of such a charge dissipation is the following hydrolysis reaction (Equation 2-5):

$$Ca^{2+} + H_2O \rightarrow CaO + 2H^+ \qquad \textbf{Equation 2-5}$$

Both pathways result in the production of hydrogen favouring the reaction in Equation 2-1 by reducing the pH in the aqueous phase surrounding the zeolite.

In addition to zeolite's catalytic capabilities, its inertness is a further advantage of the mineral. It makes natural zeolites an ideal inert filter media [79] and

studies have shown that microorganisms can attach onto the surface [101, 102]. Organic support materials such as coconut fibre [103], bark or peat [47], compost [46] or pruning waste are commonly used because of their availability, low commercial cost and provision of nutrient sources for bacteria. However microorganisms attached to the organic media cause degradation of the filter material and therefore regular filter bed replacements are required as the bed collapses and can cause additional odour during biodegradation.

The above considerations show that we can utilise a naturally occurring zeolite as a non-biodegradable matrix to support nitritifying bacteria. The zeolite also acts to buffer varying loads of ammonia. What has not been demonstrated is whether the chemical reaction of $NH_4^+ + NO_2^- \rightarrow N_2 + 2\ H_2O$ can take place at the ambient conditions of a single biofilter.

In this paper we demonstrate that the reaction indeed takes place and that it is catalysed at ambient temperatures by naturally occurring zeolite clinoptilolite.

2.2 Materials and Methods

2.2.1 Clinoptilolite

Clinoptilolite (Zeolite Australia Pty Ltd) was sieved to a grain size range of 2.4 – 4.0 mm and washed with deionised water before drying at 105 °C for at least 24 h. This will be referred to as clean Clinoptilolite throughout this thesis. The zeolite morphology was determined by using a Philips XL-20 scanning electron microscope capable of energy dispersive chemical analyses. Zeolite was mounted directly on stainless steel stubs using double-sided sticky tape with subsequent Au coating (Balzers Sputter Coating Device SCD020). The local

surface chemical element composition was obtained from the energy dispersive spectroscopy (EDS) spectra with an X-ray energy dispersive spectroscopy (X-ray EDS; Oxford Link ISIS-2000) device.

X-ray diffraction analysis (XRD) was employed to determine the chemical composition of the used clinoptilolite. The chemical composition was obtained from the pattern and the peaks recorded. Therefore 5 g samples were pulverized in duplicate with a ball mill and compacted into a holder. XRD patterns of the clinoptilolite were obtained using an Enhanced Multi Materials Analyser (EMMA) GBC Scientific Equipment Pty Ltd. A database search-match of patterns was made with Traces® software. Scans were performed at a rate of 1 ° min^{-1} and a step size of 0.05 ° and at a wavelength of 1.54059 Å (Cu).

The cation exchange capacity of the clinoptilolite for ammonium was determined by a series of batch tests. Different amounts of clinoptilolite and two different concentration ranges (A and B) of NH_4Cl solutions were used.

A. Concentration range 1 mM (batch i) and 10 mM (batch ii) NH_4Cl in de-ionised (DI) water (initial solution volume: 50 mL) with 0, 1, 2, 4, 8, 16 and 32 g clean clinoptilolite
B. Concentration range 100, 1000 and 2500 mM NH_4Cl in DI water (initial solution volume: 250 mL with 0, 50 and 500 g clean clinoptilolite

After clinoptilolite and ammonium solution were added, the closed bottles were shaken (30 rpm) with an automatic bottle shaker at room temperature. Up to 6 liquid samples were taken at the beginning (time = 0) and at regular time intervals. Total experiment run time was 24 h. Syringe filtered samples

(0.45 µm) were frozen at – 20 °C until analysis. Cation analyses were performed on an HPLC (AGILENT 1200) with a “Universal Cation HR, 3 µm, 7.0 x 53 mm” column, coupled to a conductivity detector (Alltech Model: 350). Duplicate samples were analysed by multi-injections (3 injections per sample). Methanesulfonic acid in water (3 mM) was used as a mobile phase with a flow rate of 2.5 mL min^{-1}.

2.2.2 Reaction between ammonia and nitrite

The clinoptilolite/ solution combinations were chosen based on preliminary pretests. These pretests were conducted to estimate the amount of free water clinoptilolite is capable to hold. Therefore 20 g dry clinoptilolite were submerged into water for 24 h in duplicate. After that time, water was drained through a sieve and the weight of the moist clinoptilolite was determined (results not presented). The moist zeolite was dried at 105 °C for 24 h and the weight was determined. The difference between moist and dried zeolite was used to calculate an average moisture content (retention capacity) 0.2 mL water g^{-1} clinoptilolite. The exact water content is required for further calculations (2.3.2.1). Furthermore, 50 g of clinoptilolite provided a calculated surface area of approximately 1000 cm^2 and with each magnitude less clinoptilolite the surface area degreases a magnitude.

Experiments were conducted in 120 mL serum bottles closed with rubber bungs. Gas production within these close environments was determined by the change of gas composition (gas chromatography) or monitored volumetrically. To determine the change of gas composition in the headspace of closed serum bottles filled with varying amounts of clinoptilolite as well as ammonium and

nitrite concentrations the following experiments (C to D) were conducted at room temperature:

C. 10 mL solution with a concentration of 2.5 M NH_4Cl and 1 M $NaNO_2$ was added to 50 g clinoptilolite
D. 10 mL solution with a concentration of 2.5 M NH_4Cl and 1 M $NaNO_2$ without clinoptilolite

As negative controls the following two experiments were set up and monitored at the same time and under same conditions as experiments C to D:

E. 10 mL solution with a concentration of 2.5 M NH_4Cl was added to 50 g clinoptilolite
F. 10 mL solution with a concentration of 2.5 M NH_4Cl and 1 M $NaNO_3$ was added to 50 g clinoptilolite

All experiments were performed in duplicates. After adding the compounds the serum bottles were immediately closed and the headspaces were flushed with industry grade helium for two minutes at a flow of 1 L min^{-1}.

Batch experiments were conducted to investigate the effect of temperature and the role of clinoptilolite. Before closing the bottles with rubber bungs 10 mL of 2.5 M NH_4Cl plus 1 M $NaNO_2^-$ solution were added. In these experiments (G to L) 0, 0.05, 0.5, 5.0 and 50 g clean clinoptilolite was used.

G. In a chilled water bath (12 °C)
H. At room temperature (22 °C)
I. In a heated water bath (55 °C)

To determine the concentration range of the ammonium and nitrite reaction, experiments (J to L) with 0, 0.05, 0.5, 5.0 and 50 g clean clinoptilolite in a 55 °C water bath were conducted:

J. 90 mL solution with a concentration of 100 mM NH_4Cl and 100 mM $NaNO_2$
K. 90 mL solution with a concentration of 10 mM NH_4Cl and 10 mM $NaNO_2^-$
L. 90 mL solution with a concentration of 1 mM NH_4Cl and 1 mM $NaNO_2^-$

In experiments G to L, readings were taken initially every 30 min for the first 4 h and later twice a day over a period of one week.

Nitrite (I) and nitrate (II) in water was analysed in duplicate spectrophotometrically (wavelength I = 540 nm and II = 420 nm) based on APHA Standard Methods [104].

At each sample event individual temperatures were recorded for further calculations. All determined, calculated and expected gas volumes were normalised to the temperature at which the experiment was conducted. The following equation (Equation 2-6) was used to calculate the required specific molar volume of an ideal gas v at a given temperature [mL $mmol^{-1}$], with R the universal gas law constant (8.31 [J K^{-1} m ol^{-1}]), T the temperature [K] and p the pressure [100 kPa].

$$v = \mathrm{R} * \frac{T}{p} \qquad \textbf{Equation 2-6}$$

Knowing the specific molar volume, the molar mass of the determined gas volume can be computed employing the rule of proportion (Equation 2-7).

Where *m* is the calculated molar mass [mol] at that given temperature and g is the gas volume [mL] determined during the experiment.

$$m = \frac{1}{\mathrm{v}} * g$$ **Equation 2-7**

After testing a number of curve fitting functions for the best fit, the Hill fit curve fit was used to interpolate the trend between the experimental results. The Hill equation (Equation 2-8) is a three parameter equation of a nonlinear relationship between two variables, *x* (the independent variable) and y (the dependent variable) [105]. The three parameters of the equation are *Vmax*, *c* and the coefficient *n*.

$$y = Vmax\frac{x^n}{c^n + x^n}$$ **Equation 2-8**

2.2.3 Gas analyses

2.2.3.1 Gas composition measurements

With a gas tight syringe 350 µL of headspace gas sample was taken twice. The syringe was rinsed with the first 350 µL and 300 µL of the second syringe was finally injected into the gas chromatograph (GC). Gas samples were analyses by a Shimadzu GC 2010 working with helium as carrier gas (50 mL He min^{-1}), at 40 °C, using a thermo conductivity detector (TCD) at 150 °C. A concentric packed column was installed within the GC.

2.2.3.2 VOLUMETRIC GAS MEASUREMENTS

To determine the volumetric gas production over time, a syringe was permanently connected through the rubber bung of the serum bottles. A small amount of oil was added to the syringe plunger for a more precise recording. Before daily readings were taken each syringe plunger was moved up and down to minimize resistance and to reach equilibrium.

2.3 Results and Discussion

2.3.1 CLINOPTILOLITE

The surface morphology analysis by scanning electron microscope (SEM) showed the used zeolite having a rough surface and porous structure (Fig. 2-1). X-ray energy dispersive spectroscopy (EDS) analysis revealed the presence of both, mono and multivalent cations on the zeolite surface. The presented variations in element concentration (magnification: 160 (Fig. 2-1 ii) and 2600 (Fig. 2-1 iii)) are the result of local surface element analysis of the natural zeolite resulting in spatial inconsistency of zeolite composition. The average composition of 4 X-ray EDS scans performed on zeolite are presented in Table 2-1. The confirmation of present cations will be of benefit for the catalytic reaction mentioned described in chapter 2.1. The determined cations match with the results reported by Christie [106] about the chemical composition of clinoptilolite. With an Si to Al ratio of 5.3 the clinoptilolite is clearly distinguished as an clinoptilolite- Ca [107]. Furthermore, XRD diffraction pattern (Fig. 2-2) identifies the pulverized zeolite as clinoptilolite. Therefore in this thesis the used zeolite will be referred as clinoptilolite.

Exposing different amounts of clinoptilolite samples to the same volume and concentration of NH_4Cl solution gives evidence about the effects of initial concentration on the replacement of cations. In experiment A, batch (i) initially 50, 25, 12.5, 6.25. 3.12 and 1.56 and in batch (ii) 500, 250, 125, 62.6, 31.23 and 15.62 µmol $NH_4Cl\ g^{-1}$ clinoptilolite were tested for 24 h. Results presented in Fig. 2-3 (i) show that at low NH_4Cl (1 mM) concentrations Na was exclusively replaced..

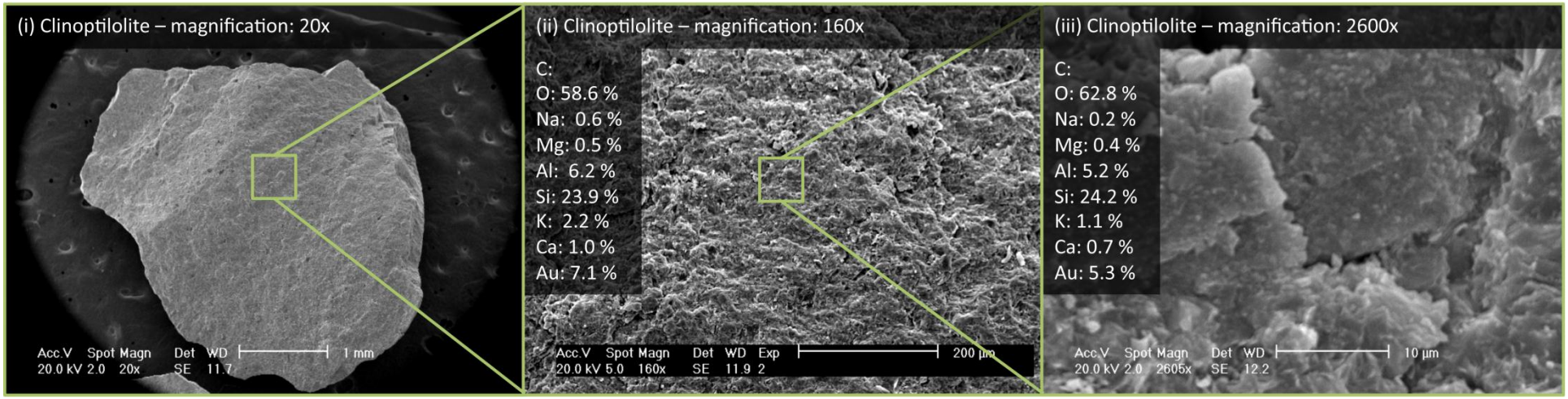

Fig. 2-1: SEM and XRD of clinoptilolite at a magnification of (i) 20, (ii) 160 and (iii) 2600 times

Table 2-1: Clinoptilolite composition used in that study determined with XRD process (average values of 4 SEM EDX runs are presented)

Components [%]	
C	0.0
O	66.6
Na	0.4
Mg	0.5
Al	4.8
Si	25.3
K	1.3
Ca	1.3

At concentrations above 50 µmol NH_4Cl g^{-1} clinoptilolite's divalent Ca began to exchange. Ca will continue to exchange while Na reaches a maximum of 55 µmol Na g^{-1} clinoptilolite when 1 g clinoptilolite is exposed to 250 µmol of NH_4Cl (Fig. 2-3 (ii)). It was found that Ca become the dominant ion exchanged cation when clinoptilolite was exposed to 500 µmol NH_4Cl g^{-1} clinoptilolite (1 g clinoptilolite exposed to 50 mL 10 mM NH_4Cl) and above.

The highest load of 500 µmol g^{-1} clinoptilolite was chosen with respect to the highest concentration measured during the experimental phase of this thesis (see 4.3.1). These cation exchange experimental results are presented as plots of s versus c, where s is the amount of adsorbed (NH_4^+) or desorbed (sum of Na, K, Ca and Mg) cations onto/ from clinoptilolite, and c the initial NH_4^+ concentration in solution exposed to one gram clinoptilolite. The results are plotted at different times (1 h, 2 h and 24 h) of measurement.

In Fig. 2-4 (i) the adsorbed and desorbed cations are plotted for the complete load range mentioned above. The plotted results indicate that ion exchange is a process occurring over time, and with increasing initial concentration higher

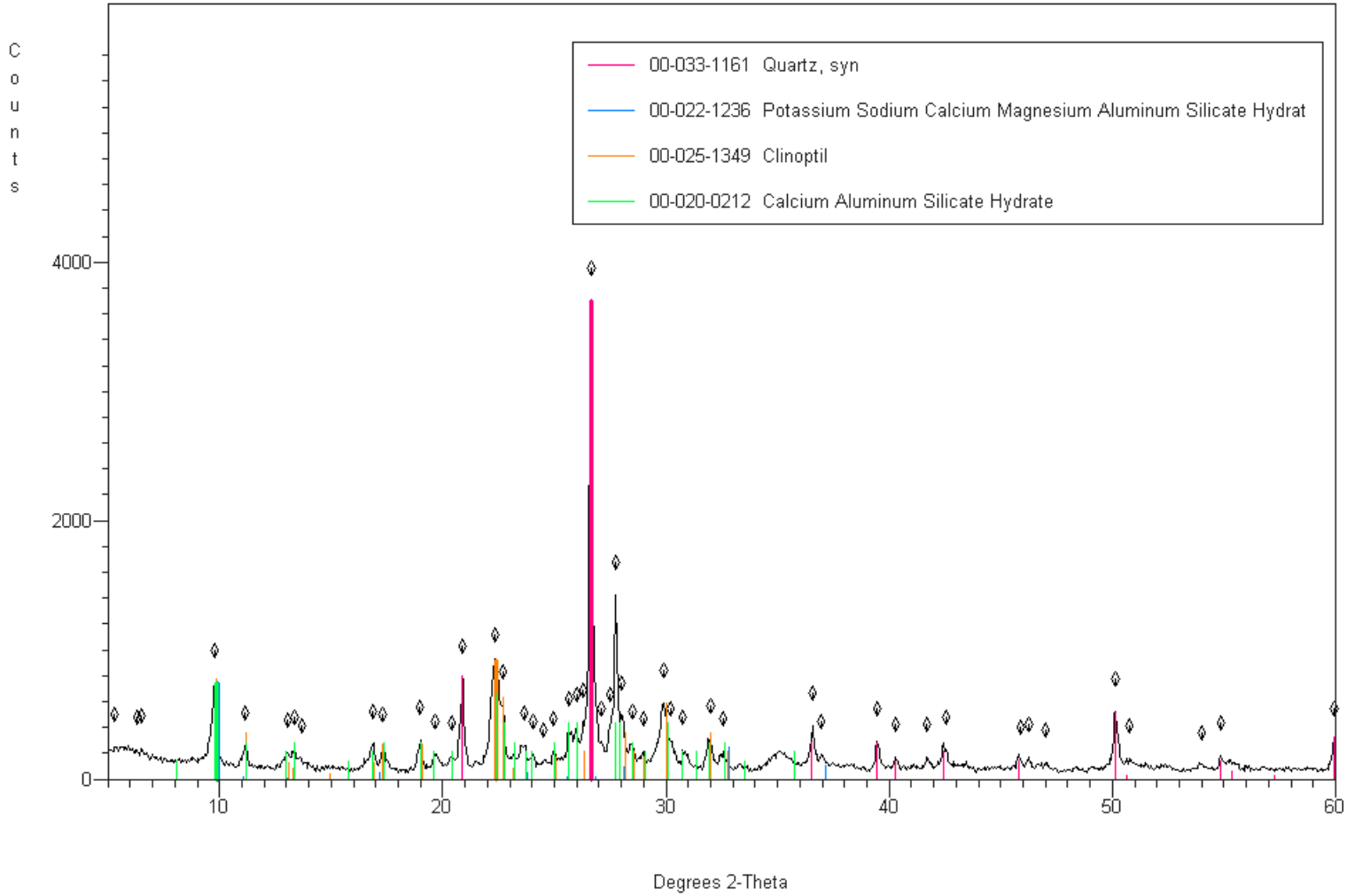

Fig. 2-2: XRD pattern of the used clinoptilolite

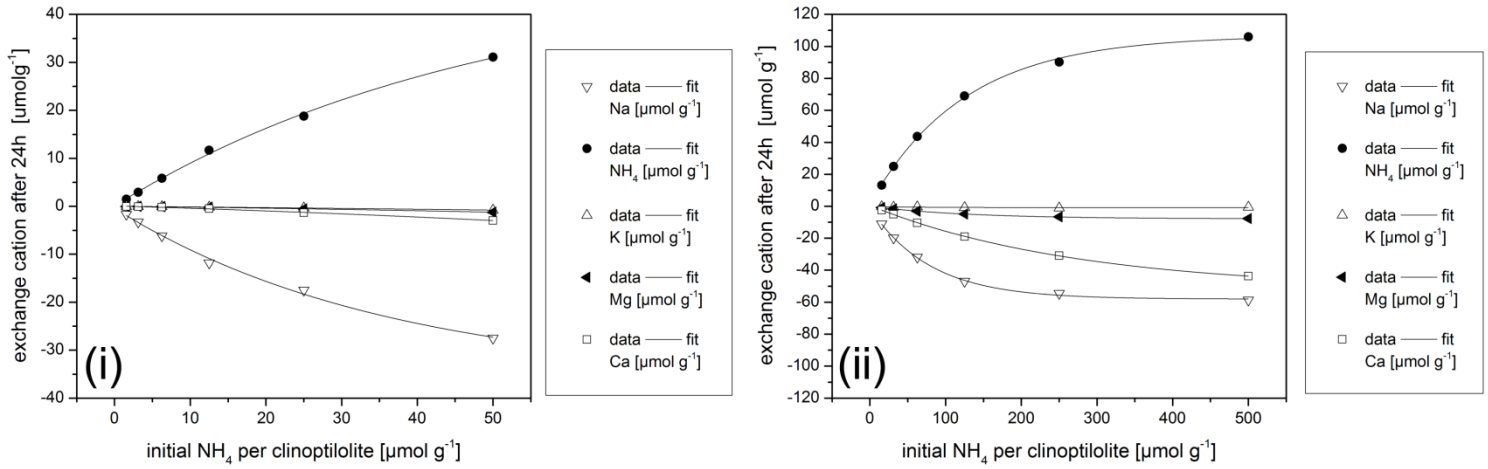

Fig. 2-3: Various amounts of clinoptilolite (0, 1, 2, 4, 8, 16 and 32 g) exposed to (i) 50 mL of 1 mM NH_4Cl resulting in an initial 50, 25, 12.5, 6.25, 3.125 and 1.5625 µmol NH_4Cl g^{-1} clinoptilolite condition and (ii) 50 mL of 10 mM NH_4Cl resulting in an initial 500, 250, 125, 62.5, 31.25 and 15.625 µmol NH_4Cl g^{-1} clinoptilolite condition (experiment A)

amounts of NH_4^+ are adsorbed and other cations are desorbed respectively. A linear relation between c and s for the load of 1.56 µmol NH_4^+ g^{-1} clinoptilolite to 125 µmol NH_4^+ g^{-1} clinoptilolite was observed (Fig. 2-4 (ii)). At initial concentrations above 125 µmol NH_4^+ g^{-1} clinoptilolite, a nonlinear ion exchange behaviour was observed (considering an intersection at 0; 0).

The results of experiment B show a clear ion exchange trend of the three initial concentrations (i = 10, ii = 100 and iii = 1000 mM NH_4Cl). Under the same condition (500 µmol NH_4Cl g^{-1} clinoptilolite) (i) 1 g clinoptilolite was exposed to 50 mL, (ii) 50 g and (iii) 500 g clinoptilolite to 250 mL solution. As shown in Fig. 2-5 (i) at low concentrations (10 mM NH_4Cl) sodium is the dominant exchanged ion but the difference to the exchanged calcium is only minimal. Exposing clinoptilolite to higher concentrations (above 100 mM) of NH_4Cl, as shown in (ii) and (iii) results in the dominance of Ca over Na cations. In batch iii 35 µmol Mg per g clinoptilolite was also measured.

That the ion exchange capacity of ammonium ion by clinoptilolite increases with increasing initial ammonium concentration is well established [108-111]. Results gathered with experiment A and B suggest the same conclusion that not only the initial NH_4^+ concentration per gram clinoptilolite effects the amount adsorbed onto the zeolite but also the concentration of NH_4^+ in solution (Fig. 2-6). That makes a reliable comparison with literature results difficult since the possible setups are endless. Further reasons making comparison of the observed ion exchange results with in literature published values difficult are:

- Different grain sizes (usually powder) and exposure time [85, 109, 112]
- Pre-treatment or preconditioning with NaOH [110] or NaCl [113]

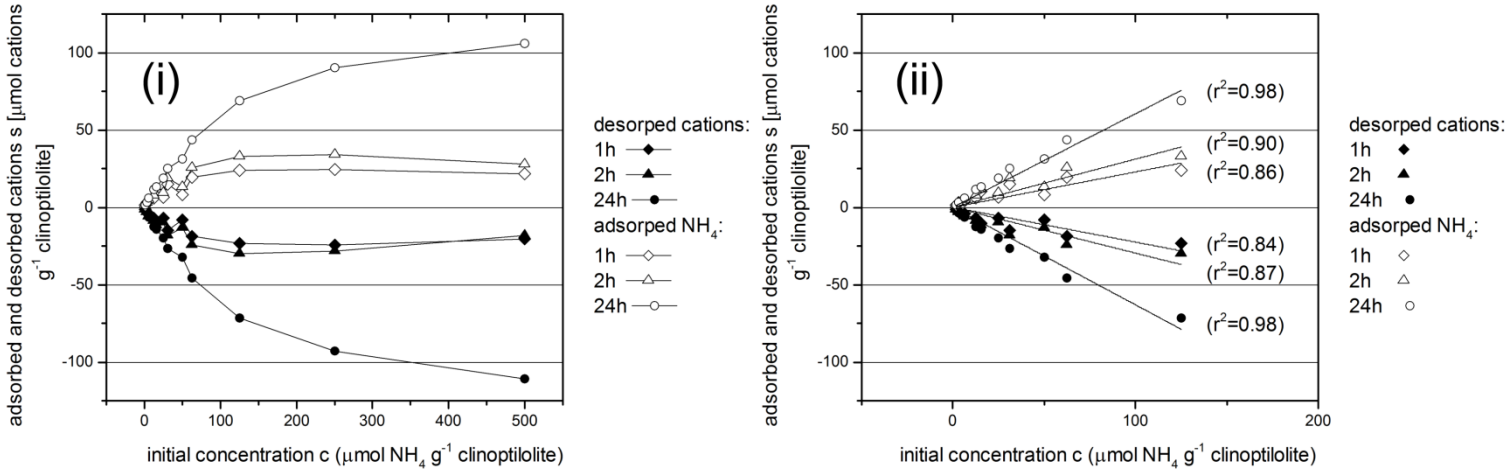

Fig. 2-4: (i) ion exchange (adsorption of NH_4^+ and desorption of other cations) at different initial concentration c (ii) ion exchange between 0 µmol NH_4^+ g^{-1} clinoptilolite to 125 µmol NH_4^+ g^{-1} clinoptilolite including a linear fit

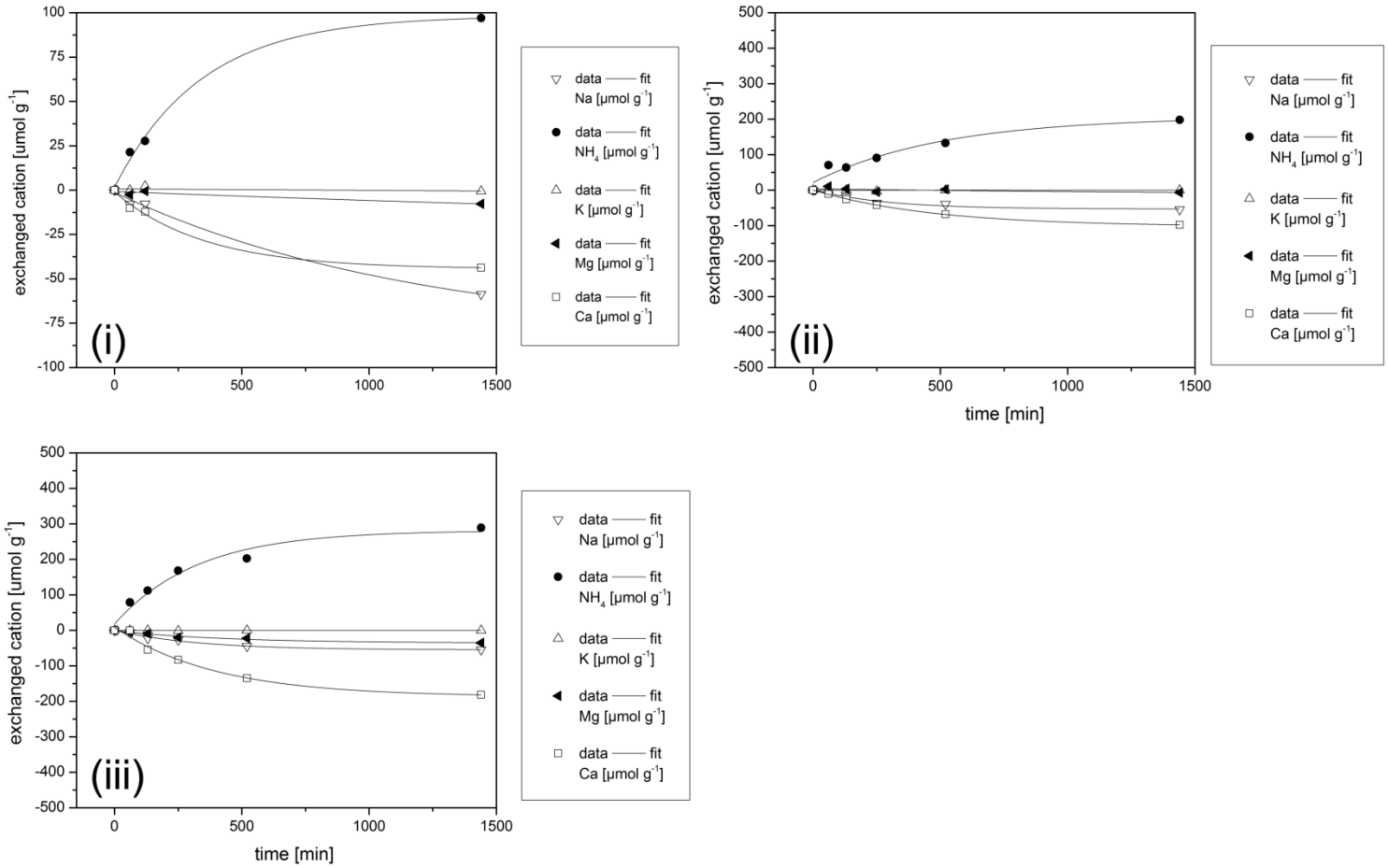

Fig. 2-5: Ion exchange behaviour of clinoptilolite at the same initial conditions of 500 µmol NH_4Cl g^{-1} clinoptilolite but (i) 1 g of clinoptilolite in 50 mL of a 10 mM NH_4Cl solution (ii) 50 g of clinoptilolite in 250 mL of a 100 mM NH_4Cl solution and (ii) 500 g of clinoptilolite in 250 mL of a 1000 mM NH_4Cl solution (experiment B)

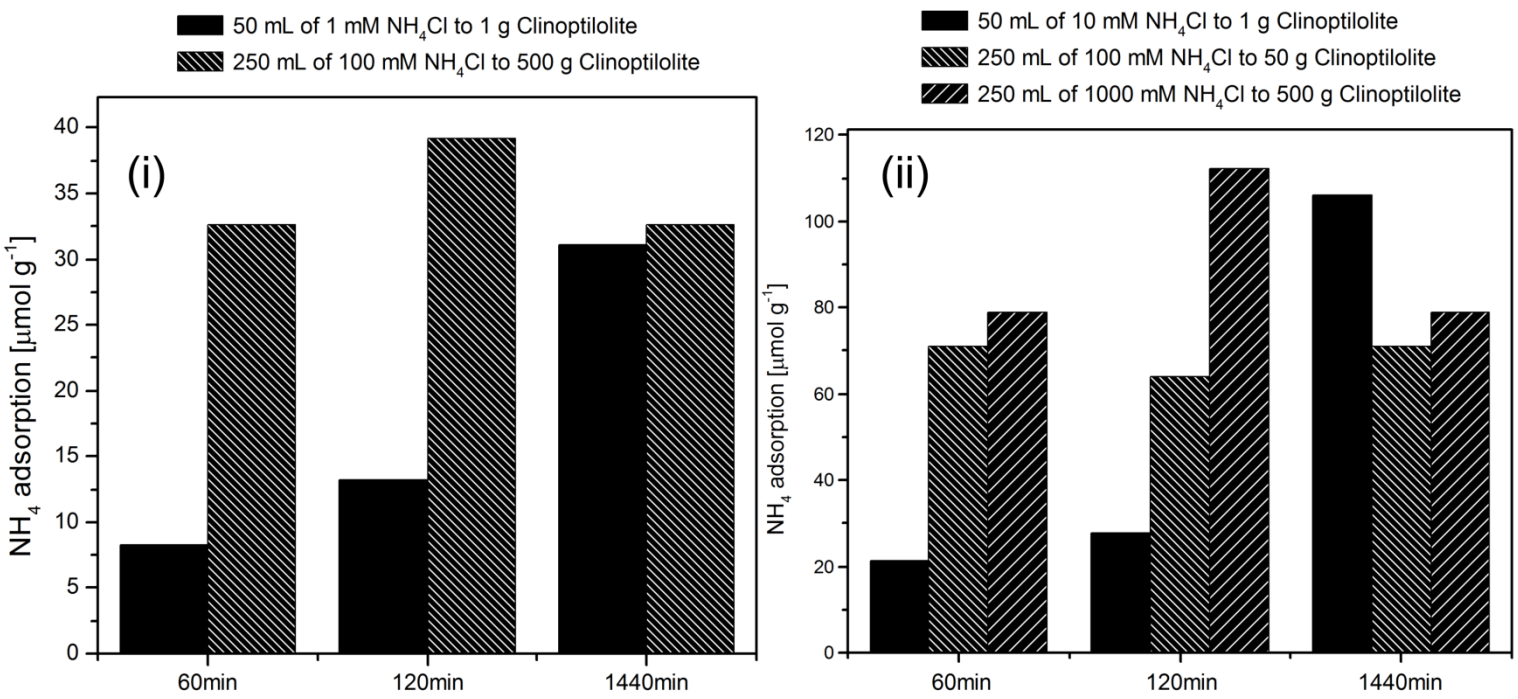

Fig. 2-6: Comparison of (i) 50 µmol NH_4^+ g^{-1} clinoptilolite and (ii) 500 µmol NH_4^+ g^{-1} clinoptilolite initial NH_4^+ concentration

In summary, it was found that the order in which the cations appeared depended on the initial NH_4Cl concentration and on the amount of clinoptilolite introduced to a NH_4Cl solution. A mass balance showed that 97 % of the ammonia adsorbed onto the clinoptilolite, was replaced by cations detectable in the remaining solution. Calcium ion appeared as the highest concentration followed by sodium and magnesium. These observations correlate with the literature [84, 85] and suggest the availability of divalent cation for dissociation of water.

2.3.2 Reaction between ammonia and nitrite

The results of the experiments C- D are presented in Fig. 2-7. N_2 gas production was observed in both experiments. Nitrogen gas production was highest in experiment C (with 6.75 mmol = 165 mL), containing the high concentration of NH_4Cl and $NaNO_2^-$ (2.5 and 1.0 M) exposed to clinoptilolite. In experiment D the N_2 gas production was observed without clinoptilolite at the same NH_4Cl and $NaNO_2^-$ concentrations of 2.5 and 1.0 mM. Results showed a 2.5 times lower gas production with a maximum of 2.7 mmol (66.3 mL). In both experiments a maximum N_2 gas production of 10 mmol (245 mL) was expected.

Within the first 4 h the observed N_2 production rate for both experiments (C- D) is a linear function over time. In this period of time in experiment C a total of 1.32 mmol (34 mL) and in experiment D a total of 0.16 mmol (4 mL) were produced resulting in a rate of 0.35 mmol h^{-1} and 0.04 mmol h^{-1}, respectively. For experiment C the volume was calculated 8.9 times more than the nitrogen production volume in experiment D indicating that catalytic effect on the reaction (Equation 2-1).

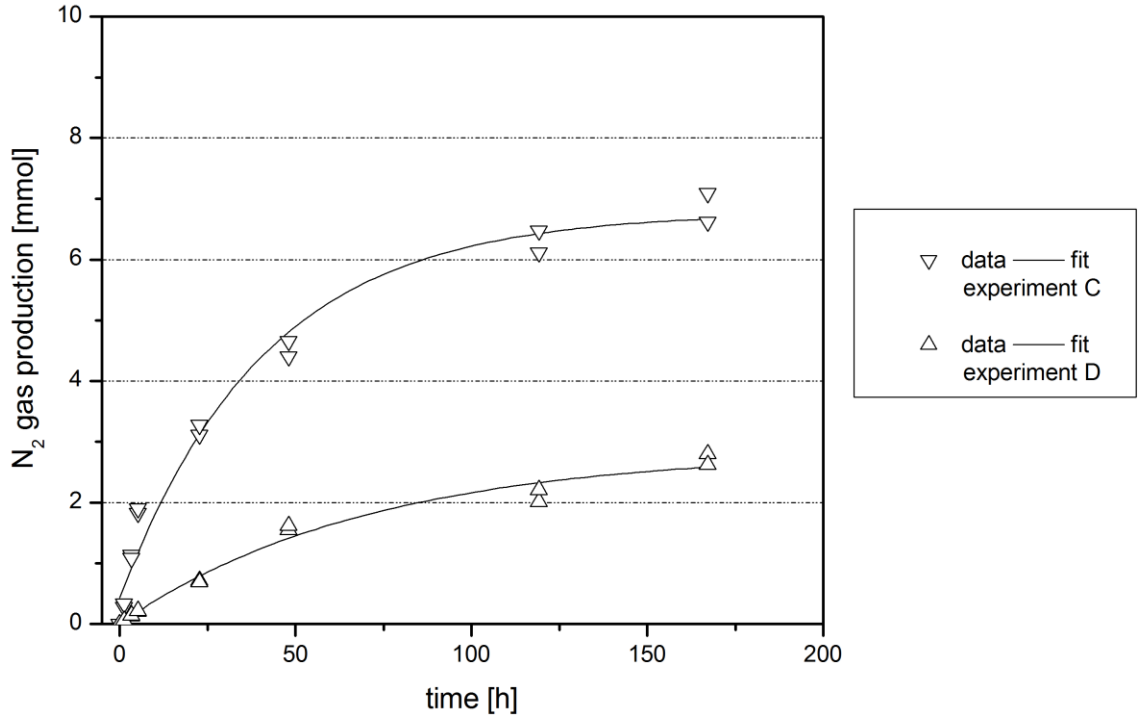

Fig. 2-7: N_2 gas production for Experiment C (10 mL of a 2.5/ 1 M NH_4Cl/ $NaNO_2^-$ solution was added to 50 g clinoptilolite) and experiment D (10 mL of a 2.5/ 1 M NH_4Cl/ $NaNO_2^-$ solution without clinoptilolite) recorded over a period of one week

Additional experiments (E and F) without nitrite did not show N_2 gas production at all. Combined with the above results presented in this section it was concluded that the reaction in Equation 2-1 remains valid. The more rapid reaction of ammonium and nitrite to N_2 in the presence of clinoptilolite also confirms the findings reported in the literature [87]. It can be suggested that a specific amount of clinoptilolite catalyses the reaction at an optimum concentration. To find the optimum clinoptilolite concentration, experiments (G - L) were conducted. Furthermore, experiments conducted and analysed with GC and volumetric method showed no significant differences in their gas production results (Appendix Fig. 7-1). For this reason from now on results presented, are determined with volumetric measurements.

The influence of temperature on the reaction rate was determined in experiments G - I. A maximum N_2 gas production of 10 mmol was expected, assuming that the introduced 10 mmol nitrite converts completely to N_2 gas. As presented in Fig. 2-8 i-iii all experiments (having the same amount of clinoptilolite (0 to 50 g)), at 12 °C, 22 °C and 55 °C produced N_2 gas over a period of one week, with a slightly higher yield at the highest temperature of 55 °C.

Fig. 2-8 iv – vi shows the gas production for the first 4 h after starting the experiment. The gas production rate increased with higher temperature. Comparisons of the experiments conducted at 12 °C and 22 °C show that the addition of clinoptilolite produces more N_2 gas, and at a faster rate.

To make comparison between experiments possible the production rate and a total N_2 gas production of those experiments were calculated and presented in Table 2-2. Table 2-2 summarises the N_2 production and rate for the first 4 h (12 °C and 22 °C) for experiments G and H as well as for the first 2 h for experiment I (55 °C). It shows, that at the highest N_2 production occurred at 55 °C and with 50 g clinoptilolite (6.77 mmol = 3.10 mmol h^{-1}) and the lowest gas production was recorded at 12 °C with 0.05 g clinoptilolite (0.09 mmol = 0.05 mmol h^{-1}).

These results strongly show the impact of clinoptilolite onto the ammonium and nitrite to N_2 conversion. However, the effect is temperature dependent. The catalytical impact of clinoptilolite in these experiments varies by a factor 1 to 4.

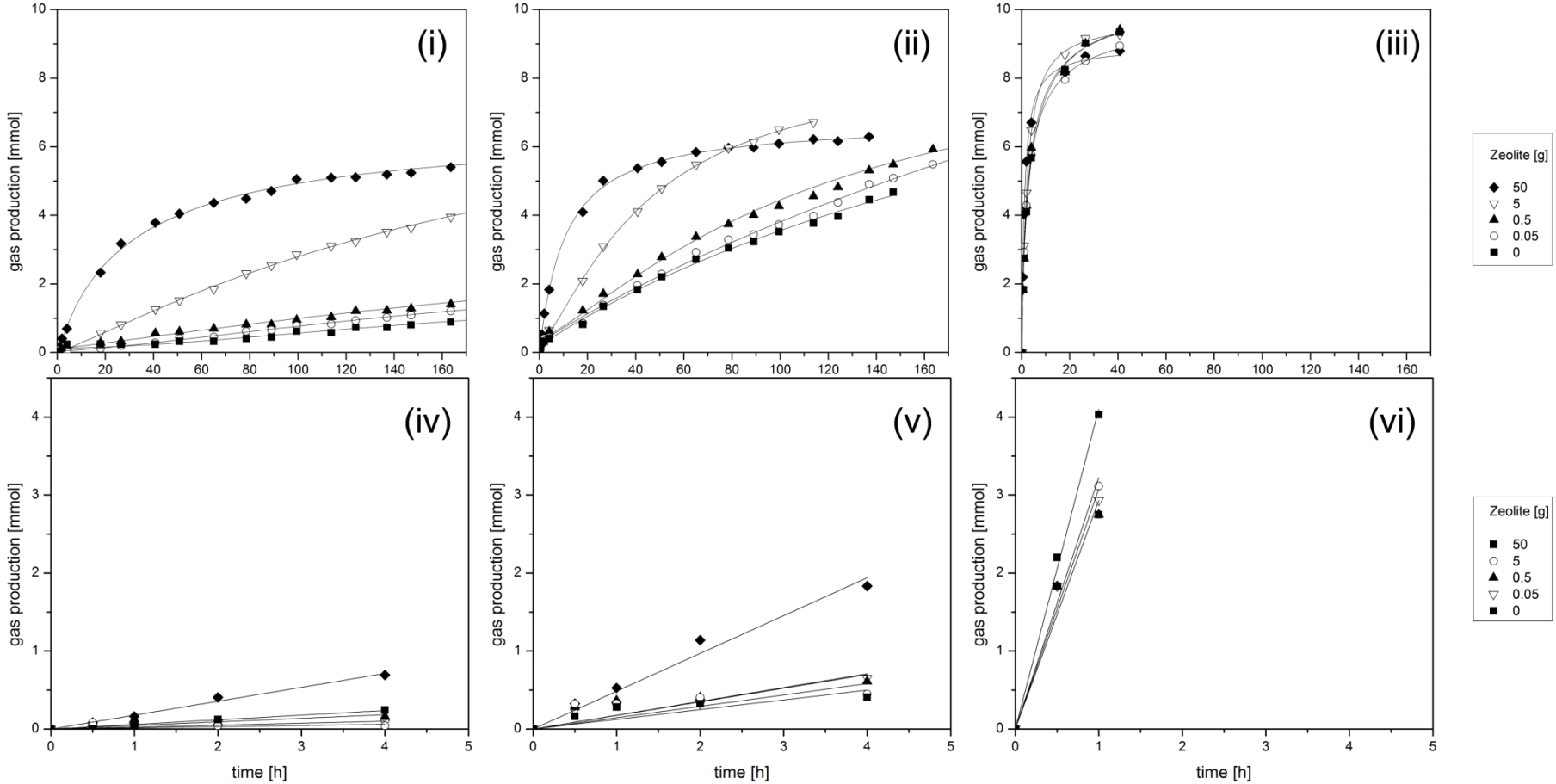

Fig. 2-8: (i) N_2 gas production and (iv) rate at 12 °C, (ii) N_2 gas production and (v) rate at 22 °C, (iii) N_2 gas production and (vi) rate at 55 °C (experiments G to I)

Table 2-2: Gas production and calculated rate for the first 4 h for experiments C and D at 22 °C as well as G and H at 12 °C and 22 °C and for experiment I the first 2 h at 55 °C for various amounts of clinoptilolite

experiment	Zeolite [g]	gas volume [mmol]			gas production rate [mmol h^{-1}]		
		12 °C	22 °C	55 °C	12 °C	22 °C	55 °C
C	50		1.32			0.35	
D	0		0.16			0.04	
G - I	50	0.37	1.95	6.77	0.19	0.48	3.10
G - I	5	0.07	0.79	5.51	0.04	0.17	2.54
G - I	0.5	0.25	0.81	5.09	0.12	0.18	2.33
G - I	0.05	0.09	0.70	5.20	0.03	0.15	2.37
G - I	0	0.09	0.55	4.99	0.05	0.12	2.26

However, the results of further experiments (Appendix Fig. 7-2 to Appendix Fig. 7-4) showed a 6.5 fold increase in production of N_2 gas when 50 g of clinoptilolite was exposed to (a) 10 mL of 40 mM of NH_4Cl and 300 mM $NaNO_2^-$ (b) 10 mL of 20 mM NH_4Cl and 150 mM $NaNO_2^-$ compared to (c) vials filled with 50 g glass beads. The glass beads (inert material) acted as substitute to the clinoptilolite to simulate similar volume and surface as provided by the clinoptilolite. A 41 times faster reaction was observed, when the N_2 gas production of 50 g clinoptilolite and 52.5 g glass beads in 10 mL of 150/ 1000 mM NH_4Cl/ $NaNO_2^-$ was compared. It was beyond the scope of this study however, to investigate those effects further.

Additional experiments (J - L) with various amounts (0, 0.05, 0.5, 5.0 and 50 g) of clinoptilolite and lower concentrations of ammonium and nitrite (100 mM, 10 mM and 1 mM) were also conducted to estimate limits of the ammonium nitrite to nitrogen reaction. No significant difference was found between the gas production with 50 g and with less clinoptilolite for the 100 mM experiment (Fig. 2-9). Approximately 5.65 mmol N_2 gas was produced (except 50 g of

clinoptilolite produced only 4.22 mmol) of the maximum expected 8.10 mmol. Only 0.36 mmol N_2 gas of the 0.81 mmol expected was produced for the 10 mM experiment within the first 60 h.

It needs to be noted, that the 0.81 mmol N_2 was produced within the first 3 h and ceased formation when additional NH_4^+ in form of NH_4Cl was added. After introducing additional NH_4^+ at 55 h, a total of 0.68 mmol N_2 was produced. That finding can be explained by the fact, that clinoptilolite is highly selective to NH_4^+ ion exchange and will adsorb NH_4^+ which is then not available for the reaction to produce N_2. Additional amount of NH_4^+ added at 120 h did not cause more gas production. This can be explained, because 0.9 mmol nitrite is the maximum concentration expected at 22 °C.

2.3.2.1 VALIDATION OF EXPERIMENTAL RESULTS WITH ABEL EQUATION

To validate the observed results, the equation (Equation 2-2) postulated by Abel [67] was employed. A model was developed, computing (a) the reduction of ammonium, nitrite and nitrous acid and (b) the resulting N_2 gas production for the first 4 h of reaction. Variables such as pH, temperature as well as constants such as pKa (NH_3 = 9.25, NO_2^- = 3.4 at 22 °C) were incorporated in the model. The pH dependency of NH_3/ NH_4^+ and NO_2^-/ HNO_2 equilibriums in aqueous phase is shown in Fig. 2-10.

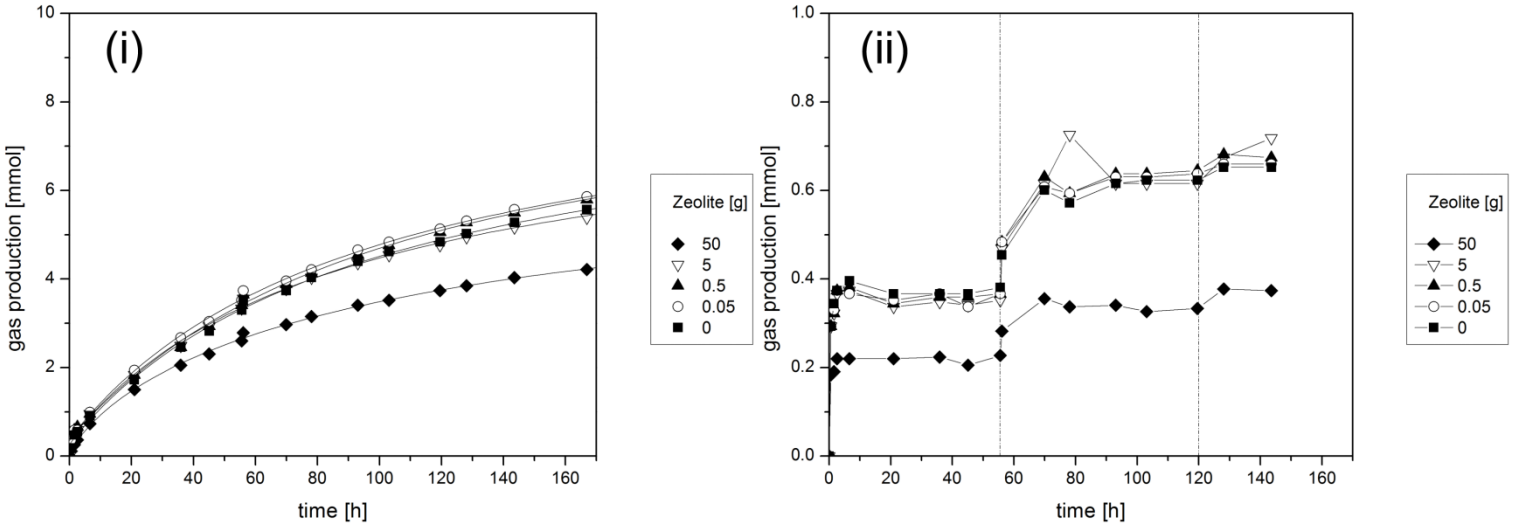

Fig. 2-9: N_2 gas production with (i) 90 mL 100 mM NH_4Cl + $NaNO_2^-$ (ii) 90 mL 10 mM NH_4Cl + $NaNO_2^-$ (additional NH_4Cl added at 55 and 120 h) and various amounts of clinoptilolite at 55 °C (experiments J and K)

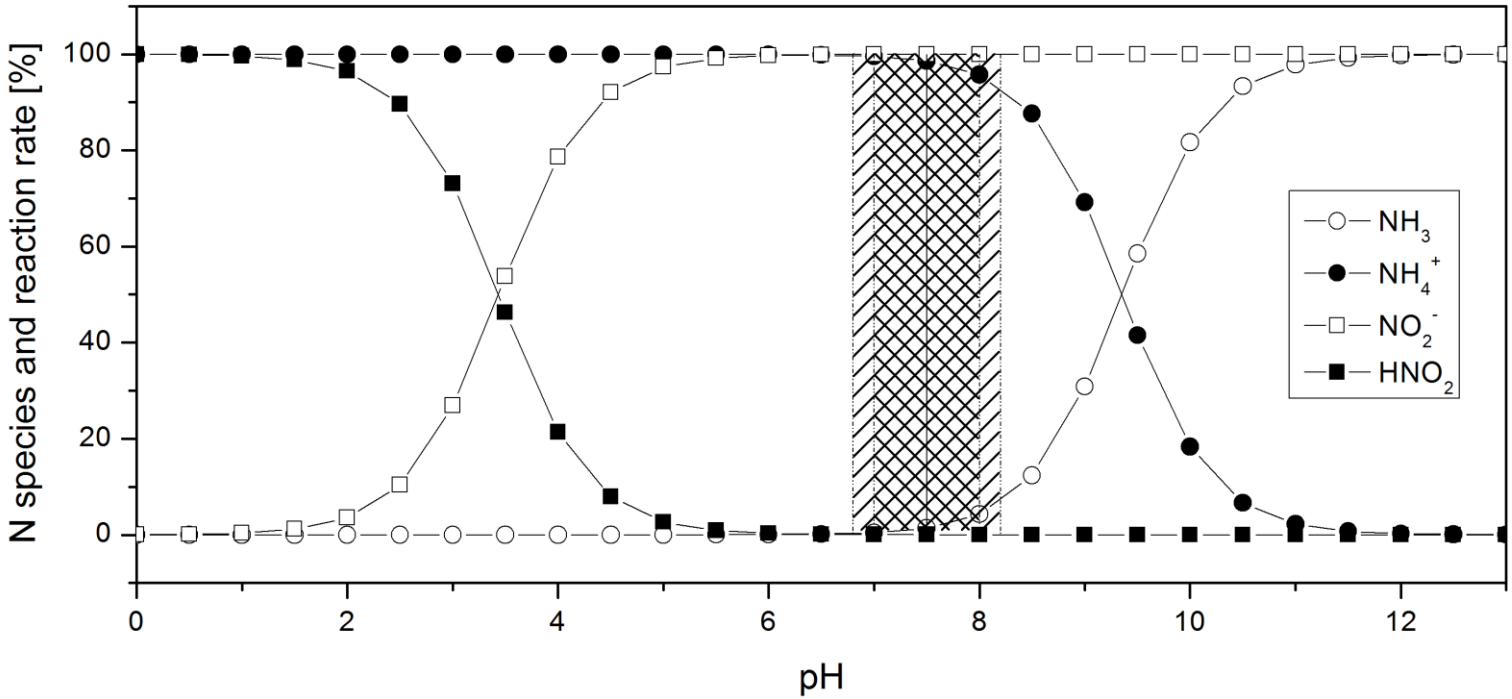

Fig. 2-10: pH dependency of NH_3/ NH_4^+ and NO_2^- and HNO_2 equilibrium's. The hatched area is the pH (6.8 – 8.2) range where nitrification is optimum [114-116] and the pH range detected during long-term experiments (Fig. 4-4)

With the applied model, the changes per minute were computed and the N_2 production was calculated as a sum over these time intervals. The model conditions were chosen based on the parameters used in experiment C to L. An initial NH_4^+ and NO_2^- concentration of 2.5 M and 1.0 M was inserted into the model and the corresponding NH_3 and HNO_2 concentrations were calculated. Temperature and pH ranges of 21°C to 23 °C (increment +1) and a pH range of 6.9 – 7.1 (increment +0.1) were chosen.

The computed model results were compared to the gas production of the zero clinoptilolite experiments D (0.16 mmol) and H (0.55 mmol), with an average of 0.36 mmol (Table 2-2). It needs to be noted, that the difference between the amount of gas produced can occur since the system is very temperature and pH sensitive, as mentioned in chapter 2.1. In addition most of the N_2 gas is possibly produced in the moist surface surrounding the clinoptilolite grains which can result in pulsed releases of gas [117]. Another reason could be the water film between the clinoptilolite grains, causing the formation of menisci which prevents or slows the diffusion of gases [118].

The modelled results and the comparison of the results with the measured values are presented in Table 2-3. Depending on pH and temperature the degree of correlation between the modelled and experimental data could be calculated. The variance of the results shows once again the importance and impact of temperature and pH on the reported reaction.

In addition the same model was used to compute and predict N_2 gas production as well as NH_4^+, NO_2^- and HNO_2 consumption over time. The computed results were also compared to the experimental results.

Table 2-3: Model results of N_2 gas production for the first 4 h calculated for three temperatures (21 °C, 22 °C and 23 °C) and three pH values (6.9, 7.0, 7.1) compared to the observed average (experiment D: 0.16 mmol and experiment H without clinoptilolite 0.55 mmol) N_2 gas production of 0.36 mmol. Results are represented in mmol as well as in mL (values in parenthesis)

pH	temperature [°C]		
	21	22	23
model results [mmol (mL)]			
6.9	0.48 (11.72)	0.4 (9.7)	0.33 (8.01)
7.0	0.38 (9.42)	0.32 (7.78)	0.26 (6.41)
7.1	0.31 (7.54)	0.25 (6.22)	0.21 (5.12)
model results correlated with measurements [%]			
6.9	37.4	13.7	-6.1
7.0	10.4	-8.9	-24.9
7.1	-11.6	-27.1	-40.0

For example, the initial condition of experiment H (10 mL containing 25 mmol NH_4^+ and 10 mmol NO_2^-, no clinoptilolite, at 22°C, pH 7.1) were inserted into the model and calculations performed for an experimental runtime of 160 h. As shown in Fig. 2-11 (i) the computed values match the observed results (± 5 %) over a period of 160 h. Simultaneously the model is computing the consumption of NH_4^+, NO_2^- and HNO_2 (Fig. 2-11 (ii)), showing a steeper decrease of HNO_2 than any of the other chemicals, indicating the possibility that HNO_2 would be the limiting factor in an ongoing experiment. The presented results also confirm, that 1 nitrogen atom from NH_4^+ and 1 nitrogen atom from NO_2^- is required (HNO_2 almost negligible at these conditions) to produce one N_2 molecule. Furthermore, it also explains why the Abel reaction is increasing in reactivity with lower pH. With decreasing pH the ratio of NO_2^- to HNO_2 (Fig. 2-10) is

changing and increasing the production of HNO_2. Therefore HNO_2 is not becoming the limiting factor in that equation at that time.

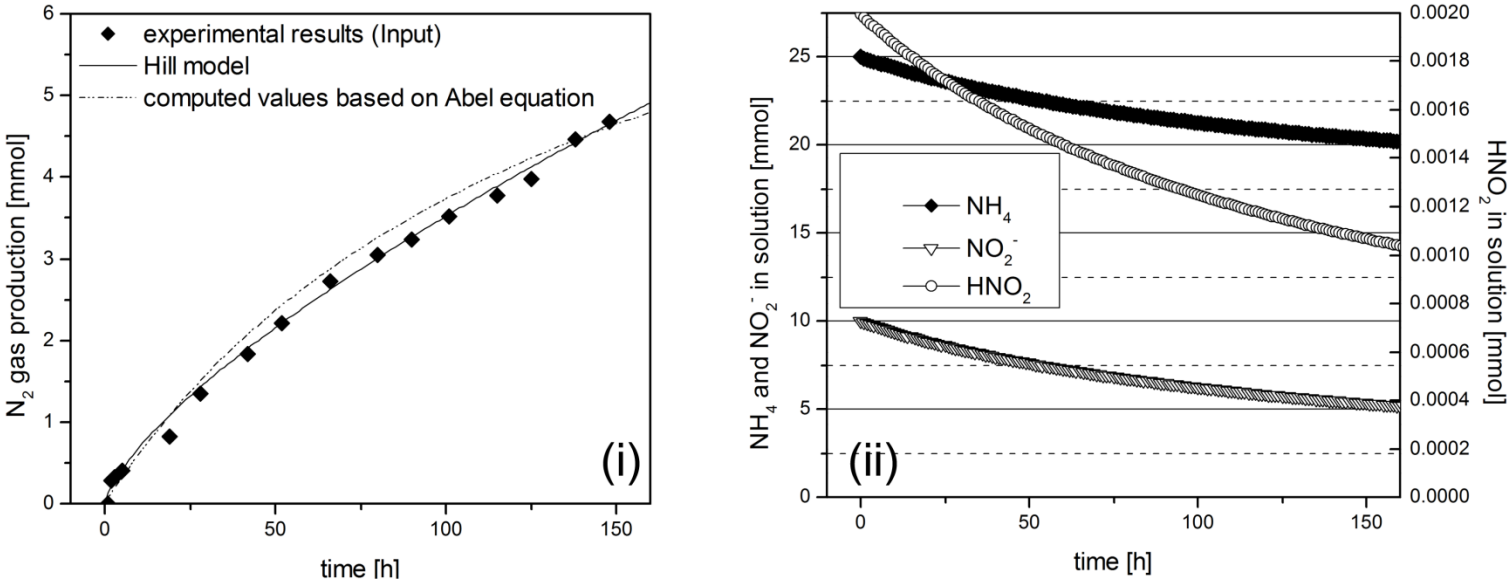

Fig. 2-11: (i) presents results observed during experiment H (no clinoptilolite 10 mL containing 25 mmol NH_4Cl and 10 mmol NO_2^- at 22°C), compared to the Hill model [105] and computed values based on the Abel equation (Equation 2-2) (ii) computed change in concentration of NH_4^+, NO_2^- and HNO_2 based on the Abel equation (Equation 2-2)

2.4 Conclusion

- Initial NH_4^+ concentration per gram clinoptilolite affects the amount adsorbed onto the zeolite but also the concentration of NH_4^+ in solution
- Reaction between NH_4^+ and NO_2 to produce N_2 can occur at room temperature (and below), and is catalysed by clinoptilolite
- Depending on the amount of clinoptilolite, temperature and pH the reaction is up to 41 times faster and more N_2 was produced than without clinoptilolite

2.5 Outlook

- The use of clinoptilolite as a biofilter media is recommended to (a) attach microorganisms and (b) as a catalyst for reaction between ammonia and nitrite
- Nitrifying bacteria attached to the clinoptilolite will utilise the adsorbed ammonia and convert ammonium present in the solution to convert it to nitrite. This conversion is limited by the high concentration of ammonium and will likely stop at the nitrite stage [119]
- Excessive concentrations of ammonium and nitrite can inhibit this reaction and therefore washing away excess ammonium and nitrite will prevent this inhibition and at the same time allow accumulated ammonium and nitrite to react to produce nitrogen gas catalysed by clinoptilolite
- The development of a moisture control system with the following properties is recommended [120]:
    - Moisture storage in filter

- Moisture recirculation and thereby backwashing compounds from top to bottom
  - Low FA and FNA concentrations in top = biological active area
  - High concentrations in bottom = chemical reaction possible

The use of such a filter design would also enable online monitoring of inlet and exit gases.

A novel way of removing ammonia: Biofilter design and development

Sebastian Vitzthum von Eckstaedt, Goen Ho, Wipa Charles, Ralf Cord-Ruwisch

Abstract

The design and development of a biofilter for the complete conversion of ammonia in gaseous waste stream to nitrogen is described in this paper. The design is based on the use of a zeolite (clinoptilolite) for the adsorption of ammonia and its oxidation to nitrite by a bacterial biofilm on the surfaces of the clinoptilolite. Moisture control is a key aspect of the design. Moisture from the gas stream condenses when leaving from the biofilter outlet and is returned to the biofilter as reflux of pure water. The water maintains a moist environment for the bacteria. It also washes down nitrite and excess ammonia to the base of the biofilter, concentrating these compounds and enabling the direct reaction between ammonia and nitrite to nitrogen gas catalysed by the clinoptilolite. Management of moisture enables balance between evaporation and condensation resulting in a non leachate system.

Keywords: biofilter, ammonia removal, clinoptilolite, moisture control, reflux

3.1 Introduction

All microorganisms need water, e.g. for nutrient transfer and mobility which requires a moist conditions in a biofilter [121]. Commonly used laboratory scale gas biofilter systems are constructed in a similar manner. Almost all filter systems have a water supply on top of the biofilter [103, 122]. Differences occur depending whether fresh water/ nutrient solution is introduced [123] or whether the water is recycled [50]. The accumulated water (leachate) from the bottom is reintroduced to the top (recycling) of the biofilter and causes a uniform filter bed [50] giving no room for the development of different microenvironments with unique capabilities. Furthermore, reintroducing the water-dissolved pollutants on top of the biofilter, leads to an increased risk of incomplete treatment and discharge. Studies reveal that leachate production is often a common problem of conventional biofilters [103, 123, 124]. Leachate contains accumulated water dissolvable pollutants (e.g. NH_3) and their degraded compounds (e.g. NO_2^-, NO_3^-). Leachate needs further treatment prior to disposal, which leads to questioning the efficiency of biofiltration [2, 103].

It is common to utilize organic packing as biofilter bed material. The organic packing has the advantage of providing additional nutrient source for the growth microorganisms [103]. The disadvantage however, is the tendency of organic materials to decompose which causes the filter bed to collapse resulting in inefficiency or eventual failure. Therefore, the application of non-biodegradable biofilter material such as zeolite promises better and long term sustainable biofilter performance. Zeolites are widely occurring inert mineral with a large specific surface area for growing microorganisms [101, 102]. Zeolites have

desired adsorption and ion exchange capabilities [125] and a great potential to be used as catalyst for the chemical reaction of ammonia and nitrite to nitrogen gas [69, 88, 126] .

The microbial oxidation of ammonia to nitrite is well known [127-129]. In the past it was shown to be difficult to provide the conditions for the subsequent reaction of ammonia and/ or nitrite to form nitrogen preventing inhibition and therefore failure of the system. Anaerobic Ammonium Oxidation (ANAMMOX) is a microbial process in which ammonium is oxidized to nitrogen gas using nitrite as the electron acceptor [130]. The slow microbial growth rate [131] and the fact that the process only occurs under strict anaerobic conditions [130-134] are the major obstacles for ANAMMOX process implementation [135]. Other processes such as denitrification [136] or shortcut biological nitrogen removal (SBNR) [137] also require conditions (anoxic, anaerobic) different to ammonium oxidation. Therefore the separation (temporal or spatial) of ammonium oxidation and the subsequent denitrification process is required. Contrary to biological treatments, the spontaneous chemical reaction between ammonia and nitrite to nitrogen gas has also been established [65, 66, 138] but so far has never been combined with biofiltration. Although chemical reactions are generally faster than microbially mediated biochemical reactions, the required high concentrations of ammonium and nitrite cause inhibition of the biological ammonium oxidation, limiting the application of this technique in the past [119].

This chapter describes the novel design concept to achieve moisture control, zero leachate production leading to a gradual compound distribution favouring microbial oxidation of ammonia to nitrite and enabling subsequent chemical

reaction between ammonia and nitrite to nitrogen gas in a single biofilter and subsequent implementation.

3.2 Design concept

We propose the application of the reflux mechanism to biofiltration, creating the required environment for simultaneous biological and chemical treatment in one system. The reflux mechanism is based on temperature differences between biofilter inlet and outlet, causing water to evaporate at the biofilter bottom and to condense at the top. Due to this condensation cycle, minimal amount of water is required for the process. This mechanism is well known from applications to crystallogenetic adsorbents [139], COD- analysis [104] and extraction chemistry [140, 141].

3.2.1 Concept of the reflux process

The process of condensation of vapours and the return of this condensate to the system from which it originated is widely accepted as reflux technique. Evaporation of water at the biofilter inlet (biofilter bottom) occurs by controlling the moisture content and temperature of the gas stream entering the biofilter to below the conditions at which the biofilter is operated. An installed cooling device on top of the filter system causes water condensation and reintroduction of pure water to the system. The water percolation through the biofilter prevents the filter from drying out, and a washdown of accumulated pollutants and metabolites is achieved. Temperatures and corresponding water content can be calculated as described below.

Application of the reflux technique to the biofiltration concept would reduce the concentration of pollutant in the top sections and increase concentration in the bottom section of the biofilter system, thereby creating a concentration gradient of the pollutant throughout the filter. This gradient allows biological activity in the top where concentrations of ammonium, nitrite and nitrate are reduced and chemical reaction in the bottom section where concentrations of the mentioned N species are increased.

3.2.1.1 FA INHIBITION OF AMMONIUM OXIDISING BACTERIA *(NITROSOMONAS)*

Conditions amenable for bacterial growth in the upper region of the filter bed are crucial for the success of this biofilter. The inhibition of ammonium oxidising bacteria *(Nitrosomonas)* is triggered at FA concentration of 0.06 – 0.41 mM NH_3 (0.83 – 5.76 mg NH_3 N L^{-1}) [142-146] or above 1.14 mM NH_3 (16 mg NH_3 N L^{-1}) [119]. The range of inhibition in the literature varies due to different environmental conditions (activated sludge or biofilm [145]) or different microbial metabolic pathways i.e. anabolism (construct molecules from smaller units) and catabolism (break down molecules into smaller units) [119]. In addition, the following further reasons for the range of inhibition can be mentioned:

- Determination of an inhibition threshold or (only) a decrease in ammonium oxidation rate [147] (not well described in literature)
- The mentioned inhibition range can also be caused by using pure, enriched cultures or mixed (wild) culture [148]
- Reactor types and operation conditions have also an influence on the inhibition concentration: Plug flow, shortcut biological nitrogen removal

(SBNR), sequencing batch reactor (SBR), single reactor sigh activity ammonium removal over nitrite (SHANON), mixing liquid) [148]

- pH and temperature also influence the range of inhibition
- Different analytical methods (microbioal (Q-PCR) or chemical determination of changes in metabolite and source concentration)

In addition it needs to be noted that changes in concentration of ammonium and its metabolites (nitrite and nitrate) can also be cause by simultaneously occurring chemical reactions (see chapter 2.1). That chemical reaction make it more difficult to determine whether the biological reaction is inhibited by high FA concentrations (anabolism/ catabolism measurements).

3.2.1.2 FA INHIBITION OF NITRITE OXIDISING BACTERIA (*NITROBACTER)*

These above mentioned reasons also affect the ability to determine a narrow inhibition range for nitrite oxidising bacteria (*Nitrobacter)*. Studies show that *Nitrobacter* inhibition occurs at a FA concentration of 8.82 mM NH_3 (124 mg NH_3 N L^{-1}) [146] or 0.43 – 0.64 mM NH_3 (6 – 9 mg NH_3 N L^{-1}) [119].

3.2.1.3 FNA INHIBITION OF AMMONIUM OXIDISING BACTERIA *(NITROSOMONAS) AND* NITRITE OXIDISING BACTERIA (*NITROBACTER)*

Toxic effects on microorganism cells may also be exerted by the nitrite un-dissociated fraction nitrous acid (HNO_2) or so called free nitrous acid (FNA) [149]. The proposed inhibition mechanism for FNA toxicity is based on the presumption that FNA causes a donation of a proton inside the cell [150]. The donated intracellular proton interferes with the transmembrane pH gradient required for ATP synthesis [151].

Nitrosomonas are reported to be inhibited at FNA concentrations of 28.57 - 45 µM HNO_2 (0.4 - 0.63 mg HNO_2 N L^{-1}) whereas *Nitrobacter* are more sensitive to FNA and are inhibited at 1.45 µM HNO_2 (0.02 mg HNO_2 N L^{-1}) [119]. Inhibition of either species would cause a reduction of biofilter performance and finally lead to biofilter failure. These mechanisms and inhibition thresholds need to be considered because the proposed biofilter system requires nitrite production and therefore FA and FNA control is essential.

3.2.1.4 FA AND FNA INHIBITION SUMMARY

The above mentioned FA and FNA concentration leading to *Nitrosomonas* and or *Nitrobacter* inhibition are summarized in Table 3-1. As described above the ratios of FA to ammonium and FNA to nitrite are highly depended on temperature and pH (Fig. 2-10). Fig. 3-1 shows the results for three temperatures (20 °C, 30 °C, 40 °C) at a pH range of 6.8 to 8.2. These temperature and pH ranges were chosen based on literature reported pH optimum for *Nitrosomonas* of 7.8 – 8.0 and *Nitrobacter* of 7.3 – 7.5 [114-116] and optimum nitrifying performance at a temperature of 20 – 30 °C [152] or 35 - 38 °C [153].

Table 3-2 summarises the results of batch experiments for three pH (7.0, 7.5, 8.0) and three temperatures (20 °C, 25 °C, 30 °C). The presented NH_x (where NH_x stands for the total NH_3 and NH_4^+) results show a varying range from 0.44 – 288.2 mM making the determination of an exact inhibition range impossible. It is uncertain if an inhibition range is reached before the ion exchange of multivalent cations will begin.

Table 3-1: FA and FNA concentration causing inhibition of *Nitrosomonas* and or *Nitrobacter*

N species	bacteria	inhibition concentrations		references
FA				J. Surmacz-Górska et al. [142]
				U. Abeling et al. [143]
	Nitrosomonas	0.06 - 0.41 mM NH_3	0.83 - 5.76 mg NH_3 N L^{-1}	D. Kim et al. [144]
				F. Fdz-Polanco et al. [145]
				A. Anthonisen et al. [146]
	Nitrobacter	> 1.14 mM NH_3	16 mg NH_3 N L^{-1}	V. Vadivelu et al. [119]
		8.82 mM NH_3	124 mg NH_3 N L^{-1}	A. Anthonisen et al. [146]
		0.43 - mM 0.64 NH_3	6 - 9 mg NH_3 N L^{-1}	V. Vadivelu et al. [119]
FNA	Nitrosomonas	28.57 - 45 µM HNO_2	0.4 - 0.63 mg HNO_2 N L^{-1}	V. Vadivelu et al. [119]
	Nitrobacter	1.45 µM HNO_2	0.02 mg HNO_2 N L^{-1}	V. Vadivelu et al. [119]

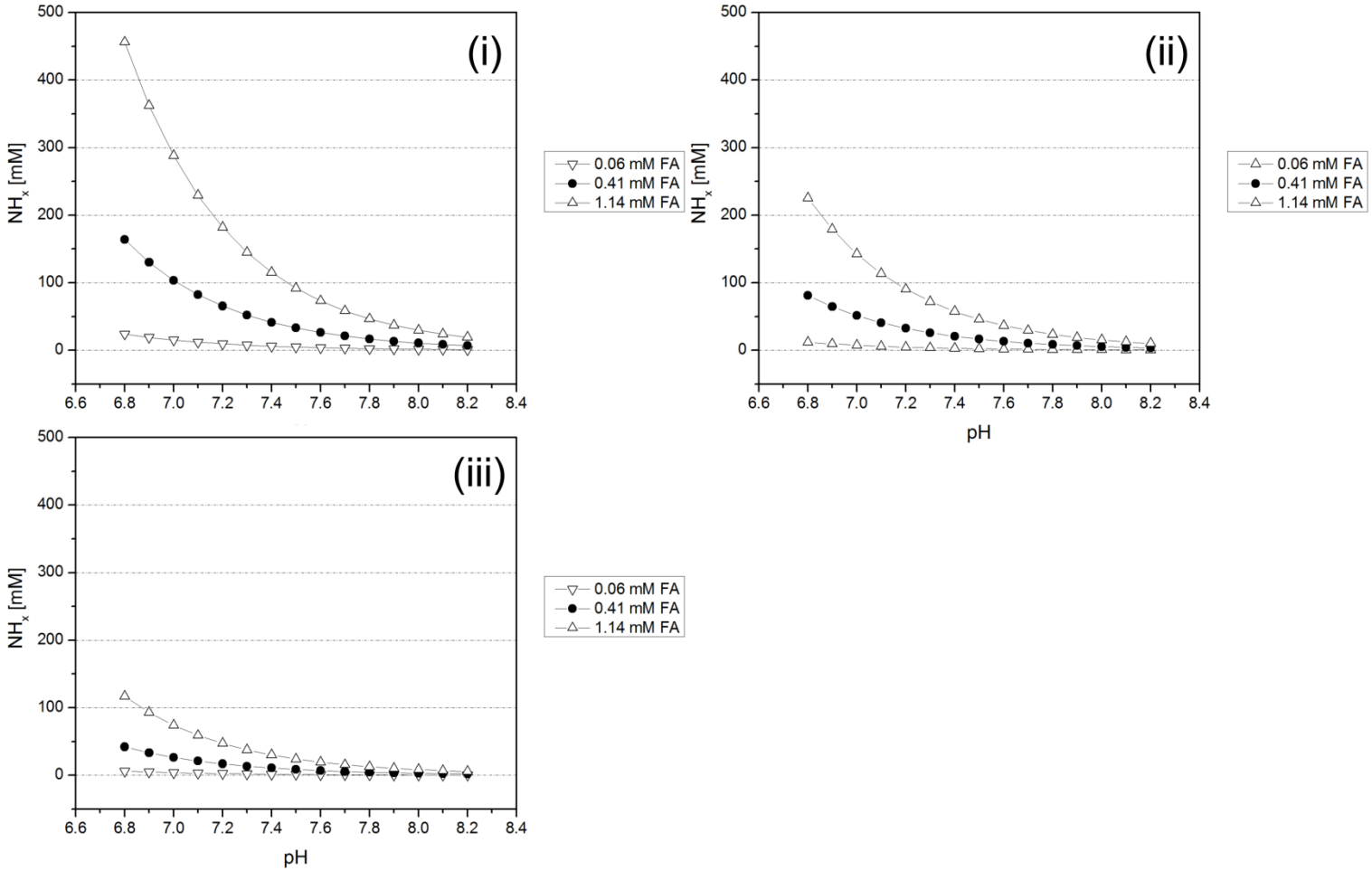

Fig. 3-1: *Nitrosomonas* inhibition ranges of 0.06 - 0.41 mM FA and 1.14mM plotted over a pH range of 6.8 – 8.2 for three temperatures (i) = 20 °C, (ii) = 25 °C and (iii) = 30 °C

Table 3-2: Required NH_x (total NH_3 and NH_4^+) concentrations at pH 7.0, 7.5 and 8.0 as well as 20 °C, 30 °C and 40 °C to realize 0.06 mM, 0.41 mM and 1.14 mM FA concentrations

		example FA [mM] concentrations		
pH	temp	0.06	0.41	1.14
	[°C]	required NH_x [mM] to achieve FA concentrations		
	20	15.17	103.64	288.17
7.0	30	7.51	51.31	142.68
	40	3.90	26.67	74.16
	20	4.84	33.05	91.91
7.5	30	2.42	16.51	45.90
	40	1.28	8.71	24.23
	20	1.57	10.73	29.84
8.0	30	0.80	5.50	15.29
	40	0.44	3.04	8.44

3.2.2 CONCEPT OF MOISTURE CONTROL

A moisture controlled filter system was developed on the basis of gas stream humidification and condensation (Fig. 3-6). It consists of an inlet dryer before the biofilter and a condenser above the biofilter.

The vapour pressure of air over water is saturated when the number of water molecules condensing equals the number evaporating from the surface of water [154]. The saturation vapour pressure at a certain temperature can be calculated according to Tentens [155] to determine the water content for a saturated gas in ps [Pa] (Equation 3-1). Equation 3-1 shows the saturation vapour pressure (610.78 [Pa]) at the temperature of 273.16 [K] multiplied by the exponential temperature ($\mathrm{T}\,[°\mathrm{C}]$) constant term and the vapour pressure of water at this temperature as 17.2694 mm Hg.

$$ps = 610.78 * \exp(T/T + 238.3) * 17.2694$$ **Equation 3-1**

Equation 3-2 allows the calculation of the water content ($wc\ [kg\ m^{-3}]$) at a certain saturation vapor pressure [156]. The molar mass of water (M = 0.018 $[kg\ mol^{-1}]$) divided by the gas constant (R = 8.314 $[J\ (K\ mol)^{-1}]$) multiplied by the ratio of saturation vapor pressure and temperature ($T\ [°C]$).

$$wc = M/R * ps/T + 273.16$$ **Equation 3-2**

Employing Equation 3-3, the evaporated or condensated water content $\Delta_{wc}\ [kg\ m^{-3}]$ between two temperatures ($T1\ and\ T2\ [°C]$) can be calculated. A positive Δ_{wc} indicates condensation; a negative Δ_{wc} implies evaporation.

$$\Delta_{wc} = wc_{T1} - wc_{T2}$$ **Equation 3-3**

The above reported mechanisms lead to the design and development of an inlet dryer (Fig. 3-6) which adjusts the moisture content of the gas stream entering the biofilter. An installed outlet dryer (Fig. 3-6) maintained the water content within the biofilter and prevented the escape of water. The outlet dryer operated on the same principle as the inlet dryer.

3.3 Implementation of the novel design concept

3.3.1 Overview

Based on the design concept, the following biofilter system was constructed. The biofilter control system consisted of an inlet dryer, a biofilter column rig, an outlet dryer and an online gas analyser (Fig. 3-2 and Fig. 3-4). The in-house

compressed air supply was used as a carrier gas for the dilution of a 1 % NH_3 in air (gas cylinder) to 50 ppm_v (2.05 µmol L^{-1} min^{-1}). All gases were transported within 0.5 mm (i.D.) Tygon tubing (antibacterial, low adsorption rate, high chemical resistance [157, 158]). Required parts were mounted to a metal frame to hold the biofilter columns, condenser, manifolds, solenoid valves, analogue flow meter (150 mm long, equipped with 16-turn high precision needle valves (4x 0-18.7 mL min^{-1} and 4x 16737 mL min^{-1}) and other electronic equipment (such as pH signal amplifier, thermocouples and wire as shown in Fig. 3-4.

The biofilter control system was capable of operating up to four biofilter columns simultaneously. It is possible to add and remove biofilter columns at any given time by changing setting in the control program. The following description is on the operation with one single column. Additional but not presented (see appendix DVD's) experiments as listed below were conducted with the three extra ports on the biofilter control system:

- Gathering information with an rotating drum setup,
- Breakthrough experiments with wet, dry and coated clinoptilolite,
- Incubation and breading microorganisms onto the clinoptililite, and
- Experiments with one and two fifth of the complete filter volume (see layer formation described in chapter 4.2.5 and 4.3)

3.3.2 BIOFILTER COLUMN

An upflow biofilter column was constructed as shown in Fig. 3-5. A stainless steel mesh installed within the biofilter provided support to hold up to 1 L filter material and simultaneously provided 300 mL homogenization (mixing) space at the bottom. A pH probe was installed approximately 2.5 cm above the stainless

steel mesh and connected to a data logging module (see ADAM modules inchapter 3.3.5) for automated pH data acquisition. The biofilter column was operated at room temperature (21 ± 1 °C).

Clinoptilolite (Zeolite Australia PTY LTD) was used as a non-degradable filter media sieved to 2.4 – 4.0 mm. Prior to use the clinoptilolite was incubated at a composting facility (Southern Metropolitan Regional Council) for a period of 6 months. After that period, the clinoptilolite was harvested and carefully washed to clean the filter material from accumulated dust and organic material. One litre drained but moist clinoptilolite was placed within the biofilter column.

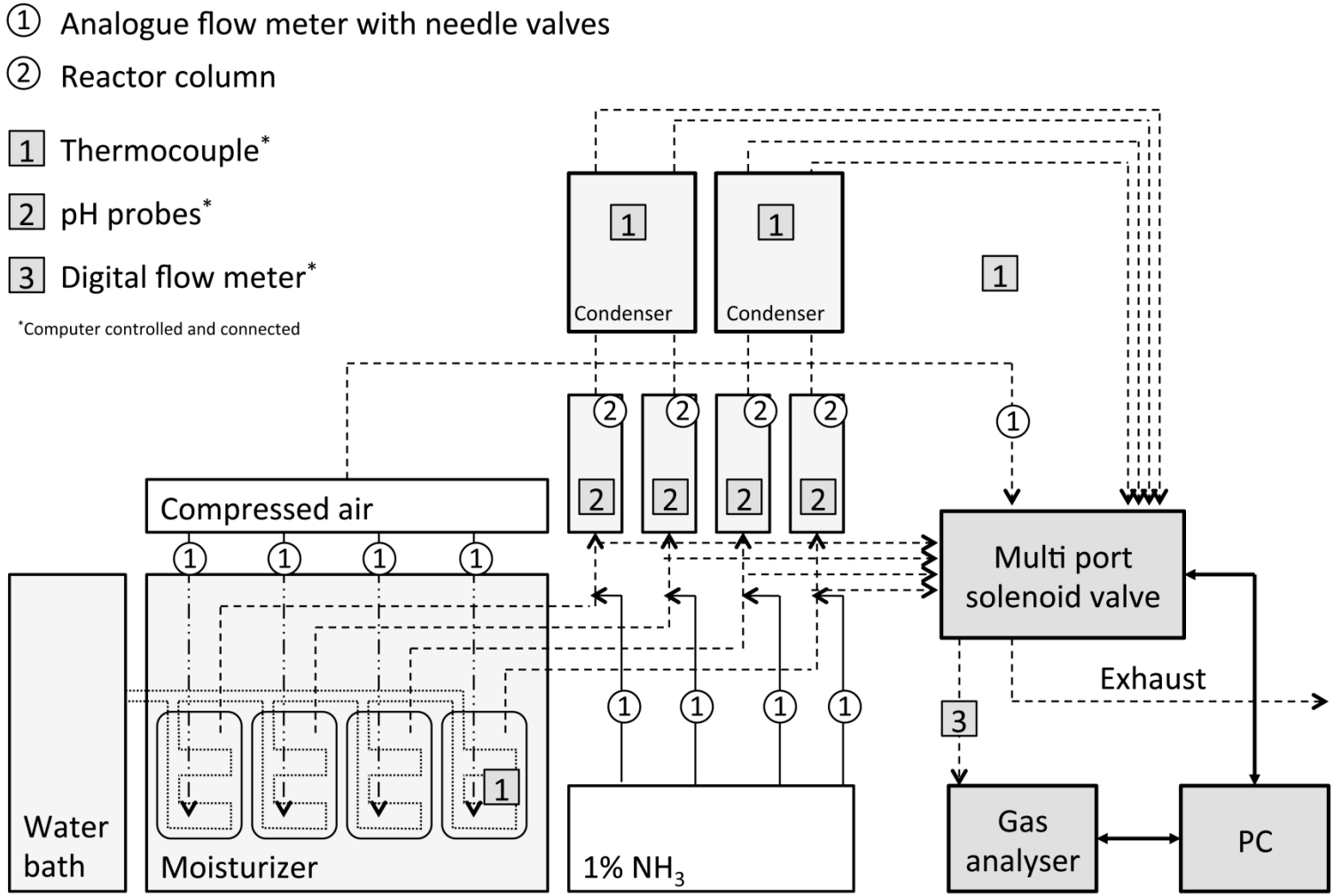

Fig. 3-2: Flow chart of the biofilter system (operating four individual biofilter columns)

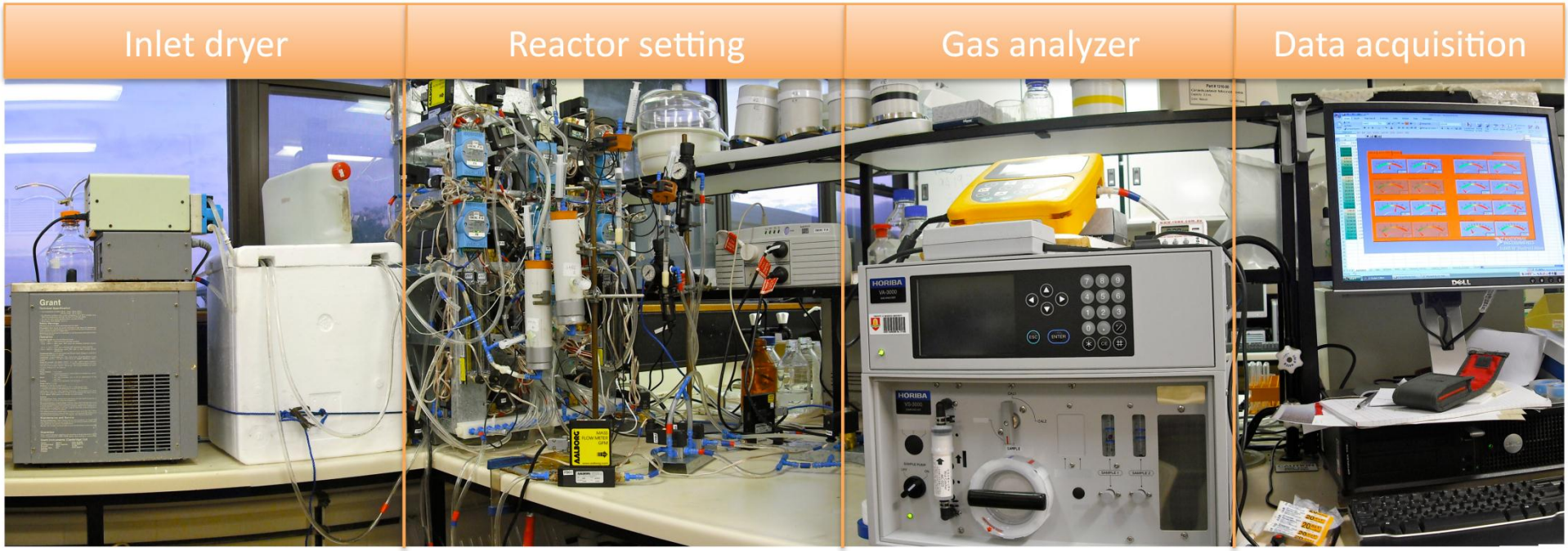

Fig. 3-3: Equipment overview

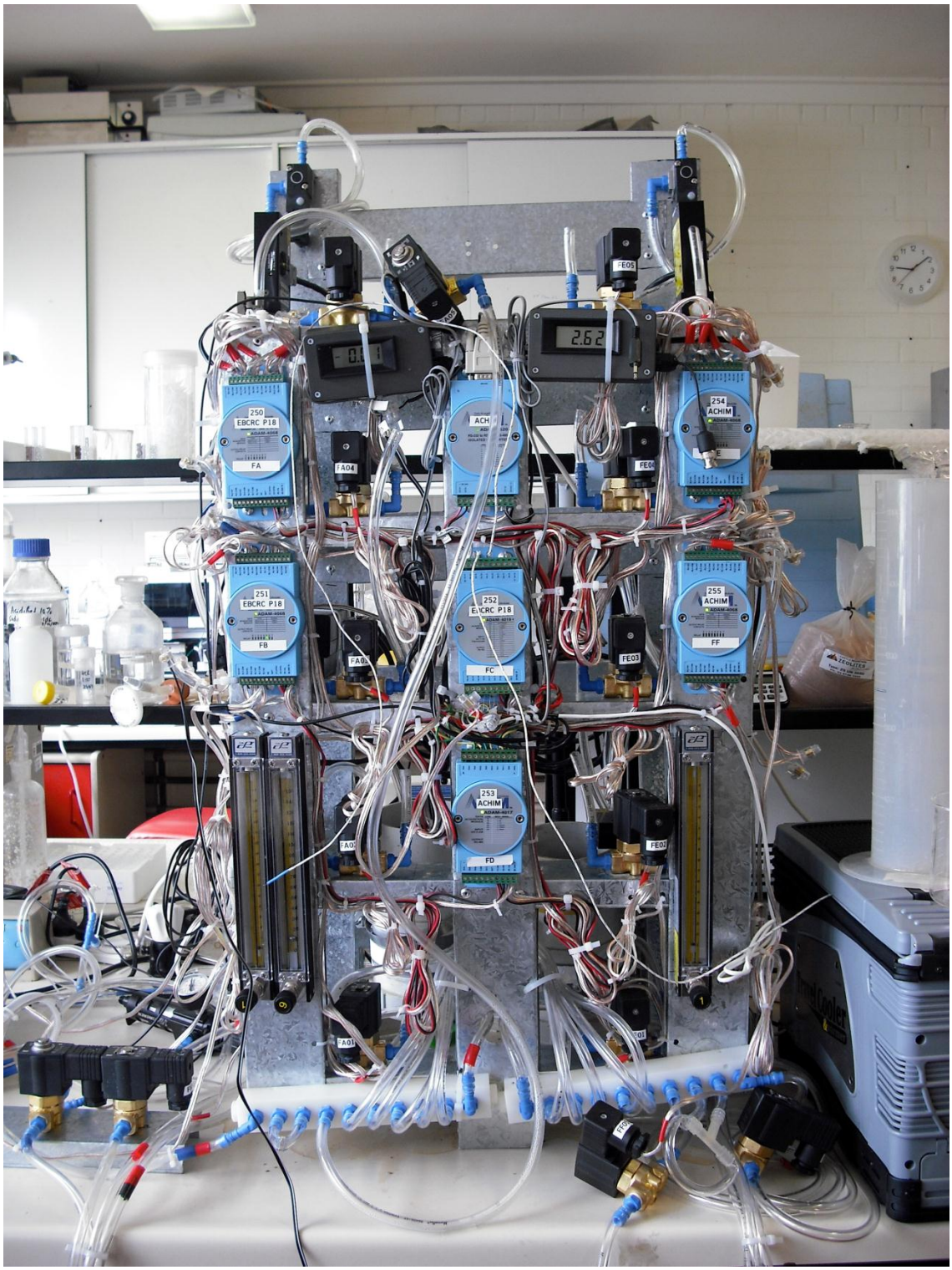

Fig. 3-4: The Modular Adam Research Visual INstrument (MARVIN) biofilter setup

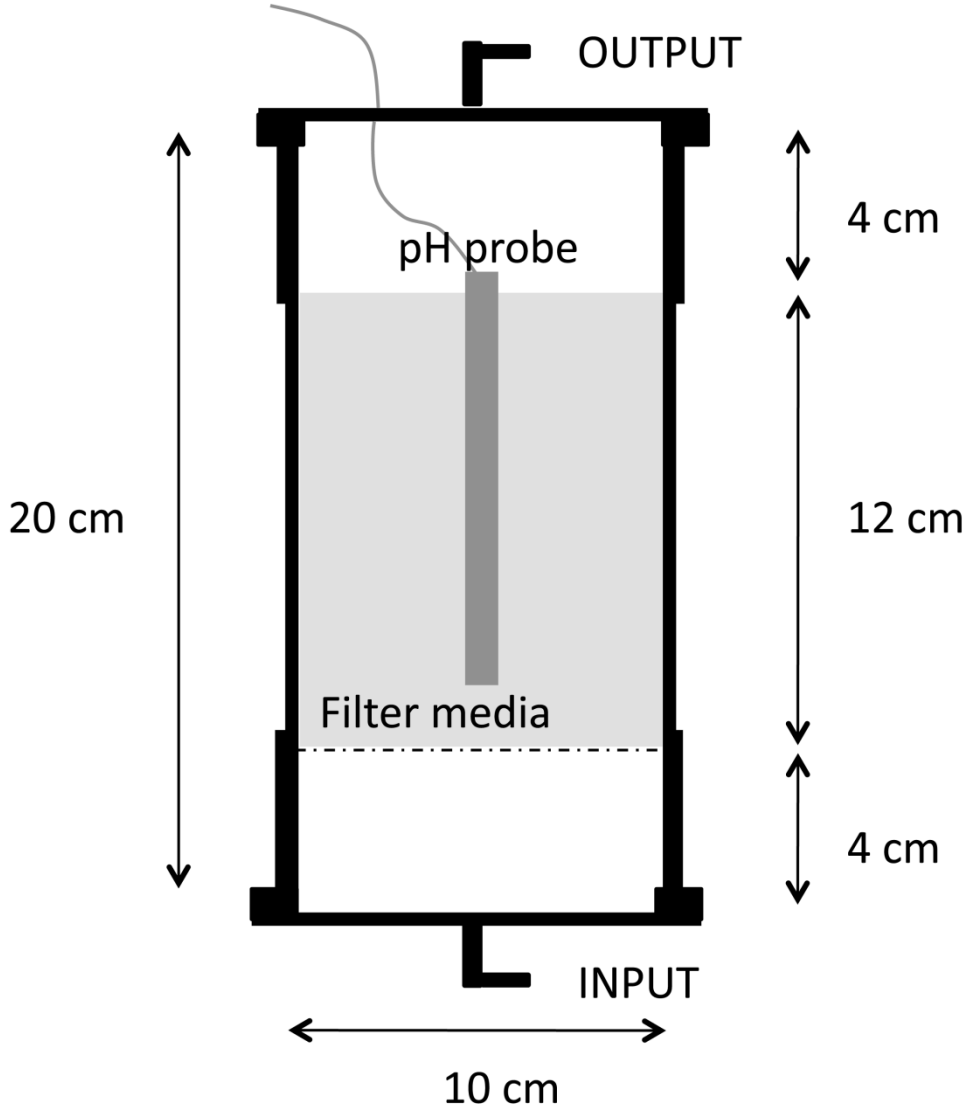

Fig. 3-5: Schematic of the biofilter column design

3.3.3 MOISTURE CONTROL

As mentioned previously, moisture control is the essence of the novelty in the development of the biofilter and intended to be an outcome of our research work.

3.3.3.1 INLET DRYER

The inlet air (1 L min^{-1}) was introduced into the moisturizer vessel at the bottom of a chilled (9 °C) water reservoir (Fig. 3-6). The moisturizer vessel contained a maximum of 4.5 litre of deionised water (plus approximately 1 litre headspace). At the top of the vessel, ports were installed for a raw gas inlet (in house gas supply) and a moisturised gas outlet (dust free). The water level in the vessel was checked using an adjustable level gauge on top of the vessel. The temperature within the vessel was maintained by a heat exchanger, which was connected to a water bath capable of cooling and heating. A thermocouple within the moisturizer was connected to a PC for data acquisition and visualization of the temperature.

The inlet dryer setup permitted trapping of dust particles and contaminants from the gas stream (e.g. oil) in the water. The clean and cool moist gas left the vessel at the top in a Tygon tube that was exposed to room temperature (21.6 °C). A known amount of 1 % NH_3 in air (gas cylinder) was introduced to the gas stream before the biofilter inlet using a t-piece in order to achieve 50 ppm_v NH_3. In that way the risk of adsorption or leaching through the tubing was minimized. Due to the temperature difference between the introduced gas stream from the moisturiser vessel (chilled and saturated) and the biofilter

column (see Fig. 3-6) (operated at room temperature of 21 ± 1 °C), evaporation in the bottom layer occurred.

The evaporation of water has additional effects:

- Compound accumulation in the bottom layer due to water evaporation,
- Water distribution to layers above the bottom layer.

A water content of 9 mg L^{-1} can be calculated under the assumption that the gas leaving the moisturizer was fully saturated at 9 °C. When this gas stream entered a water phase at a higher temperature the water content per litre of gas will increase due to evaporation. Under the assumption that the gas reaches saturation during passage through the moist biofilter (operated at 21 °C) an increase in water content of 9.5 mg L^{-1} to a total 18.5 mg L^{-1} was calculated. At a flow rate of 1 L min^{-1} a total discharge of 13.75 mL d^{-1} can be expected. Additional measurements of the biofilter moisture content showed a total water content of 250 mL L^{-1} biofilter material. Further calculations reveal that the biofilter would theoretically be dried out after 18 days unless the water is replenished.

3.3.3.2 OUTLET DRYER

To prevent water loss, a condenser was installed on top of the biofilter column and aligned with the outlet of each biofilter. A Tygon tube was vertically installed within the condenser which was operated at the same temperature (9 °C) as the inlet dryer (see Fig. 3-6). By cooling the gas in the PVC tube the moisture condensed (see Fig. 3-6) on the tubing wall and dripped back into the biofilter. The water inventory of the biofilter remained. The percolation of the clean

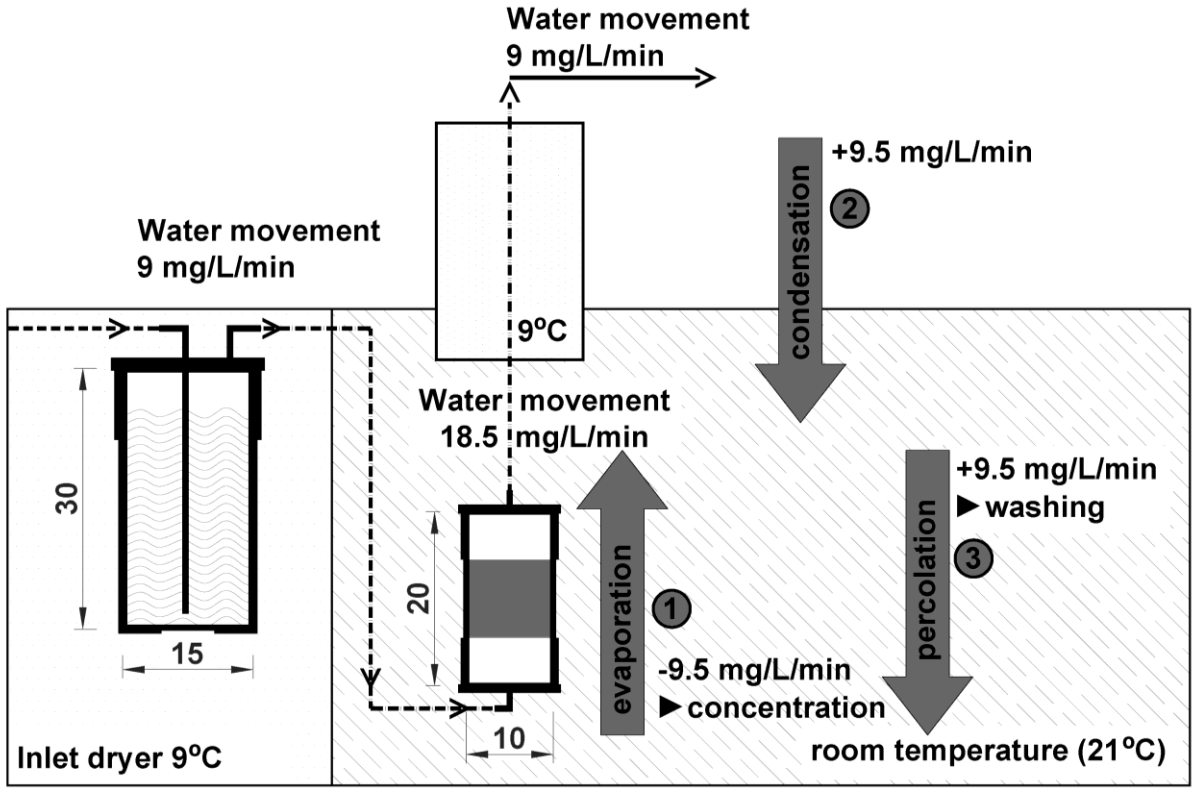

Fig. 3-6: Schematic diagram of gas flow consisting of the three temperature zones. (1) Evaporation of water from the biofilter due to introducing gas containing lower water content. This causes the gas to gain moisture of 9.5 mg L^{-1} min^{-1} (2) Condensation of moisture in the gas by cooling the gas to lower temperature with the result that 9.5 mg L^{-1} min^{-1} condenses and is reintroduced into the biofilter and (3) 9.5 mg L^{-1} min^{-1} water percolates and thereby washing accumulated compounds to the bottom where the process begins again.

condensate through the biofilter allowed wash-down of soluble compounds accumulated over the depth of the biofilter. These compounds accumulated at the bottom where due to continuous introduction of dry gas (saturated at lower temperatures) the reflux process starts again and cause an additive increase in accumulated compound concentration.

Another advantage of installing an outlet dryer is a dry gas. Most available gas analysers are sensitive to moisture in the gas stream making long-term online monitoring impossible. Online monitoring however, is highly beneficial, allowing the automated data acquisition for collecting complete datasets for accurate mass balance calculations. A dry gas stream can be obtained by various physical or chemical methods e.g. activated carbon [27], silica gel [28, 29], potassium hydroxide (KOH) or pellets [30]. But the use of such adsorbents has the disadvantage of adsorbing compounds of interest and requiring additional measurements of the adsorbed compounds [31-35]. The installation of a condenser above the biofilter resulted in dry enough gas so that online continuous monitoring could be employed.

3.3.4 GAS ANALYSER

An HORIBA VA/ VS 3000 multigas analyser (Horiba International Corporation) equipped with nitric oxide (NO_x), nitrogen dioxide (N_2O) and NH_3 sensors was used for gas analysis. The principle measurement of the HORIBA multigas analyser are non-dispersive infrared (NDIR) sensors [159]. Each individual sensor provided a 4 - 20 mA signal accessible through an analogue connector at the back of the analyzer. The accuracies of the measurements were checked regularly with standard gas mixes (Detectagas 100 ppm NH_3 in nitrogen,

Detectagas 100 ppm NO_x in nitrogen and Detectagas 100 ppm N_2O in nitrogen provided by BOC Scientific Centre).

3.3.5 COMPUTER CONTROL

The hardware and software setup descried throughout the thesis was developed and designed by the author. The Modular Adam Research Visual INstrument (MARVIN) was developed to fulfil the following tasks:

1. Automation
    a. Online monitoring
    b. Solenoid valve control
    c. Automated gas sampling and analysis
    d. Data processing and real time visualization
    e. Run and execute multiple or single experiments under different conditions (filter volume, filter load, concentrations. Flow rate, duration of experiment simultaneously
2. Capability to control, interact and schedule via internet and any internet connected device globally

All accessories (e.g. sensors and solenoid valves) were controlled and connected to a computer by an ADAM 4520 interface module (Advantech's ADAM). ADAM modules are sensor-to-computer devices with multiple types and ranges of analogue input (ADAM 4017 and 4019+) or relay outlets (ADAM 4068). These modules and accessories (e.g. values and condensers) were operated at 12 VDC. The status and the analogue input values of each individual ADAM module was updated every 150 ms which allows high-resolution data acquisition.

Two analogue modules (ADAM 4017 and 4019+) were employed to record the voltage and current of the HORIBA multi gas analyser (NH_3, N_2O and NO_x), four thermocouples (wire type K thermocouple, www.jaycar.com.au), four digital flow meters (12 VDC 0-20 sL min^{-1} Cole-Parmer) and the pH probes (Fig. 3-3).

With each of the four connected relay modules (ADAM 4068) it was possible to control up to eight On/Off low-power switches. For example, direct operated two port open/ closed valves (SMC Corporation, VX22) and direct operated three port solenoid valves (SMC Corporation, VX32), were controlled by the ADAM 4068 modules to control the gas flow.

3.3.5.1 HARDWARE

All electronic devices (sensors and solenoid valves) were connected to a computer by a series of seven Advantech's ADAM modules of the 4000 series [160] as shown in Fig. 3-7.

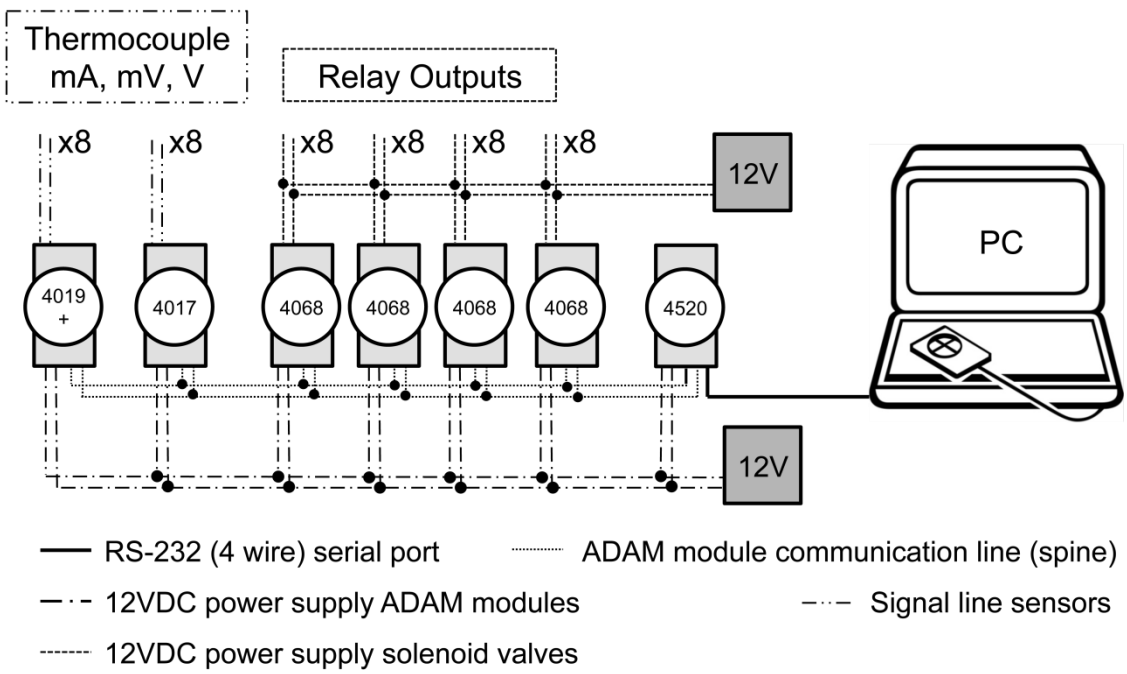

Fig. 3-7: Computer control, ADAM module wiring and connections

These ADAM modules are sensors to computer interfaces, which are remotely controlled through a set of commands issued in American Standard Code for Information Interchange (ASCII) format and transmitted in RS-485 protocol. A computer can only understand numbers, so an ASCII code is the numerical representation of a character. The RS-485 network allows the connection of up to 256 ADAM modules with a two-wired connection with a maximum communication distance of 1200 m. The host computer is connected to a RS-485 network via an isolated RS-232 to RS-422/ 485 converter module (ADAM 4520).

The modules are designed for standard industrial unregulated 24 VDC power supply but accept any power unit that supplies power within the range of +10 to +30 VDC. In the setup presented in this thesis all modules were powered by an external 12 VDC power supply. The low power supply allowed the author the save adjustments and changes of the setup without the help of a trained electrician.

Four relay output modules (ADAM 4068) were connected to the ADAM 4520 converter. Each module provides eight relay channels allowing the ON/ OFF control of up to 32 low-power switches such as solenoid valves. The solenoid valves used in this study were powered with a separate 12 VDC power supply to minimize the risk of interference between the power to operate the modules and activate the solenoid valve.

Furthermore, two eight channel analogue input modules (ADAM 4017 and 4019+) were connected to the setup. The ADAM 4017 is a 16-bit, 8 channel analog input module that provides programmable input ranges on all channels

(Table 3-3). In this study two pH probes and up to 4 digital flow meter [161] were connected to the ADAM 4017 module. The ADAM 4019+ is a universal input module providing the data acquisition of 4 ~ 20 mA and all thermocouple types (Table 3-4). This module was used to acquire the values of 4 thermocouples type K and the voltage outlet of three gas analyser sensors [159].

The voltage, current and temperature are converted within the modules to digital data. When prompted by the host computer, the module sends the data to the host through the standard RS-485 interface.

3.3.5.2 SOFTWARE (LABVIEW)

Labview (short for Laboratory Virtual Instrumentation Engineering Workbench) is a graphical programming language developed and distributed by National Instruments [162] and has the purpose to automate laboratory setups. Labview programs consist of a backend where the actual programming happens and the frontend where information are visualized and the user can also setup and change parameter. A modular constructed Labview program was developed by the author to control all ADAM modules (see section 3.3.5.1) for data acquisition. The modular design of the backend allowed flexible and fast adjustments of the program and the complex program structure remained easy to overview. One module is called sub.vi, e.g. the module operating the timer is called timer.vi. A simplified flow chart of the developed sub.vis is shown in Fig. 3-8.

Table 3-3: Technical Specification of ADAM 4017

Capability	Info
Channel	8
Input Type	mV, V, mA
Input Range	±150 mV, ±500 mV, ±1 V, ±5 V, ±10 V, ±20 mA
Isolation Voltage	3000 VDC
Fault and Over-voltage protection	With stands over-voltage up to ±35 V
Sampling Rate	10 sample/sec (total)
Input Impedance	Voltage: 20 Mol Current: 120r
Accuracy	±0.1% or better
Power Consumption	1.2 W @ 24VDC
I/O Connector Type	10 pin plug-in terminal

Table 3-4: Technical Specification of ADAM 4019+

Capability	Info
Channel	8
Resolution	16 bits
Input Type	V, mV, mA, T/C
Input type and temperature range	V: ±1 V, ±2.5 V, ±5 V , ±10 V mV: ±100 mV , ±500 mV mA: ±20 mA (with 120 Ω resister) 4~20mA (with 120 Ω resister) Thermocouple: J 0 to 760 °C K 0 to 1370 °C T -100 to 400 °C E 0 to 1400 °C R 500 to 1750 °C S 500 to 1750 °C B 500 to 1800 °C
Isolation Voltage	3000 V_{DC}
Sampling Rate	10 samples/sec (total)
Input Impedance	Voltage: 20 MΩ, Current: 120Ω
Accuracy	±0.1% or better
Power Consumption	1.0W @ 24V_{DC}
I/O Connector Type	10 pin plug-in terminal
Burn-out Detection	4~20mA and all thermocouple input

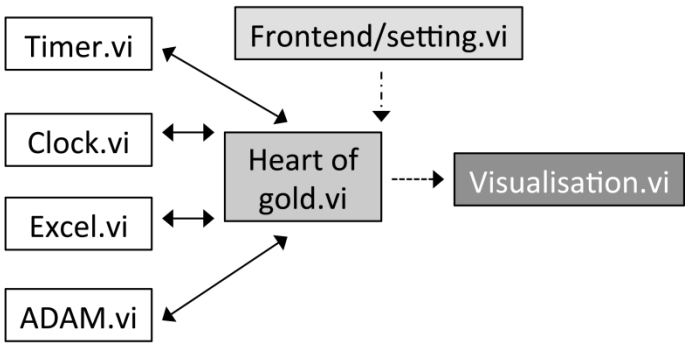

Fig. 3-8: Software modules (subvi's) of the Labview program controlling, monitoring and scheduling MARVIN

Each of the sub.vis operates independently but is activated and provided with necessary parameters from the "Heart of gold" subvi. The Heart of gold subvi controlls all processes beginning with timing, scheduling the gas stream to the analytical instrument, acquiring the values from all sensors, processing the results and finally visualizing and saving them into Microsoft Excel 2007 (Microsoft, Redmond, WA, USA).

The ADAM.vi issued all processes and information required for the communication with the ADAM modules (acquiring data but also switching solenoid valves ON/ OFF). The individual ADAM modules, except ADAM 4520 (described in 3.3.5.1), were identified by the software using a unique hexadecimal address. This two digit hexadecimal value allows addressing up to 256 ADAM modules. For the communication with the ADAM modules a six-digit hexadecimal string containing the address of the module and the command for either gathering the values of the input modules (ADAM 4017 and 4019+) or the syntax to switch the solenoid valve (ADAM 4068). Thereby it can be distinguished between the acquisition of a single data channel, a combination of channels or all channels together. For example: to open (OFF) all relays of the

ADAM 4068 module “00” and to close (ON) only channel 1 the commend “01” need to be send. For the eight channel modules the option of either ON (1) or OFF (0) is possible. Resulting in a total channel ON/ OFF combination for a single ADAM module of 256 (2^8) which can also be written as a two-digit hexadecimal number (00 – FF). For example to have only channel 1 at the ADAM module 255 (FE) closed the circle the #FE0001\r and to close all eight circles #FE00FF\r need to be send. Similar options exist for the acquisition of a single or all analogue values digitalized by the ADAM 4017 and 4019+ modules.

As shown in Table 3-3 and Table 3-4 show that the maximum total sampling rate for each module is 100 msec. To protect the system of an over run (overload) the ADAM.vi’s were updated every 150 msec and visualized the gathered results at the frontend of the program (see below). Within the ADAM subvi the acquired sensor signals (voltage, current and temperature) were converted in real time into scientific unites. Data points were obtained several times per second, the gathered data for the individual experiments were saved into an Excel file only ten times a day. This allowed minimizing the data storage capacity but real-time visualisation.

Before the data could be processed within Excel, a warning dialog box was activated (Fig. 3-9) to avoid conflicts between Labview (which acts in this case as an Excel user) and a possible other user. The activation of the warning dialog box was a part of the Excel subvi as illustrated in Fig. 3-10.

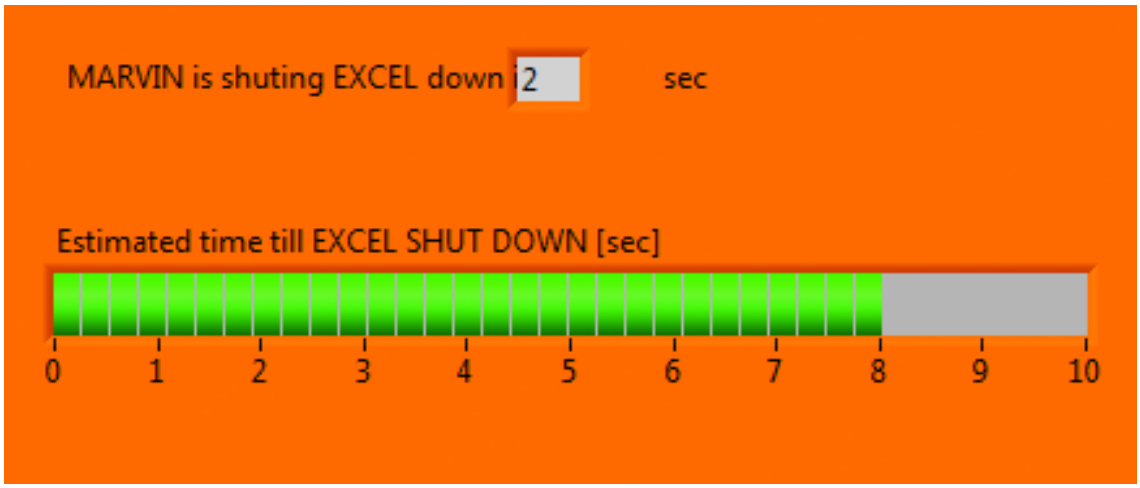

Fig. 3-9: Excel shout down warning

After Labview had taken control over Excel the existence of a file name in a predefined folder was checked (File exist?). That file name was previously generated by the heart of gold subvi based on the analysed sample port of the biofilter system. If the file doesn't exist a new Excel workbook (New Excel) with 6 statistic sheets (average, quartile 1, minimum, median, maximum, quartile 3) including the header was created and saved as a new file (Create & Name). In the statistic sheets, for each sampling event the basic statistic functions for each parameter, are saved automatically in a single Excel row subsequently.

If the file already exists, the file was opened. To determine how many sampling events were already saved in the file the existing sheets were counted (Count Sheets) before a new sheet was created (New Sheet) for each individual sampling event. The new sheet was named after the sampling time (yymmdd_hhmmfs) and the values from the sampling procedure were inserted. Depending upon the number of previous sampling events a new line at the end of the statistic sheets was inserted (New Row), and the functions were

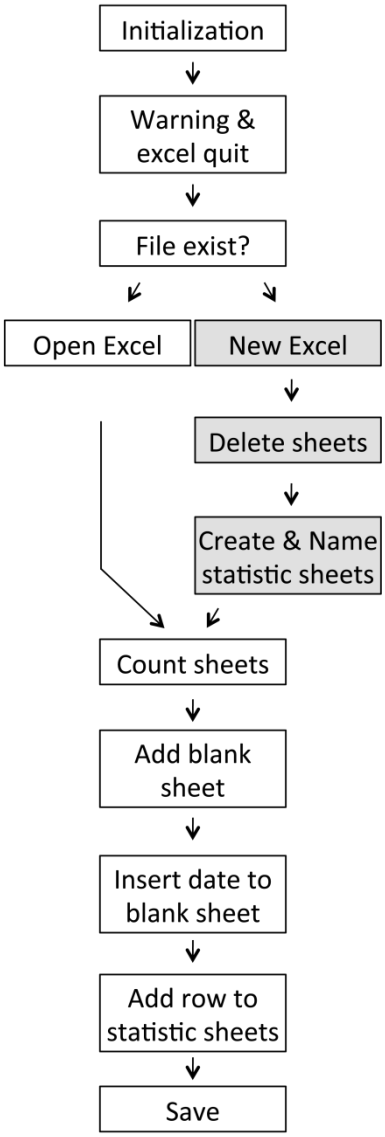

Fig. 3-10: Excel vi construction flow chart

processed. The file was saved (Save), and depending on other settings (not described in here), Excel remained open or was closed automatically.

As mentioned before the Labview programs also consist of the frontend. The frontend of the program developed for this study contained four tabs(settings, Port, Data, Results) as shown in Fig. 3-11 (activated data page).

Fig. 3-11: Frontend MARVIN, visualization off 16 sensor readings

On the data page, sensor information (from 16 sensors) was visualized and presented with the responding units. The setting tab allowed adjustments to timing and frequency of sampling as well as to the path of saving the file. Changes to the setup of ADAM modules can be made on the Port tab and the Results tab showed additional results calculated with the results and values presented on the Data tab.

3.3.6 Preliminary Experiment

The biofilter system was constantly fed with 2.05 µM (50 ppm_v) ammonia (NH_3) in air gas stream with a volume load of 60 L L^{-1} h^{-1} for a period of 300 days. Inlet and outlet gas concentrations (NO_x, N_2O and NH_3) were measured and monitored with the above mentioned setup. The dissociation of NH_3 into water

where it became NH_4^+ as well as the metabolites of the oxidation of NH_4^+ to NO_2^- and NO_3^- were determined by using the following sampling procedure.

3.3.6.1 SAMPLING PROCEDURE

The 1 L biofilter media was manually separated into 200 mL lots (layers) for analysis of the surrounding liquid. Subsamples of 10 g clinoptilolite of each homogenized layer were washed for 1 min in 10 mL deionised water (manually stirring) for further analysis. Eluents were syringe filtered (0.45 µm), frozen (below -20 °C) and stored until analysis. The liquid was analysed for NH_4^+ and other cations (built up as a result of NH_4^+ ion exchange onto clinoptilolite) and for biological NH_4^+ metalloids (NO_2^- and NO_3^-).

3.3.6.2 SAMPLE ANALYSES

Ammonium measurements were run on duplicate samples (each sample injected and analysed three times) using an AGILENT 1200 series HPLC with a “Universal Cation HR, 3 µm, 7.0 x 53 mm” column coupled to a conductivity detector (Alltech Model: 350). A mobile phase of 3 mM methanesulfonic acid was used at a flow rate of 2.5 mL min^{-1}.

NO_2^- and NO_3^- in the surrounding liquid were spectrophotometrically analyzed in duplicates based on APHA Standard Methods [104].

3.4 Results and Discussion

The setup was operated for a period of 300 days. During that time no additional water was added and no leachate was produced. That provides the essential conditions for continuous biological activity within the biofilter, and minimises

the risk of “only” stripping/ washing the compounds out of the polluted gas. Initially two biofilters were commissioned, but after 6 months of operation, two more biofilter columns were operated simultaneously. These adjustments and setup changes could be performed without the help of a professional electrician since all electronic devices used were powered with 12 VDC. All data were automatically acquired in a regular and schedule procedure at least 10 times a day. A moisture sensitive multi gas detector (HORIBA VA/ VS 3000) [159] was connected to the outlet gas and operated without failure for the whole time. In addition, the automation and the PC controlled operation allowed the monitoring of the system from outside the lab via VPN (virtual private network) connection.

Results of preliminary experiments presented in biofilter depth profiles (Fig. 3-12) determined at day 0 and 300 indicate a change of concentration (a) over time and (b) over the depth of the biofilter column. As expected the introduced NH_3 (inlet) is converted to NH_4^+. However, the measured concentration of NH_4^+ and NO_2^- are above the inhibition concentration (see chapter 2.1), allowing no biological ammonium oxidation. In contrast, it was not possible to detect any NO_2^- nor NH_4^+ in the top layer of the reactor column. From the results, it can be postulated that the biological oxidation of NH_4^+ occurred in the top section, and the metabolites were washed down the bottom of the reactor with the introduction of the pure water to the top of the reactor. Within the 300 days a steep concentration gradient over depth developed with high concentrations of nitrite at the bottom of the Biofilter column.

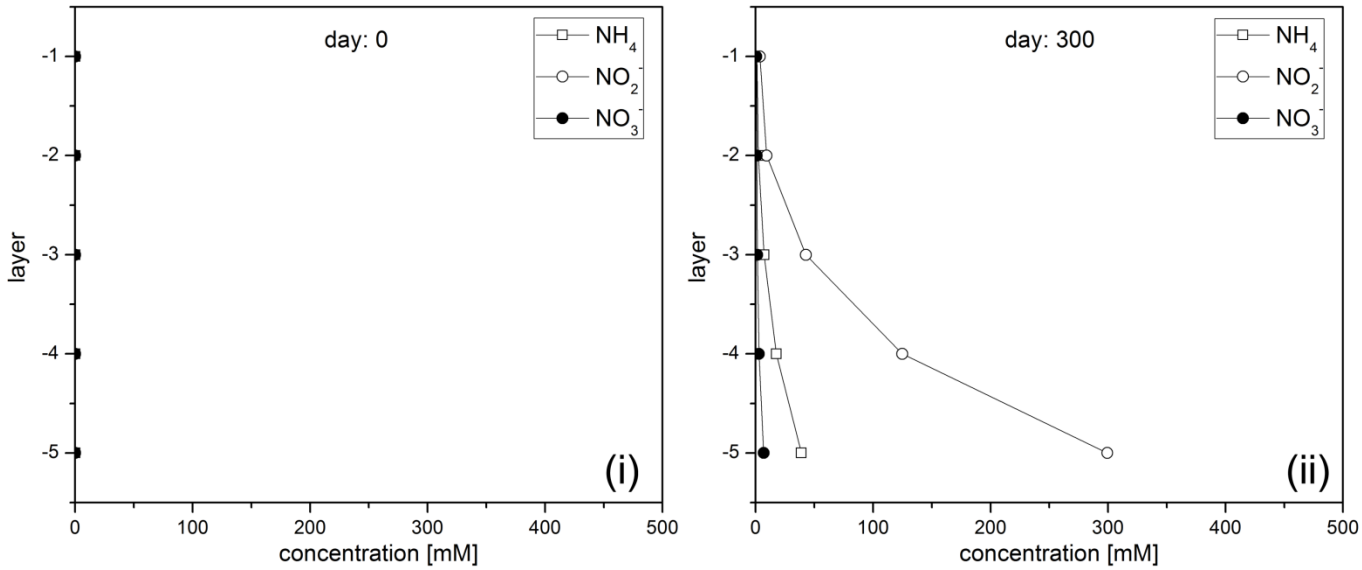

Fig. 3-12: Biofilter depth profile for NH_4^+, NO_2^- and NO_3^- for day 0 and 300 showing the differences in distribution over the biofilter depth

It is beyond the aims of that chapter to discuss these finding in more detail, but more detailed information about the biofilter performance are presented in chapter 4.

The following mechanism and principles of the reflux can be claimed:

1. The gas introduced at the bottom of the biofilter causes evaporation of the biofilter containing moisture
2. Water transport from the bottom to the top resulting in sustainable water supply through the biofilter
3. Condensation of moisture leaving from the biofilter allowed (a) the production of dry outlet gas for online gas monitoring with moisture sensitive gas detector [159] and (b) the reintroduction of condensate
4. The cycle of vaporising and condensing the water in the biofilter caused (a) a stable biofilter moisture inventory and (b) a gravitationally washing of compounds to the bottom of the biofilter
5. The addition of the reintroduced condensate caused a concentration gradient across the biofilter with (a) accumulation of the compounds at the bottom and (b) lower concentrations on top of the biofilter
6. Low concentrations in the upper layer preclude biological inhibition and favour biological reaction such as the nitrification of ammonium to nitrite
7. High concentrations of ammonium, nitrite and nitrate allow chemical reactions such as the reaction of $NH_4NO_2 \rightarrow N_2$ and 2 H_2O (favoured at high concentration [126, 163])

If necessary, saturated bottom parts of the biofilter can be replaced instead of the whole biofilter. The detailed information about the layer formation and the

chemical reaction of NH_4NO_2 to N_2 and 2 H_2O will be presented in chapter 4. [163].

3.4.1 Relevance/ Future Application

Long-term and upscaled experiments are recommended for a more complete understanding of the biofilter performance. It is suggested to continue with the model compound ammonium to study (a) the biological oxidation (nitrification) to nitrate followed by (b) the spontaneous chemical reaction of NH_4NO_2 to N_2.

Pollutants that do not biological, chemical or biochemical degrade in the way described above the reflux process could be used to accumulate those pollutants in the bottom of a filter column. That would allow the replacement of high concentrated pollutant from the bottom of the filter and further use of the above filter material. Such a modular filter construction could help saving filter material and consequently saving costs.

3.5 Conclusions

- By developing a moisture recycle system (reflux) that replenishes water from the top the (exact) moisture for long term operation was maintained without leachate production.
- A concentration gradient is achieved across the filter bed for the development of microenvironments.
- The moisture reflux enabled accumulation of metabolites in the bottom of the biofilter and prevented inhibition in the upper layer.

3.6 Acknowledgement

We acknowledge support of this research by the Environmental Biotechnology Cooperative Research Centre (EBCRC), Zeolite Australia for the kind supply of clinoptilolite and Southern Metropolitan Regional Council (SMRC) for the allocation of the existing filter system. We also like to acknowledge the help of Dr Sebastian Bochmann for sharing his chemical expertise.

A novel way of removing ammonia: Long-Term evaluation of ammonia and total nitrogen removal

Sebastian Vitzthum von Eckstaedt, Goen Ho, Wipa Charles, Ralf Cord-Ruwisch

Abstract

Ammonia in air is of major health and environmental concern and existing ammonia removal systems are costly or unreliable. A novel biofilter system employing the reflux process was continuously operated for a period of 300 days. Inoculated zeolite (clinoptilolite) as packing material provided microorganisms for ammonia removal from an air stream (2.05 µmol L^{-1}) at a volume load of 1 L L^{-1} min^{-1}. Depth profile analysis showed the development of a steep gradient of ammonia and nitrite from the inlet to the outlet over time. Aside from the well-known ammonium adsorption on clinoptilolite, consistent microbial nitrification took place. After 160 days of operation, high concentrations of ammonium (140 mM), nitrite (1 M) and nitrate (375 mM) accumulated at the bottom of the biofilter where they reacted to nitrogen gas. Nitrogen mass balance showed that ammonia was removed from the effluent gas and no nitrogen species (ammonium, nitrite and nitrate) accumulated in the column. The mass balance analyses also show that under the complete aerobic conditions, 100 % of the ammonia introduced into the biofilter was converted to nitrogen gas. This reaction is known to be catalysed at room temperature by clinoptilolite.

Keywords: ammonia biodegradation, reflux process, clinoptilolite filter, long-term investigation, nitrite reduction

4.1 Introduction

Biofiltration is a common and widely accepted method to treat ammonia from air streams [51, 164, 165]. In the process of biofiltration the ammonia is initially dissolved in the water phase followed by microbial degradation (nitrification) to nitrite and nitrate. Under aerobic conditions nitrite and nitrate accumulate to high concentrations inhibiting the nitrifiers unless flushing removes them as leachate. Nitrifiers, like all life forms depend on the availability of free water moisture making water essential in a biofilter. In gas biofiltration, nitrifying organisms are commonly attached to organic or inorganic filter material. Organic filter materials such as coconut husks [103], compost [46] or pruning waste [47] provide additional nutrient source but have the disadvantage that they biodegrade [47, 166]. In contrast, inorganic filter materials such as ceramic [40], polyurethane foam [167] and zeolite [168] have no source of additional nutrients but are not biodegradable. Foglar et al. [101] demonstrated the possibility to attach nitrifying organisms to zeolite. Zeolites are wildly available porous aluminosilicate minerals with the capability to selective ion exchange [169-171] and surface adsorption [172-174]. Li et al. [69] and Yeom et al. [88] reported catalytical effects of zeolite on the reaction of NH_4NO_2 to N_2 and 2 H_2O at room temperature. This concept was demonstrated by our research presented previously [126].

Sufficient moisture supply without leachate production is a key issue in biofiltration. Leachate can be of major concern when containing accumulated pollutants and their metabolites [103, 175, 176]. A previous study demonstrated effectively that the water moisture control can be achieved by applying the

reflux process to biofiltration [120]. Moisture leaving the biofilter is condensed and reintroduced to the top of the biofilter. The pure water condensate percolates through the filter bed and washes pollutants and metabolites to the bottom. By doing so, a gradual distribution of compound is established. The reflux process provides a dry outlet gas which allows continuous online monitoring for precise mass balances and data acquisition.

The aim of this study was to demonstrate the efficacy of a novel reflux biochemical filter system over an extended time using a bench scale biofilter. Depth profiles of the filter bed demonstrated layer formation suggesting that biological and chemical reactions were taking place in the different layers (microenvironments) of the biofilter.

4.2 Materials and methods

4.2.1 Experimental set-up

The laboratory scale biofilter contained a moisture control unit, four biofilter columns, two condensers and gas analyser units. A multiple gas detector for NH_3, N_2O and NO_x (HORIBA VA/ VS 3000, detection range: 0 – 100 ppm ± 0.5 %) was used. Biofilter components e.g. water bath, solenoid valves and sensors (digital flow meter, thermocouples and analyser outputs) were monitored and controlled by a computer where the acquired data were automatically processed. The experimental set up was previously described in detail [120]. In this paper relevant aspects of the design, which are directly related to the filter operation, are described in brief.

4.2.2 BIOFILTER

An up-flow biofilter was constructed using a 10 cm internal diameter PVC pipe with a total height of 20 cm. Headspaces on top (4 cm) and at the bottom (4 cm) of the biofilter column served as mixing and homogenization areas. One litre of moist zeolite clinoptilolite (Zeolite Australia Pty Ltd) formed a bed depth of 13 cm with a calculated surface area of 10 m^2. Prior to being used, the clinoptilolite was sieved (2.4 – 4.0 mm), washed and inoculated with microorganisms for 6 months by placing in a biofilter at an operating composting facility of Southern Metropolitan Regional Council (SMRC), Perth, Western Australia. Since clinoptilolite is known to be an media microorganisms attach to [79, 101, 177] it was assumed that during the inoculation time a varaity of microorganisms attached to the clinoptilolite.

The biofilter was operated at room temperature (21 ± 1 °C). The flow of the carrier gas (laboratory compressed air supply) was adjusted to 1 L min^{-1} resulting in a True empty Bed Residence Time (TBRT) of 27 sec. From a gas cylinder, 1 % ammonia in air was spiked into the gas stream to achieve a 2.05 µmol L^{-1} min^{-1} (50 ppm_v) input concentration. Over the duration of experiments, pH was never adjusted, and no water or carbon source was added.

4.2.3 MOISTURE CONTROL

A moisture control method based on the principle of evaporation and condensation was employed [120]. The configuration of humidifier, biofilter and condenser at different temperatures resulted in the reflux mechanism. By evaporating water from the bottom and reintroducing the condensation water on

top of the biofilter a stable water regime was established. The reflux mechanism ensured a constant water content in the biofilter but also led to the accumulation of water-soluble compounds in the bottom of the biofilter by washing the compounds down and evaporating the water from the bottom. This enabled the formation of a concentration gradient of water-soluble compounds along the depth of the biofilter. Furthermore, due to the reflux process, the development of biological and chemical microenvironments (layers) within the filter bed resulted in sustainable NH_3 removal.

4.2.4 Computer monitoring and control

The biofilter is part of a computer controlled and monitored (Labview 8.5.1) laboratory scale test facility as described in detail in Vitzthum von Eckstaedt et al. [120]. All recorded data were processed and stored automatically in Microsoft Excel 2007 workbook. OriginPro 8.5 (OriginLab Corporation) was utilized for graph generation.

4.2.5 Manual clinoptilolite sampling

To verify variation in the biofilter activity as a result of stratification, and to obtain a more detailed understanding of its performance in addition to on-line analysis, the biofilter operation was periodically stopped and its clinoptilolite content was separated into five layers for analyses. The biofilter was opened and the clinoptilolite removed in 200 mL lots. The individual samples were homogenized. Subsamples were taken to analyse the liquid surrounding the clinoptilolite particles to determine the sodium, ammonium, potassium, magnesium and calcium, nitrite and nitrate content. The pH of the moisture in the clinoptilolite layers was also determined from these extractions.

For the analysis of the liquid surrounding the clinoptilolite particles (water content: 0.2 mL g^{-1} clinoptilolite) 10 g of clinoptilolite were washed in 10 mL deionised water by manually shaking for 1 min. Further subsamples were taken for the extraction of ammonium adsorbed onto the clinoptilolite. Ammonium was desorbed from the surface of clinoptilolite particles by shaking (48 h at 60 rpm) 2 g clinoptilolite in 50 mL of a 4 M KCl solution [178]. Both resulting aliquots were filtered through a 0.45 µm syringe filter and the filtrate was frozen (- 20 °C) until required for analysis.

4.2.6 Batch experiments

It was postulated, that the nitrogen disappearance observed in the biofilter [120] was due to nitrogen gas production. To verify this batch experiments were carried out. Four serum bottles were filled with clinoptilolite from the bottom of the biofilter in order to determine the gas production rate and its composition. It was also of interest to show that the observed reaction was not biological and therefore 2 of the 4 serum bottles were autoclaved. For the headspace gas composition analyses, all serum bottles were flushed with oxygen for two minutes at a flow of 1L min^{-1}. The gas sampling procedure is described below. Briefly, samples were taken and immediately analysed once a week for 64 days. To avoid overpressure, volumetric gas measurements were conducted as well.

4.2.7 Chemical analyses

4.2.7.1 Liquid analyses

An AGILENT 1200 series HPLC with an “Universal Cation HR, 3 µm, 7.0 x 53 mm” column connected to a conductivity detector (Alltech Model: 350)

was employed to analyse the cation samples in duplicates (3 injections per sample). Methanesulfonic acid (3 mM) was used as the mobile phase at a flow rate of 2.5 mL min^{-1}.

Nitrite and nitrate were measured in duplicate spectrophotometrically at the wavelength of 540 nm and 420 nm respectively. The KCl solution containing the ammonia desorbed from the clinoptilolite was analysed in duplicate spectrophotometrically at a wavelength of 425 nm. The analysed cations represented the cations from the clinoptilolite which were replaced by ammonium. Ammonia, nitrate, and nitrite analysis was based on APHA Standard Methods [104].

4.2.7.2 GASEOUS ANALYSES

Headspace gas sample was taken twice with a gas tight 350 µL syringe. The syringe was flushed with the first 350 µL of sample. With the flushed syringe 350 µL sample was taken and 300 µL injected into the gas chromatograph (GC). Gas samples were analysed by a Shimadzu GC 2010 working with helium as carrier gas (50 mL He min^{-1}), at 40 °C, using a thermo conductivity detector (TCD) at 150 °C. A concentric packed column was installed within the GC.

4.2.8 DNA EXTRACTION AND PCR

To determine the presence of ammonia monooxygenase (amoA-1F and amoA-R2 primer) and nitrous oxide reductase (zosZ1F and reverse primer), DNA was extracted from 1 g clinoptilolite samples using a modified protocol of an Ultra Clean Soil DNA Isolation Kit [179]. The clinoptilolite samples were taken from all five layers at various times (day 0, 147, 238, 265 and 328). For each sample,

50 µl DNA was stored in the freezer (-20 °C). The reaction mixture contained in a final volume of 25 µL: 1 µL of DNA (about 50 ng mL^{-1}), 2.5 µL of 10xbuffer, 2.5 µL of $MgCl_2$ (25 mM), 0.5 µL of dNTP (10 µM), 2.5 µL of each forward and reverse primer (10 pmol mL^{-1}) and 0.1 µL of TagTi polymerase (5 U mL^{-1}). The PCR machine was programmed at (a) 94 °C for 5 min, (b) 35 cycles at 94 °C for 1 min, (c) 1 min annealing at 55 °C, 58 °C and 59 °C for Eubacteria and amoA, nosZ and Pla, respectively; and (d) followed by a final temperature of 72 °C for 90 sec.

PCR products were checked by electrophoresis on 1 % agarose gels including 2 µL SYBERsafe per 50 mL gel [180]. A mix of 5 µL ladder solution and 3 µL loading dye was added to the 10 µL sample (including positive and negative control) and 3 µL loading dye reagent. A voltage of 80 V was applied for 60 min before the gel product was analysed and photographed under UV light.

DNA extraction and PCR analyses were performed at least in triplicate to ensure the validation of the presented results.

4.3 Results and Discussion

4.3.1 Ammonia removal behaviour of the Biofilter

Initial trials with ammonia adsorption of the used clinoptilolite confirmed literature findings [126]. According to Karadag et al. [108] gradual ammonia accumulation in the column would result in an increased ammonia build-up in the exit gas. In order to prolong the column lifespan, direct conversion of ammonia to nitrate or nitrite by bacteria is desired. Therefore clinoptilolite inoculated at an operating biofilter with a developed biofilm, was used in our

study. This biofilm coated clinoptilolite biofilter column was operated at an ammonia loading rate of 2.05 µmol NH_3 L^{-1} carrier gas (air) L^{-1} filter volume min^{-1} (50 ppm_v). The development and performance of this clinoptilolite biofilter was recorded over 300 days (Fig. 4-1 to Fig. 4-3).

The continuous and constant input of ammonia resulted in a steady accumulation of total nitrogen (Fig. 4-1). A NH_3, N_2O or NO breakthrough was not detected at any time leading to the conclusion that all introduced ammonia-

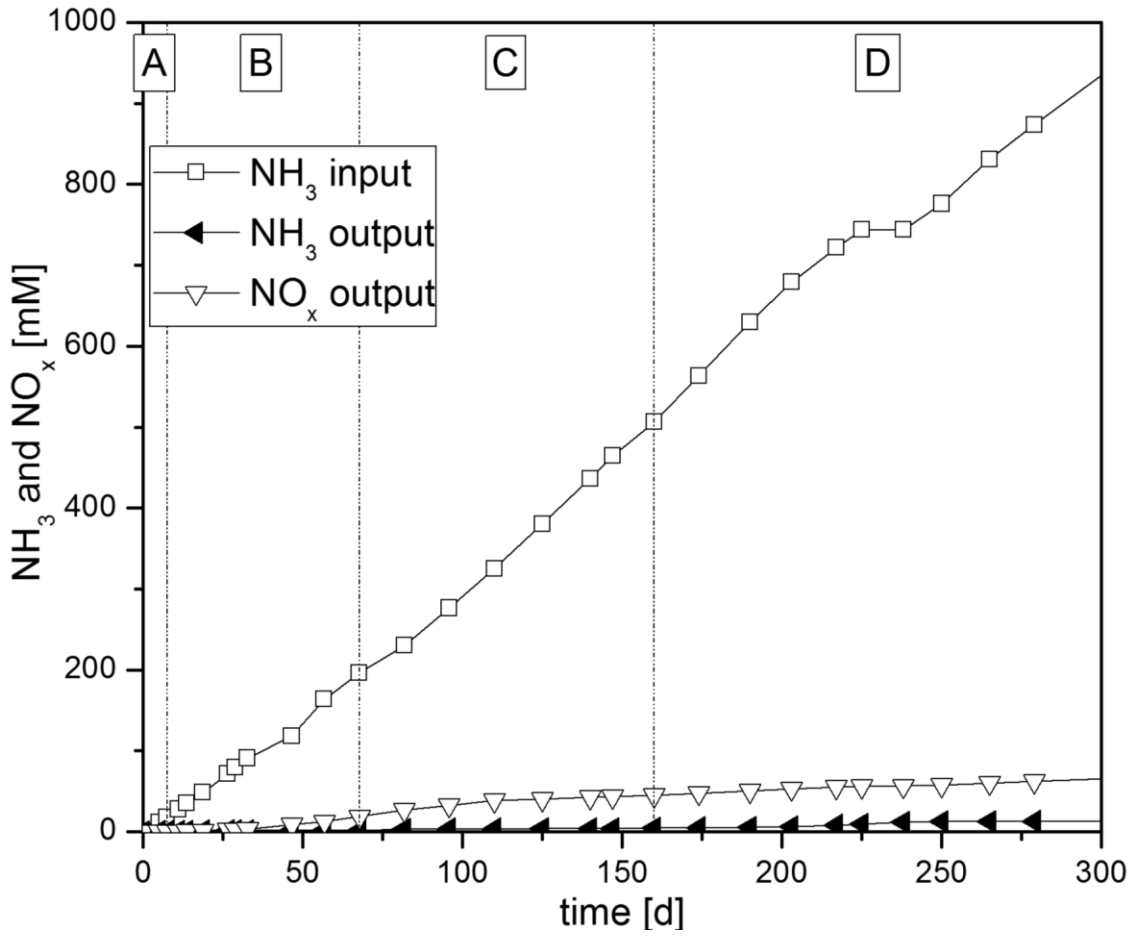

Fig. 4-1: Accumulative N species in inlet and outlet gas stream (data points reduced to the dates where both, gas and liquid samples, were available and analysed (complete data set on appendix DVD). Furthermore, the results were separated into phases A-D)

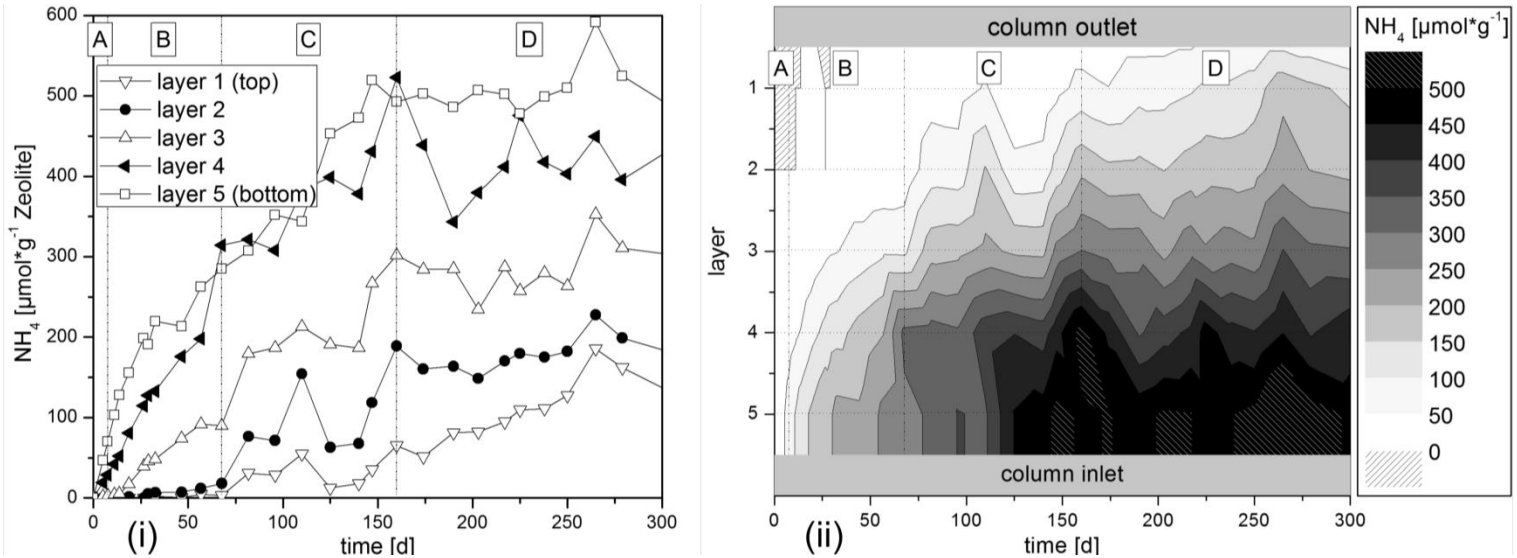

Fig. 4-2: (i) NH_4^+ adsorbed onto clinoptilolite in 5 layers over time presented in a conventional line plot (ii) NH_4^+ adsorbed onto clinoptilolite interpolated over depth and time presented as a contour plot; results separated into phases A-D

nitrogen remained within the biofilter column or leaved as a non-analysed nitrogen species such as nitrogen gas (N_2).

As expected, ammonia built up in the column over time, mainly at the gas inlet (bottom of the column, Fig. 4-2). This caused the build-up of a vertical ammonia gradient throughout the column as demonstrated in Fig. 4-2 (i) and (ii). Fig. 4-2 (i) shows a conventional line graph of the results measured in the individual layers over time. The fact that the top layer contained less than 10 % of the total ammonia suggests that the column was not yet saturated. A contour plot as shown in Fig. 4-2 (ii) visualized the development of spatial distribution of e.g. ammonia more clearly where the grey scale represents the concentration in the biofilter column. In addition to ammonia build-up in the liquid surrounding the clinoptilolite (Fig. 4-3 (ii)) there is evidence of microbial conversion of ammonia to oxidized metabolites nitrate and nitrite in each layer of the column (Fig. 4-3 (iii) and (iv)). The pH over the depth and over time is presented in Fig. 4-4. To characterize the biofilter column performance the time course was divided into four phases (A-D).

4.3.2 Physical adsorption - Phase A (first 7 days)

Within the first 7 days prior to the full development of microbial activity the introduced ammonia gas dissolved in the water causing the pH to increase from 7.3 to 8.5 in the bottom layer (Fig. 4-4). Clinoptilolite as the filter media adsorbed the dissolved ammonium while microbial communities were being established (Fig. 4-2 and Fig. 4-3). At this stage, no further N species were detected in the water or outlet gas.

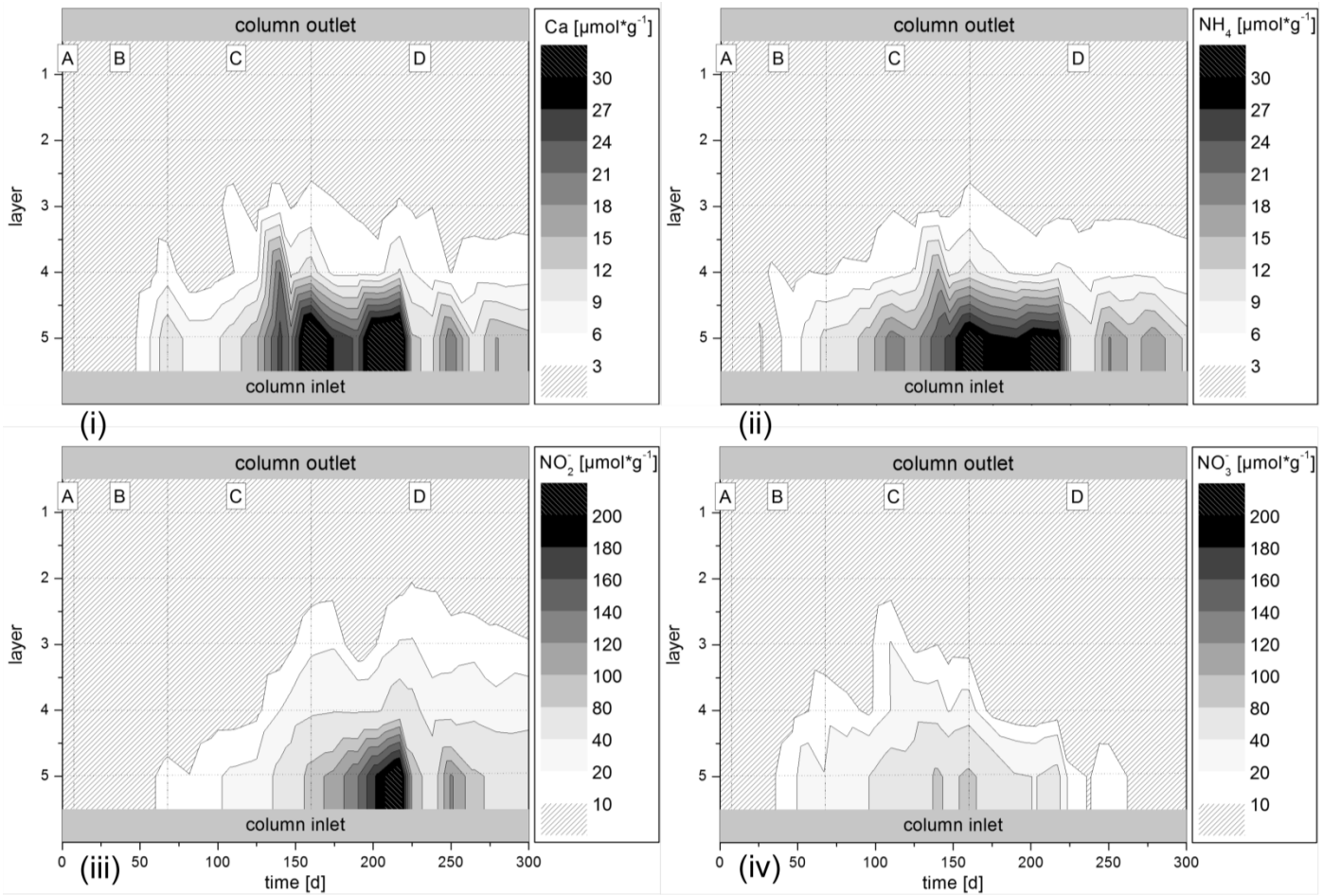

Fig. 4-3: Presence of (i) calcium (Ca), (ii) ammonium (NH_4^+), (iii) nitrite (NO_2^-) and (iv) nitrate (NO_3^-) in water surrounding the clinoptilolite interpolated over depth and time presented as an contour plot, results separated into phases A-D. Results are expressed per g of clinoptilolite (0.2 mL of moisture is associated with 1 g of clinoptilolite)

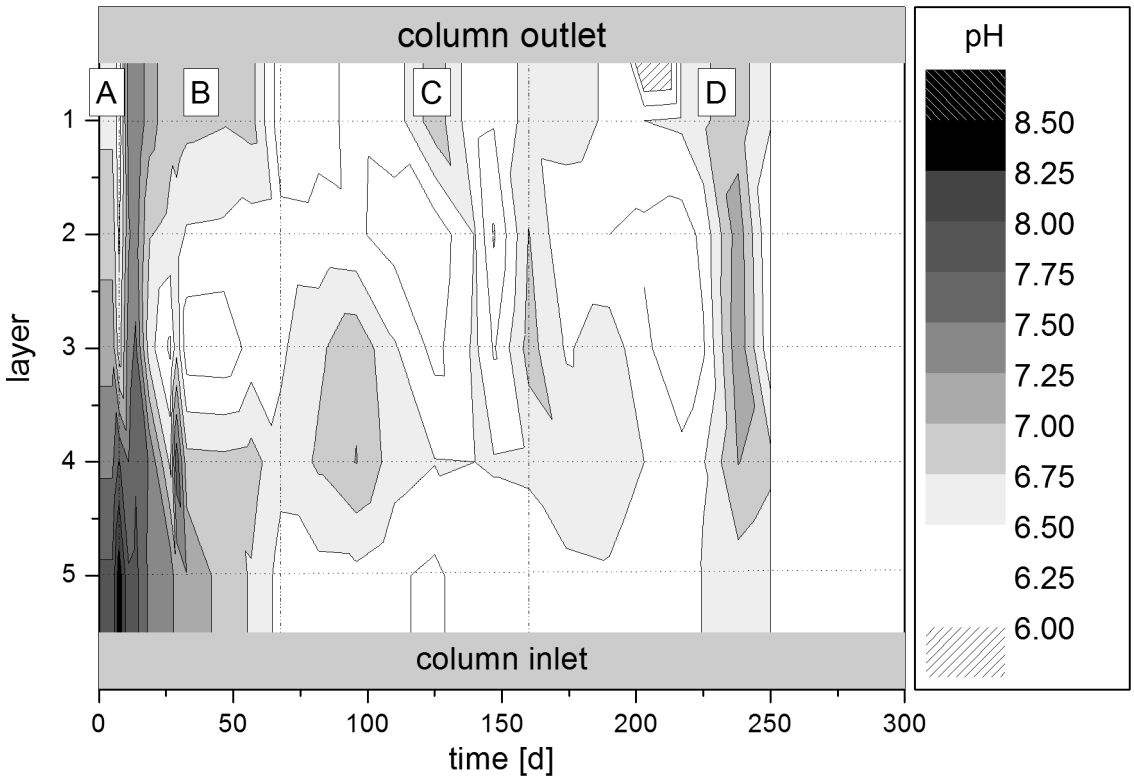

Fig. 4-4: pH distribution over the depth of the biofilter column interpolated over time

4.3.3 Nitrification - Phase B (day 7 to 67)

During phase B, the pH gradually decreased from 8.5 to 6.5 (Fig. 4-4). Over the period of 60 days the continued ammonium adsorption in the bottom layer triggered the release of cations as shown for the example of calcium in Fig. 4-3 (i). As the clinoptilolite in the bottom layer approached saturation, the ammonium adsorption rate slowed down, causing an ammonium accumulation increase in the layer above (Fig. 4-2 and Fig. 4-3). The build-up of nitrate and nitrite (12.5 µmol g^{-1} and 31 µmol g^{-1} respectively

4.3.4 Nitrogen accumulation - Phase C (day 67 to 160)

Nitratification continued until a maximum level of nitrate of 87.5 µmol g^{-1} clinoptilolite (bottom layer) was reached on day 160. The pH in the bottom layer

remained stable at between 6.5 and 6.2 (Fig. 4-4) during the 100 days of phase C. The nitrite built up to higher levels (92.5 µmol g^{-1}) than nitrate which is usually observed in the presence of high ammonia concentrations (Fig. 4-3).

The ammonium adsorbed onto the clinoptilolite reached a plateau at 500 µmol g^{-1} clinoptilolite in the bottom layer (Fig. 4-2). The corresponding maximum of ammonia in the surrounding liquid phase was approximately 33 µmol g^{-1}. Because of the low liquid volume available in the filter (0.2 mL per g of clinoptilolite) the resulting ammonia concentration was 140 mM.

4.3.5 Nitrogen loss - Phase D (day 160 – 300)

After the ammonium had reached saturation level in the bottom layer it was expected that the continued ammonia input would either result in build-up of ammonium in the layer above or in continued nitrate or nitrite build-up. However, neither nitrate nor nitrite or ammonia significantly accumulated in any of the layers above the bottom layer even though a continuous stream of ammonia entered the system. Regular measurements of the biofilter column outlet (every 3 h) confirmed that no significant NH_3, N_2O and NO_x left the system. The detected approximate 5 % NO_x in the output shown in Fig. 4-1 can be explained by a possible cumulating error occurring over the period of 300 days.The fact that both nitrate and nitrite concentrations decreased within the biofilter (87.5 µmol g^{-1} to 2 µmol g^{-1} and 229 µmol g^{-1} to 70 µmol g^{-1}, respectively) suggests that a nitrate/ nitrite consuming reaction occurred (Fig. 4-3). The ammonium adsorbed onto the clinoptilolite in the bottom layer remained stable at about 500 µmol g^{-1} at a pH of 6.5 (Fig. 4-4).

The nitrogen in the form of ammonia introduced into the biofilter and the nitrogen accumulated as ammonium (in liquid phase as well as adsorbed onto clinoptilolite), as well as nitrite, nitrate and nitrogen leaving from the biofilter did not match. Mass balances provided clear evidence of nitrogen disappearance in a form not detected from day 160 onwards (Table 4-1). As on day 300, a greater 100 % efficiency shows a reduction of the sum of all nitrogen species (ammonium, nitrite and nitrate) accumulated in the reactor. A greater 100 % efficiency implies more nitrogen is leaving than entering the reactor. This will be discussed further and in more detail in section 4.3.9 below.

Note: The correlation of N species computed for the first 110 days showed significant correlation with a coefficient of determination (r^2) of 0.86 to 0.99. However attempts to correlate the results later sampling events (day 110 to 300) or over for the complete time (day 0 to 300) did not reveal correlation (r^2 between 0.07 to 0.61). Fig. 4-8 and Table 4-1 contain reduced and summarised findings. All data can be found on the appendix DVD's attached to the thesis.

Table 4-1: Nitrogen species appearance in the complete filter column presented for days 0, 7, 67, 160, 220 and 300

time	input	zeolite	surrounding liquid			difference	nitrogen removal efficiency
	NH_3-N	NH_4-N	NH_4-N	NO_2^--N	NO_3^--N		
[d]	[µmol]	[µmol]	[µmol]	[µmol]	[µmol]	[µmol]	[%]
0	0	0	0	0	0	0	0.00
7	17477	16745	174	302	375	-118	-0.68
67	199850	178985	3772	4519	11386	1189	0.72
160	506229	396075	12598	38686	32400	26470	8.25
300	955200	385929	4096	29119	785	535271	113.33

4.3.6 LAYER ABOVE THE BOTTOM LAYER

Similar phases as described for the bottom layer also occurred in the layer above, although less pronounced. Ammonium build-up in the layer above the bottom layer (layer 4) reached the saturation at the same time as the bottom

layer. All layers above the bottom layers reached lower levels as expected with a lower NH_3 concentration in the gas stream reaching these layers.

4.3.7 MICROBIOLOGY

In order to establish whether bacteria with the key enzymes ammonia mono-oxidase (amoA) and nitrate reductase (nosZ) were present, a standard DNA analysis (see 4.2.8) was carried out. Samples taken on days 0, 147, 238, 265 and 328 showed the presence of both enzymes after 147 days in the bottom layer of the lab biofilter column. The in Table 4-2 presented results indicate that amoA and nosZ for the SMRC zeolite (day 0) samples could not be found. This leads to the conclusion that (a) the incubation at the existing biofilter (SMRC) had no effect or (b) the amount of amoA and nosZ containing microorganisms have been too small to be detected. Furthermore, it can be speculated that if the appearance of those key enzymes from day 147 onwards are (a) due to the development of the small amount possibly attached microorganisms to the zeolite or (b) an incubation from another source occurred. It was beyond the scope of the thesis to find answers to this phenomenon.

Band intensity of nosZ was weaker than of amoA suggesting denitrifying microbes were less prevalent than ammonia oxidizers. These results explain the observed conversion of ammonia to nitrite as a biologically catalysed step.

Table 4-2: ammonia mono-oxidase (amoA) and nitrate reductase (nosZ) results of samples taken on 4 points in time.

sample	Amoa	NosZ
SMRC Zeolite (day 0)	-	-
Filter Zeolite (day 147)	+	+
Filter Zeolite (day 238)	+	+
Filter Zeolite (day 265)	+	+
Filter Zeolite (day 328)	+	+

4.3.8 BIOLOGICAL ACTIVITY AND BIOFILTER PERFORMANCE

High concentrations of ammonium in the biofilter column were achieved due to the low water content of 0.2 mL g^{-1} clinoptilolite. Ammonium concentrations of up to 140 mM (day 160) were measured in the bottom layer of the biofilter. At the observed pH of 6.4 and a temperature of 21.6 °C the highest free ammonia (FA) concentration of 0.15 mM (2.1 mg NH_3 N L^{-1}) was calculated for this particular time. Inhibition of ammonium oxidizing bacteria (AOB, *Nitrosomonas*) triggered by free ammonia (not been detected below 16 mg NH_3 N L^{-1} [119]) has not been reached in the system. The same authors showed that nitrite oxidizing bacteria (*Nitrobacter*) inhibition at a FA concentration of 6 – 9 mg NH_3 N L^{-1} [119] occurs which may have occurred in the biofilter.

Toxic effects on microorganism cells may be exerted by the nitrite un-dissociated fraction nitrous acid (HNO_2) or so called free nitrous acid (FNA) [149]. FNA is known to be toxic to nitrifyers by interfering with the proton gradient [150]. In contrast to natural nitrifying environments (e.g. soil, wastewater) where nitrite rarely builds up our experiments showed significant nitrite build up of up to 980 mM (13.7 g N L^{-1}) at day 217. *Nitrosomonas* bacteria are reported to be inhibited at FNA concentrations of 0.4 -0.63 mg HNO_2 N L^{-1} whereas *Nitrobacter* are more sensitive to FNA and are inhibited at 0.02 mg HNO_2 N L^{-1} [119]. The FNA inhibited areas for *Nitrosomonas* and *Nitrobacter* (Fig. 4-5) develop over time and biofilter depth.

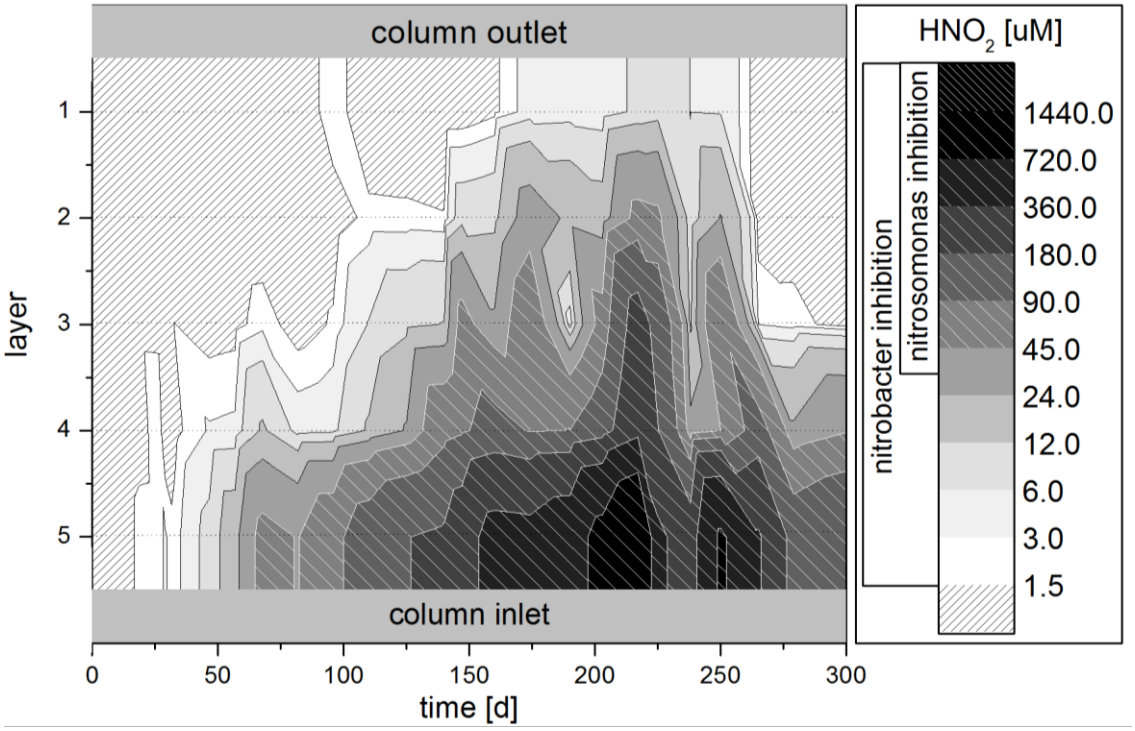

Fig. 4-5: *Nitrosomonas* and *Nitrobacter* inhibition by FNA plotted over the biofilter column depth and over time

For example, at the bottom layer nitrite concentrations of up to 980 mM (13.7 g NO_2^- N L^{-1}) were measured on day 203. At a pKa of 3.4 this would result in a FNA concentration of 1.4 mM (19.2 mg HNO_2 N L^{-1}) at a pH of 6.3 at 21 °C. Complete inhibition of both nitrifyers is expected at this concentration about 30 times above the *Nitrosomonas* inhibition threshold and 3 magnitudes above the *Nitrobacter* inhibition threshold. However, nitrite concentration measured at the same time in the top layer of the biofilter column at 4.52 mM (63.3 mg NO_2^- N L^{-1}) and calculated FNA concentrations of 3.75 µM (0.05 mg HNO_2 N L^{-1}) at pH 6.5 indicate that *Nitrosomonas* bacteria (ammonium oxidizing) were not inhibited. From the results presented in Fig. 4-5 it can be concluded that *Nitrobacter* were inhibited early (day 20) in the bottom layer and in the whole biofilter from day 100. At this time the highest nitrate concentration (350 mM) was also measured. A complete *Nitrosomonas* inhibition caused by FNA

concentration could not be detected. However, inhibition occurred from day 60 onwards in the bottom layer. Lower concentrations measured in the top layers indicate the possibility of continuous ammonium oxidation. Despite FNA concentration above the inhibition threshold, nitrite concentration in the bottom layer continued to increase.

The design of the described column enables an upward movement of pure water vapour with the gas stream and a continuous downwards percolation of the condensed water from the top of the column [120]. This counter current reflux not only allows the build-up of very high concentrations of metabolites but also removes potentially toxic species such as FNA from areas where nitrification is occurring. Also by ammonia being able to move upwards in the column while nitrite and nitrate only move downwards (leaching by condensate) the existence of a layer with low nitrite concentrations and adequate ammonia concentrations is feasible.

4.3.9 NITROGEN LOSS

Mass balance calculations of the N species remaining in the filter system (NH_4^+, NO_2^-, NO_3^-) and those leaving from the biofilter column in the form of gas (NH_3, N_2O and NO_x) indicate a mass loss of N over time with an increasing trend (Fig. 4-6). This apparent N loss was occurring to an extent that all incoming ammonia was retained in the column while there was no significant build-up of any N species (phase D). Even more pronounced, over a period of about 20 weeks the total soluble N-species decreased in spite of continuous ammonia addition.

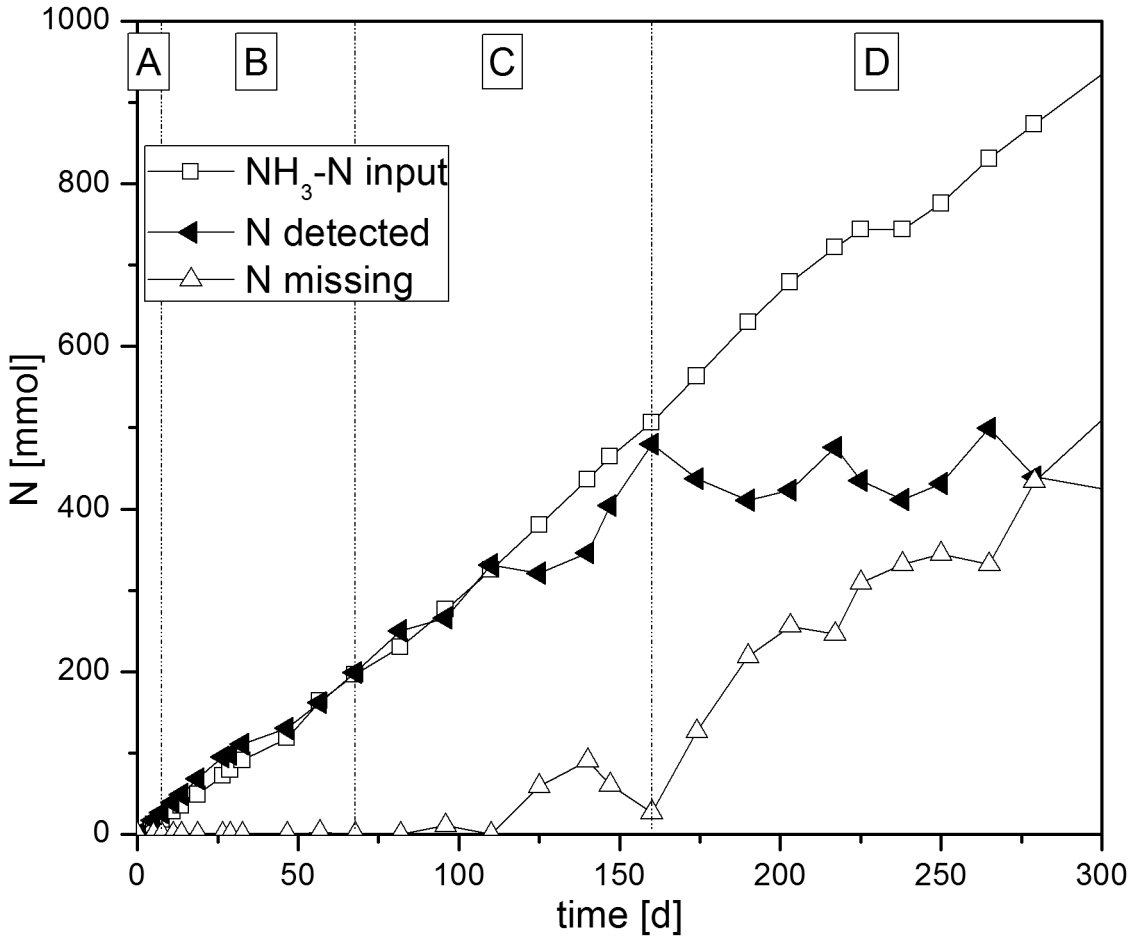

Fig. 4-6: N balance for the complete biofilter column (data points reduced to the times where both, gas and liquid samples, where available and analysed. Furthermore, the results were separated into phases A-D)

The most likely species of nitrogen explaining the N loss would be N_2. However, biological denitrification as an N_2 producing reaction can be excluded, since the biofilter was flushed with air at all times, not allowing the oxygen free conditions needed for effective denitrification. Further there was no organic material present that could serve as the essential electron donor for denitrification.

To test the hypothesis of NH_4NO_2 reacting chemically to N_2 and 2 H_2O, four sterile 120 mL serum bottles were filled with 10 g of homogenized biofilter media from layer 5. After closing the bottles with rubber bungs the headspace

was flushed with industry grade oxygen for two minutes with a flow rate of 1 L min^{-1} in order to produce an N_2 gas free environment. A positive over pressure in the bottles was created in order to minimize N_2 diffusion from the atmosphere into the closed bottles. To prevent biological activity within these bottles two of the four bottles were autoclaved. The change of gas composition was monitored for 64 days and analyses were performed weekly. Results observed from the autoclaved and non-autoclaved bottles showed significant N_2 gas production over time.

The GC and volumetric measurements over the period of 64 days showed the average total N_2 gas production of 1.15 mmol (28.13 mL) for the autoclaved clinoptilolite and 0.99 mmol (24.26 mL) for the bioactive Fig. 4-7. Clinoptilolite samples taken and analysed before and after the experiment revealed a decrease of all nitrogen species surrounding and adsorbed onto the clinoptilolite (Fig. 4-8 and Table 4-3). A total nitrogen mass balance (NH_4^+, NO_2^- and NO_3^- in water plus NH_4^+ adsorbed onto clinoptilolite) showed an expected calculated N_2 N gas production of 1.18 mmol (29.03 mL) and 0.91 mmol (22.27 mL) for the autoclaved and biological active samples. Measured and expected N_2 gas production of the autoclaved and bioactive experiments match to 97 % and 109 % respectively. The difference was possibly caused by analytical errors due to solid and liquid analyses. Under the assumption the biofilter is homogeneous (which it was not) by extrapolating the observed findings about 900 g (720 mL) of the total 1250 g (1000 mL) clinoptilolite present in the filter system are sufficient to allow the conversion of 2.05 µmol L^{-1} min^{-1} (2952 µmol d^{-1}) of ammonia N.

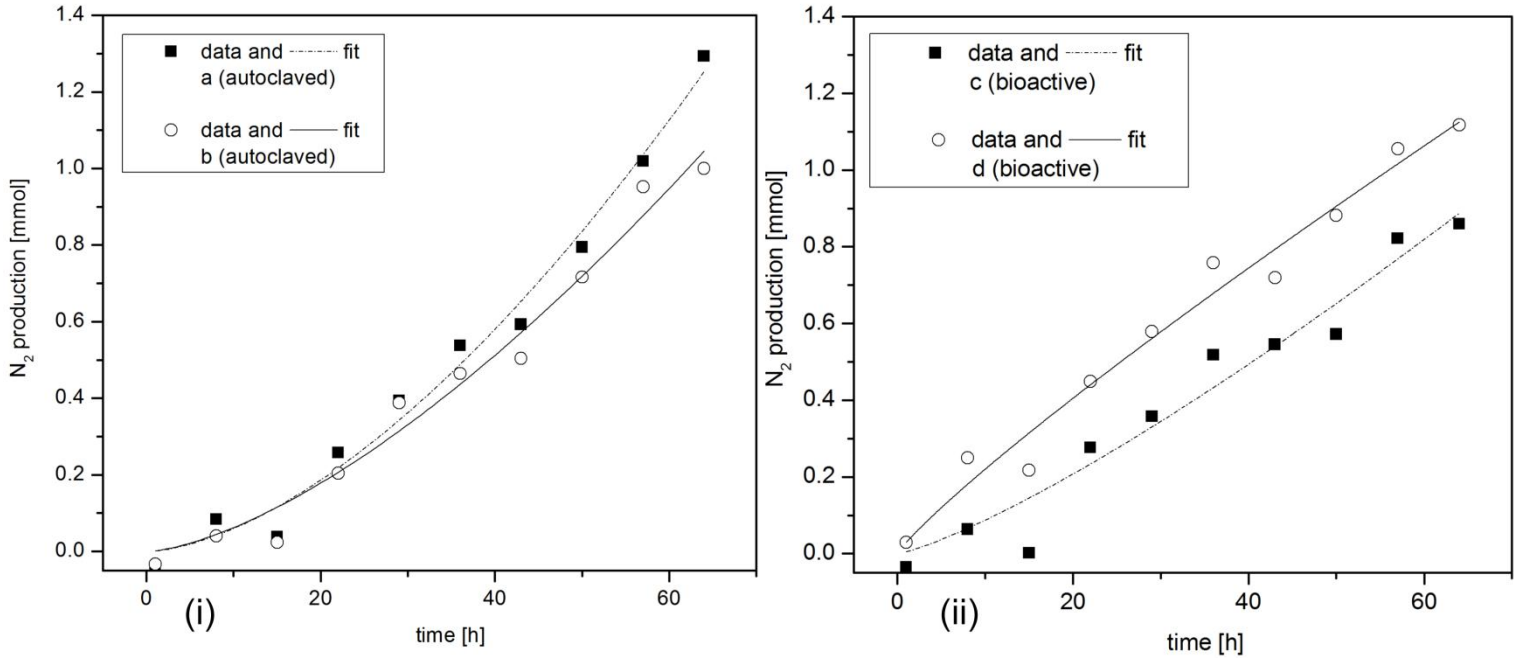

Fig. 4-7: N_2 gas production in duplicate with (i) autoclaved and (ii) bioactive clinoptilolite over a period of 64 days

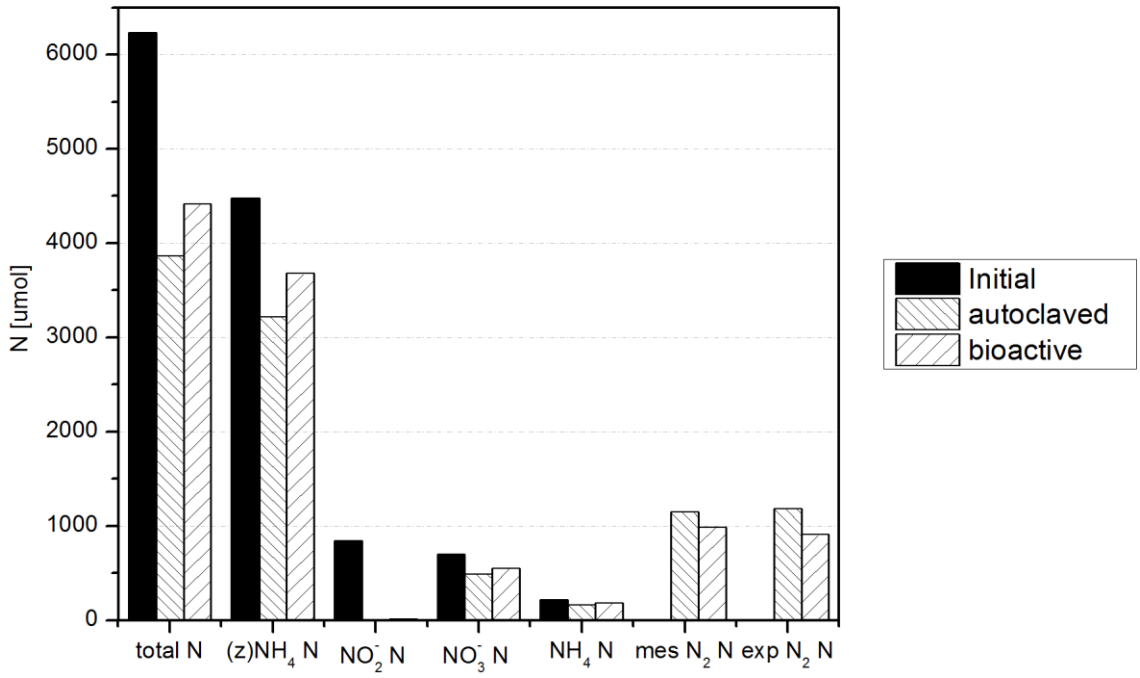

Fig. 4-8: Nitrogen mass balance of initial, autoclaved and bioactive clinoptilolite. (NH_4^+) represents the amount of NH_4^+ adsorbed onto clinoptilolite. mes N_2 N is the amount of N_2 gas measured whereas exp N_2 is the amount expected based on the N loss from the nitrogen species in liquid and adsorbed onto clinoptilolite

Table 4-3: autoclaved vs. bioactive clinoptilolite. (z)NH_4^+ N represents the NH_4^+ adopted onto clinoptilolite. mes N_2 N stands for the N_2 N measured and the exp N_2 N presence the nitrogen expected to occur based on the NO_2^- N, NO_3^- N, NH_4^+ N and (z)NH_4^+ N changes between t=0 and t=64 days. Correlation [%] indicates how exact the expected and measured results match

	NO_2^- N	NO_3^- N	NH_4 N	(z)NH_4 N	total N N	mes N_2 N	exp N_2 N	correlation
	[µmol/ experiment]							[%]
t=0	841	698	218	4476	6232			
autoclaved (t= 64d)	1.5	487	164	3214	3867	1146	1183	97
bioactive (t= 64d)	9.0	549	181	3677	4417	988	908	109

The results presented above indicate the well-established chemical reaction of nitrite and ammonia (see Equation 2-1) took place in the bottom layer of the biofilter. Considering the reaction kinetics of ammonia with nitrite to N_2 [65, 67] and the high concentrations encountered in the column, our observed N loss was due to the spontaneous chemical reaction of ammonia with nitrite [65]

$$NH_4^+ + NO_2^- \rightarrow N_2 + 2H_2O$$ **Equation 4-1**

Abel et al. [67] describes the kinetics of the reaction as a third order reaction involving NH_4^+, HNO_2 and NO_2^- (Equation 4-2):

$$d(N_2)/dt = k[NH_4^+][NO_2^-][HNO_2]$$ **Equation 4-2**

The appropriate k constant has been the subject of discussion in a number of publications [68, 70], but in this study we use the k constant of $3.67*10^{-3}$ [unit less] at 25 °C [67]. Interestingly this reaction is not only dependent on nitrite and ammonium but also on the concentration of free nitrous acid. This means the reaction will proceed faster at lower pH values with a maximum velocity at around the pKa value (3.4) of the NO_2^- / HNO_2 equilibrium. In order to estimate whether the observed N production over 64 days correlates with the model described by Abel et al [67], the rate of N produced in the batch experiment was compared to the model predictions at three different pH (constant) values. At a temperature of 22 °C the Abel model predicted at initial ammonium (93.2 mM) and nitrite (360.3 mM) concentrations as in the batch experiment, rates that are 400, 130 or 42 times less than observed in the batch experiments for the pH values of 6, 5.5 and 5 respectively. As shown in batch experiments conducted with and without clinoptilolite [126] that clinoptilolite acts as a catalyst for the

reaction. The much higher rates observed in the biofilter could also be due to lower pH than measured using extracted water.

4.4 Conclusions

- The results demonstrate a long-term stable operation of a novel clinoptilolite biofilter for ammonia removal from air streams
- The novelty of the biofilter is due to its operation using reflux of condensed moisture producing pure water washing soluble substances to the bottom of the biofilter. Moisture control is key to the operation of the biofilter system
- The wash down of ammonia and nitrite from top layers of the biofilter enables biological nitrification to proceed uninhibited
- Concentrated ammonia and nitrite at the bottom of the biofilter layer result in chemical reaction to produce nitrogen gas catalysed by the biofilter matrix clinoptilolite

4.5 Acknowledgement

We acknowledge support of this research by the Environmental Biotechnology Cooperative Research Centre (EBCRC), Zeolite Australia for the supply of zeolite clinoptilolite and Southern Metropolitan Regional Council (SMRC) for making available their biofilter system. Our thanks also go to Dr Lucy Skillman and her colleagues for providing the facilities and equipment required for the microbiology work. For the help in question related to chemistry I would like to thank Dr Sebastian Bochmann.

Conclusions and recommendations for further work

5.1 The development and testing of a biofilter system for sustainable ammonia removal from air and conversion to nitrogen

A biofilter system has been developed and operated successfully for a period of 300 days. Ammonia at a concentration of 50 ppm_v (2.05µmol L^{-1} min^{-1}) was continuously introduced into a one litre clinoptilolite biofilter. Breakthrough of ammonia or metabolites was not detected in the outlet gas. Biological activity was demonstrated through microbial tests and the observed production of nitrite and nitrate. Regular analyses of inlet gas concentration and accumulation of nitrogen species in the biofilter (ammonium adsorbed onto clinoptilolite, ammonium, nitrite and nitrate present in liquid surrounding the clinoptilolite)

provided clear evidence of nitrogen losses. GC analysis in batch experiments revealed nitrogen as the end product.

5.2 The use of clinoptilolite as an non biodegradable filter material as biofilm carrier and catalyst

Zeolite clinoptilolite was used as an inert filter material, providing surfaces for microorganisms to grow. The clinoptilolite also provided an adsorption capacity or buffer for ammonium adsorption. Microbiology tests demonstrated the presence of nitrifying bacteria attached onto the surface. Results of batch experiments showed the catalytic effect of clinoptilolite on the reaction of ammonium nitrite at room temperature to nitrogen gas.

5.3 The natural development of biological and chemical microenvironments (layer) without pH or water adjustment to allow the operation of the system without further additions

Regular depth profiles of clinoptilolite in the biofilter showed the development of distinct chemical and biological layers. Observed concentration profiles clearly demonstrated that biological and chemical reactions occurred in separate areas with biological conversion of ammonium to nitrite above the bottom layer and chemical reaction of ammonium nitrite to nitrogen gas in the bottom layer. No additional carbon was needed as nitrification is a chemotrophic process.

5.4 The application of the reflux method to biofiltration in order to maintain moisture content within the biofilter and achieve layer formation and gradual distribution of ammonium, nitrite and nitrate to achieve areas with biological and chemical microenvironments

For the extended time of operation (300 days) no water was added while biological activity continued. Depth profiles showed steep concentration gradients over the biofilter depth. The concentration distribution was achieved gradually with low ammonium, nitrite and nitrate concentrations measured on top and (very) high concentrations on the bottom of the biofilter column. Condensing vapour at the outlet and returning the pure water condensate into the top of the column achieved the concentration profile.

5.5 Spatial separation due to layer formation allows simultaneous biological degradation of ammonium to nitrite and nitrate as well as the chemical reaction of ammonium nitrite catalysed by clinoptilolite at room temperature

Biological ammonia conversion to nitrite and nitrate was observed for the 300 days of experiment. However, due to the high concentrations accumulated in the bottom of the biofilter column over time, it is deduced that the biological active area shifted to higher biofilter clinoptilolite areas. The accumulated high concentrations in the bottom and the presence of clinoptilolite as a catalyst allowed the chemical reaction of ammonium nitrite to nitrogen.

5.6 Achieve a dry gas outlet of the biofilter to allow continuous online monitoring with moisture sensitive equipment

An online gas detector was operated for 300 days, analysing the gas composition of the leaving gas without additional gas drying.

5.7 Development of a biofilter system without leachate production and zero additional water supply to reduce water usage

Careful control of the reflux process achieved balance between vapour produced in the biofilter and condensate returned to the column. No leachate was produced and no water needed to be added.

5.8 Future recommendations

In this final chapter, future recommendations and ideas based on the findings presented above are presented. It is recommended to test the experimental setup to treat different compounds such as hydrogen sulphide (H_2S) or organic compounds such as limonene or butanone. After studying the treatment of further single compound we suggest the treatment of a “real” odourous gas produced at a waste treatment facility. It would be also interesting to know if other zeolite different to clinoptilolite (heulandite or synthetic zeolites) also catalyse the reaction and perform as biofilm carrier. Changes in volume load (gas introduced per volume biofilter) and changes in filter design (size and form) need to be tested as well. Instead of condensing the water from the exit gas, the use of a spray system providing pure deionized water on top of the filter need to be tested. That will also help to calculate or minimise the energy consumption.

5.8.1 Questions to be answered in further work

- Is zeolite/ clinoptilolite necessary at all? Is it possible to use different inorganic filter media?
- Is incubation/ inoculation of filter media essential?
- What are the to be expected energy costs to run a condenser in a scaled up operation?
- Are there other fields where such a computer controlled system can be applied?
- Are there further areas where the reflux technology can be applied?

5.8.2 Things to consider during Scale Up

- Larger Zeolite particles to ensure a low back pressure. (thought from the author: an increase of 50 times larger seems reasonable)
- Resulting in a more stable mash/ floor with reinforcement beams to hold the weight (thought from the author: installing a number of beams to (a) insure stability and (b) to ensure constant and uninterrupted flow)
- Consider to use an alternative to an energy intensive cooling device, cooling due to intelligent gas management or filter construction
- It is possibly best to construct in a square instead of round shape
- Consider a concrete basin coated with chemical resistant material

[1] P. Boeker, T. Hamacher, D. Mannebeck, P. Wimmer, and G. Horner, "Methodik und Technik der Online-Geruchsmessung," *Gefahrstoffe Reinhaltung Der Luft,* vol. 63, 2003.

[2] G. M. Nisola, E. Cho, J. D. Orata, M. C. F. R. Redillas, D. M. C. Farnazo, E. Tuuguu, and W. J. Chung, "NH_3 gas absorption and bio-oxidation in a single bioscrubber system," *Process Biochem,* vol. 44, pp. 161-167, Jan 1 2009.

[3] S. Wing, R. Horton, S. Marshall, K. Thu, M. Tajik, L. Schinasi, and S. Schiffman, "Air pollution and odor in communities near industrial swine operations," *Environ Health Perspect,* vol. 116, pp. 1362-8, Oct 1 2008.

[4] X. Li, X. Zhang, and L. Lei, "Preparation of CuNaY zeolites with microwave irradiation and their application for removing thiophene from model fuel," in *Separation and purification technology* vol. 64, ed, 2009, pp. 326-331.

[5] P. Poulsen and P. Kalluri, "Gaseous Oxygen Uptake in Porous Media at Different Moisture Contents and Airflow Velocities," *Journal of the Air and Waste Management Association,* vol. 59, p. 676, Jun 1 2009.

[6] E.-H. Lee, H. W. Ryu, and K.-S. Cho, "Removal of benzene and toluene in polyurethane biofilter immobilized with Rhodococcus sp. EH831 under transient loading," *Bioresource Technology,* pp. 1-8, Jul 4 2009.

[7] J. Vansickly. (2009). *Juries Rule Livestock Not Odor Nuisance*. Available: http://nationalhogfarmer.com/facilities-equipment/manure-handling/0215-juries-rule-livestock-nonnuisance/index.html

[8] G. Sun, H. Guo, J. Peterson, B. Predicala, and C. Laguë, "Diurnal odor, ammonia, hydrogen sulfide, and carbon dioxide emission profiles of confined swine grower/finisher rooms," *Journal of the Air and Waste Management Association,* vol. 58, pp. 1434-48, Nov 1 2008.

[9] J. Sweeten and J. Miner, "Odor intensities at cattle feedlots in nuisance litigation," *Bioresource Technology,* vol. 45, pp. 177-188, 1993.

[10] D. Shusterman, "Critical review: the health significance of environmental odor pollution," *Archives of Environmental Health* Jan 1 1992.

[11] M. A. McGinley and C. M. McGinley, "The 'gray line'between odor nuisance and health effects," *AWMA 92nd Meeting and Exhibition,* 1999.

[12] W. Bruvold, S. Rappaport, and T. Wu, "Determination of nuisance odor in a community," *Journal of the Water Pollution Control Federation,* Jan 1 1983.

[13] R. Ames, "Acute health effects from community exposure to n-propyl mercaptan from an ethoprop (Mocap®)-treated potato field in Siskiyou County, California," *Archives of Environmental Health,* Jan 1 1991.

[14] K. Thu, K. Donham, R. Ziegenhorn, S. Reynolds, P. S. Thorne, P. Subramanian, P. Whitten, and J. Stookesberry, "A control study of the physical and mental health of residents living near a large-scale swine operation," *Journal of Agricultural Safety and Health,* Jan 1 1997.

[15] Erste Allgemeine Verwaltungsvorschrift zum Bundes–Immissionsschutzgesetz (Technische Anleitung zur Reinhaltung der Luft – TA Luft), Berlin: Aug 22 2002.

[16] Government of Sout Australia, "Environment Protection Act 1993," pp. 1-186, 18/11/ 2010.

[17] J. Jager, A. Bockreis, I. Steinberg, C. Rohde, and U. Laser, "Einsatz eines alternativen Abluftreinigungsverfahrens kombiniert mit dem bestehenden biologischen Abluftreinigungsverfahren in einer mechanisch-biologischen Restabfallbehandlungsanlage," 2005.

[18] VDI 3881 Blatt 1: Olfaktometrie – Geruchsschwellenbestimmung - Grundlagen, Berlin: 1986.

[19] DIN EN 13725: Luftbeschaffenheit – Bestimmung der Geruchsstoffkonzentration mit dynamischer Olfaktometrie, Berlin: 2003.

[20] St. Croix Sensory, "Comparison of Field Olfactometers in a Controlled Chamber using Hydrogen Sulfide as the Test Odorant," pp. 1-13, May 16 2003.

[21] VDI Richtlinie 3882: Olfaktometrie - Bestimmung der Geruchsintensität, Berlin: 1992.

[22] OdourTech. (2011). *Odour Experts*. Available: http://www.odotech.com/en/

[23] K. Persaud and G. Dodd, "Analysis of discrimination mechanisms in the mammalian olfactory system using a model nose," *Nature,* vol. 299, pp. 352-355, 1982.

[24] K. C. Persaud, "'Electronic Nose'--New Condition Monitoring Devices for Environmental Applications," *Chemical Senses,* vol. 30, pp. i252-i253, Jan 1 2005.

[25] A. Romain, J. Delva, and J. Nicolas, "Complementary approaches to measure environmental odours emitted by landfill areas," *Sensor Actuat B-Chem,* vol. 131, pp. 18-23, Apr 14 2008.

[26] K. Kleeberg, M. Schlegelmilch, and J. Streese, "Odour abatement strategy for a sustainable odour management " *Proceedings (CD-ROM) of Sardinia,* Jan 1 2005.

[27] S. Sircar, T. Golden, and M. Rao, "Activated carbon for gas separation and storage," *Carbon,* vol. 34, pp. 1-12, 1996.

[28] G. Vyalkina, Z. Nabutovskii, V. Popov, and E. N. Turevskii, "Drying compressed natural gas with silica gel," *Chemistry and Technology of Fuels and Oils,* Jan 1 1985.

[29] S. Petrescu and M. S. Secula, "Mathematical modeling of gas drying by adsorption," *Environmental Engineering and Management Journal,* Jan 1 2008.

[30] M. Trimborn, "Biofilter/Biowäscher an Tierhaltungsanlagen als relevante Quelle von Lachgas durch Ammoniakabscheidung?," 2006.

[31] J. Helminen, J. Helenius, E. Paatero, and I. Turunen, "Adsorption Equilibria of Ammonia Gas on Inorganic and Organic Sorbents at 298.15 K," *Journal of Chemical and Engineering Data* vol. 46, pp. 391-399, 2001.

[32] S. Kuo, E. Pedram, and A. Hines, "Analysis of ammonia adsorption on silica gel using the modified potential theory," *Journal of Chemical and Engineering Data* Jan 1 1985.

[33] Y. Liang, X. Quan, J. Chen, J. Chung, J. Sung, and S. Chen, "Long-term results of ammonia removal and transformation by biofiltration," *Journal Of Hazardous Materials,* Jan 1 2000.

[34] E. Richter, R. Kleinschmidt, E. Pilarczyk, K. Knoblauch, and H. Jontgen, "Thermal desorption of nitrogen oxides from activated carbon," *Thermochimica Acta,* vol. 85, pp. 315-318, 1985.

[35] L. White and C. Schneider, "Physical Adsorption from Mixtures of Gases. II. Oxygen - Argon on Silica Gel at 0°," *Journal of the American Chemical Society,* Jan 1 1949.

[36] J. Koziel. (2011, 07/07/). *Iowa State University*. Available: http://www3.abe.iastate.edu/odor/

[37] A. Van Harreveld, "From odorant formation to odour nuisance: new definitions for discussing a complex process," *Water Science & Technology,* vol. 44, pp. 9-15, 2001.

[38] VDI 3475 Blatt 3: Emissionsminderung Anlagen zur mechanisch-biologischen Behandlung von Siedlungsabfällen, Berlin: 2007.

[39] J. Devinny, M. Deshusses, and T. Webster, "Biofiltration for air pollution control," p. 299, Jan 1 1999.

[40] N. Kim, M. Hirai, and M. Shoda, "Comparison of organic and inorganic packing materials in the removal of ammonia gas in biofilters," *Journal Of Hazardous Materials,* Jan 1 2000.

[41] K. James R Kastner, "Comparison of chemical wet scrubbers and biofiltration for control of volatile organic compounds using GC/MS techniques and kinetic analysis," *Journal of Chemical Technology & Biotechnology,* vol. 80, pp. 1170-1179, 2005.

[42] C. Rodrigues, D. De Moraes, S. Da Nobrega, and M. Barboza, "Ammonia adsorption in a fixed bed of activated carbon," *Bioresource Technology,* vol. 98, pp. 886-891, 2007.

[43] K. Ciahotný, L. Melenová, H. Jirglova, and O. Pachtova, "Removal of ammonia from waste air streams with clinoptilolite tuff in its natural and treated forms," *Adsorption,* Jan 1 2006.

[44] J. Devinny and J. Ramesh, "A phenomenological review of biofilter models," *Chemical Engineering Journal,* vol. 113, pp. 187-196, 2005.

[45] J. Streese, M. Schlegelmilch, K. Heining, and R. Stegmann, "A macrokinetic model for dimensioning of biofilters for VOC and odour treatment," *Waste Management,* vol. 25, pp. 965-974, 2005.

[46] K. Demeestere, H. Van Langenhove, and E. Smet, "Regeneration of a compost biofilter degrading high loads of ammonia by addition of gaseous methanol.," *Journal of the Air and Waste Management Association,* vol. 52, p. 796, 2002.

[47] E. Pagans, X. Font, and A. Sánchez, "Adsorption, absorption, and biological degradation of ammonia in different biofilter organic media," *Biotechnology & Bioengineering,* vol. 97, pp. 515-525, 2007.

[48] E. Pagans, X. Font, and A. Sánchez, "Coupling composting and biofiltration for ammonia and volatile organic compound removal," *Biosystems Engineering,* vol. 97, pp. 491-500, 2007.

[49] E. Dumont, Y. Andrès, P. Le Cloirec, and F. Gaudin, "Evaluation of a new packing material for H_2S removed by biofiltration," *Biochemical Engineering Journal,* Jan 1 2008.

[50] T. Sakuma, T. Hattori, and M. A. Deshusses, "The effects of a lower irrigation system on pollutant removal and on the microflora of a biofilter," *Environmental Technology,* vol. 30, pp. 621-627, Aug 8 2009.

[51] J. Goncalves and R. Govind, "Analysis of biofilters using synthetic macroporous foam media.," *Journal of the Air and Waste Management Association,* Jan 1 2009.

[52] H. Taghipour, M. Shahmansoury, B. Bina, and H. Movahdian, "Operational parameters in biofiltration of ammonia-contaminated air streams using compost-pieces of hard plastics filter media," *Chemical Engineering Journal,* vol. 137, pp. 198-204, 2008.

[53] O. Lambrecht. (2011, 05/07/). *Das Geschäft mit den Schweinen*. Available: http://www.tagesschau.de/wirtschaft/schweinemast100.html

[54] T. R. Haug, "The practical handbook of compost engineering," p. 717, Jan 1 1993.

[55] E. Smet, H. Van Langenhove, and K. Maes, "Abatement of high concentrated ammonia loaded waste gases in compost biofilters," *Water, Air and Soil Pollution,* vol. 119, pp. 177-190, 2000.

[56] Y. Chung, C. Huang, and C.-p. Tseng, "Reduction of H_2S/NH_3 production from pig feces by controlling environmental conditions," *Journal of environmental science and health Part A,* vol. 31, pp. 139-155, 1996.

[57] B. Weckhuysen, L. Vriens, and H. Verachtert, "Biotreatment of ammonia- and butanal-containing waste gases," *Applied Microbiology and Biotechnology,* vol. 42, pp. 147-152, Jan 1 1994.

[58] J. L. Gerberding, "Toxicological Profile for Ammonia," Atlanya2004.

[59] G. Busca and C. Pistarino, "Abatement of ammonia and amines from waste gases: a summary," *Journal of Loss Prevention in the Process Industries,* vol. 16, pp. 157-163, Jan 1 2003.

[60] W. Ferguson, W. Koch, and L. Webster, "Human physiological response and adaption to ammonia," *Journal of Occupational Medicine,* Jan 1 1977.

[61] S. Morsing, J. Strom, G. Zhang, and P. Kai, "Scale model experiments to determine the effects of internal airflow and floor design on gaseous emissions from animal houses," *Biosystems Engineering,* vol. 99, pp. 99-104, Jan 1 2008.

[62] J. Clemens, M. Trimborn, P. Weiland, and B. Amon, "Mitigation of greenhouse gas emissions by anaerobic digestion of cattle slurry," *Agriculture Ecosystems and Environment,* vol. 112, pp. 171-177, Jan 1 2006.

[63] A. G. Megaritis and C. Fountoukis, "Response of fine particulate matter concentrations to changes of emissions and temperature in Europe," *Atmos Chem …,* 2012.

[64] A. P. Tsimpidi, V. A. Karydis, and S. N. Pandis, "Response of inorganic fine particulate matter to emission changes of sulfur dioxide and ammonia: the eastern United States as a case study.," *Journal of the Air & Waste Management Association (1995),* vol. 57, pp. 1489-1498, Dec 2007.

[65] M. E. Millon, "Note sur la decomposition du nitrate d'ammoniaque (note on the decomposition of ammonium nitrate)," *Annales de chimie et de physique,* vol. 3, pp. 255-256, Jan 27 1847.

[66] N. Kolarow and B. Popjankow, "Über die Kinetik der Zersetzung von NH_4NO_2 in Lösungen," *Monatshefte für Chemie,* Jan 1 1965.

[67] E. Abel, H. Schmid, and J. Schafranik, "Kinetik der Stickstoffentwocklung aus Ammoiumnitrit," *Zeitschrift für Physikalische Chemie (Ergänzungsband Bodenstein Festband),* pp. 510-522, 1931.

[68] J. Dusenbury and R. Powell, "Reactions of Nitrous Acid. I. Ammonium Nitrite Decomposition1," *Journal of the American Chemical Society,* vol. 73, pp. 3266-3268, 1951.

[69] M. Li, Y. Yeom, E. Weitz, and W. Sachtler, "An acid catalyzed step in the catalytic reduction of NO_x to N_2," *Catalysis Letters,* vol. 112, pp. 129-132, 2006.

[70] C. Harrison, M. Malati, and N. Smetham, "Solvent and deuterium isotope effects on the decomposition of ammonium nitrite solutions," *Journal of Solution Chemistry,* vol. 25, pp. 505-514, 1996.

[71] K. Suzuki, T. Noda, G. Sastre, N. Katada, and M. Niwa, "Periodic Density Functional Calculation on the Brönsted Acidity of Modified Y-Type Zeolite," *The Journal of Physical Chemistry C,* vol. 113, pp. 5672-5680, 2009.

[72] M. Yadav, M. Patil, and R. Jasra, "Acetoxylation and hydration of limonene and alpha-pinene using cation-exchanged zeolite beta," *Journal of Molecular Catalysis,* vol. 297, pp. 101-109, Jan 1 2009.

[73] M. Li, Y. Yeom, E. Weitz, and W. Sachtler, "Possible reasons for the superior performance of zeolite-based catalysts in the reduction of nitrogen oxides," *Journal of Catalysis,* vol. 235, pp. 201-208, 2005.

[74] C. Colella and A. Gualtieri, "Cronstedt's zeolite," *Microporous and Mesoporous Materials,* vol. 105, pp. 213-221, 2007.

[75] Wikipedia. (2006, 05/07/). *Zeolite structure*. Available: http://en.wikipedia.org/wiki/Zeolite

[76] P. Cooksay, "ZelAmm General Description," 2003.

[77] J. Kim, E. Rene, and H. Park, "Performance of an immobilized cell biofilter for ammonia removal from contaminated air stream," *Chemosphere,* vol. 68, pp. 274-280, 2007.

[78] T. Sakuma, M. Aoki, T. Hattori, and D. Gabriel, "A Conceptual Model for the Treatment of Ammonia Vapors in a Biotrickling Filter," *Annual Meeting and Exhibition of the Air and Waste Management Association,* vol. 690, pp. 1-16, Jan 1 2004.

[79] D. McNevin and J. Barford, "Biofiltration as an odour abatement strategy," *Biochemical Engineering Journal,* vol. 5, pp. 231-242, Jan 1 2000.

[80] J. Carpenter, "Influence of structural features on Zeolite characterization by constraint index testing," 2010.

[81] A. Grossale, I. Nova, E. Tronconi, D. Chatterjee, and M. Weibel, "The chemistry of the $NO/NO_2^-NH_3$," *Journal of Catalysis,* vol. 256, pp. 312-322, 2008.

[82] Z. Wu, Y. An, Z. Wang, S. Yang, H. Chen, Z. Zhou, and S. Mai, "Study on zeolite enhanced contact-adsorption regeneration-stabilization process for nitrogen removal," *Journal Of Hazardous Materials,* vol. 156, pp. 317-326, 2008.

[83] A. F. Mumpton and R. J. Boles, *Mineralogy and geology of natural zeolites*, 1981.

[84] T. Perrin, J. Boettinger, D. Drost, and J. Norton, "Decreasing nitrogen leaching from sandy soil with ammonium-loaded clinoptilolite," *Journal of environmental quality,* vol. 27, pp. 656-663, 1998.

[85] R. Juan, S. Hernández, J. Andrés, and C. Ruiz, "Ion exchange uptake of ammonium in wastewater from a Sewage Treatment Plant by zeolitic materials from fly ash," *Journal of hazardous materials,* vol. 161, pp. 781-786, 2009.

[86] A. Zeotech, "Zeolite a versatile air pollutant adsorber," Feb 29 2008.

[87] E. Pidko, R. van Santen, and V. Kazansky, "Chemical Reactivity of Cation‐Exchanged Zeolites," PhD, 2008.

[88] Y. Yeom, M. Li, A. Savara, W. Sachtler, and E. Weitz, "An overview of the mechanisms of NO_x reduction with oxygenates over zeolite and [gamma]-Al_2O_3 catalysts," *Catalysis Today,* vol. 136, pp. 55-63, 2008.

[89] J. Weitkamp, "Zeolites and catalysis," *Solid State Ionics,* vol. 131, pp. 175-188, 2000.

[90] Q. Sun, Z. X. Gao, H. Y. Chen, and W. M. H. Sachtler, "Reduction of NO_x with ammonia over Fe/MFI: Reaction mechanism based on isotopic labeling," *Journal of Catalysis,* vol. 201, pp. 88-99, 2001.

[91] M. Brandle and J. Sauer, "Combining ab initio techniques with analytical potential functions. A study of zeolite-adsorbate interactions for NH_3 on H-faujasite," *Journal of Molecular Catalysis A: Chemical,* 1997.

[92] J. Eckert, C. M. Draznieks, and A. K. Cheetham, "Direct observation of host-guest hydrogen bonding in the zeolite NaY/chloroform system by neutron scattering.," *Journal of the American Chemical Society,* vol. 124, pp. 170-171, Feb 16 2002.

[93] F. Gilles, J. L. Blin, H. Toufar, M. Briend, and B. Su, "Double interactions between ammonia and a series of alkali-exchanged faujasite zeolites evidenced by FT-IR and TPD-MS techniques* 1," *Colloids and Surfaces A: Physicochemical and Engineering Aspects,* vol. 241, pp. 245-252, 2004.

[94] D. Das and M. C. Upreti, "Probable reaction mechanism and nature of active sites in catalytic cracking of hydrocarbons over zeolites LaX and PrX - part.I," *Indian journal of chemistry. Sect. A,* vol. 34, pp. 512-51521, Sep 20 1991.

[95] I. Batonneau-Gener, S. Degorce, P. Ayrault, O. Ducreux, P. Magnoux, and S. Mignard, "Determination of the 5A zeolite acidity: an infrared study," in *Studies in Surface Science and Catalysis*, 2008, pp. 857-860.

[96] V. Zabolotskii, N. Shel'deshov, and N. Gnusin, "Dissociation of water molecules in systems with ion-exchange membranes," *Russian Chemical Reviews,* vol. 57, pp. 801-808, 1988.

[97] G. N. Vayssilov and N. Rösch, "Influence of Alkali and Alkaline Earth Cations on the Brönsted Acidity of Zeolites," *The Journal of Physical Chemistry B,* vol. 105, pp. 4277-4284, 2001.

[98] L. A. M. M. Barbosa and R. A. van Santen, "Theoretical study of the enhanced Brönsted acidity of Zn^{2+} ‐ exchanged zeolites," *Catalysis Letters,* vol. 63, pp. 97-106, 1999.

[99] E. Sousa-Aguiar, V. Camorim, F. M. Zanon Zoti, and R. L. dos Santos, "A Fourier transform infrared spectroscopy study of La-, Nd-, Sm-, Gd- and Dy-containing Y zeolites," *Microporous and Mesoporous Materials,* vol. 25, pp. 25-34, Jan 1 1998.

[100] J. W. Ward, "A spectroscopic study of the surface of zeolite Y: the adsorption of pyridine," *Journal of Colloid and Interface Science,* vol. 28, pp. 269-278, 1968.

[101] L. Foglar, L. Sipos, and N. Bolf, "Nitrate removal with bacterial cells attached to quartz sand and zeolite from salty wastewaters," *World Journal of Microbiology and Biotechnology,* vol. 23, pp. 1595-1603, 2007.

[102] A. Hedström, "Ion exchange of ammonium in zeolites: a literature review," *Journal of environmental engineering,* vol. 127, pp. 673-681, 2001.

[103] G. Baquerizo, J. Maestre, and V. Machado, "Long-term ammonia removal in a coconut fiber-packed biofilter: Analysis of N fractionation and reactor performance under steady-state and transient conditions," *Water Research,* vol. 43, pp. 2293-2301, Jan 1 2009.

[104] APHA, *Standard Methods for the Examination of Water and Wastewater*, 21 ed. Washington, D.C.: American Public Health Association, 2005.

[105] A. Hill, "The mode of action of nicotine and curari, determined by the form of the contraction curve and the method of temperature coefficients," *The Journal of Physiology,* vol. 39, p. 361, 1909.

[106] T. Christie, B. Brathwaite, and B. Thompson, "Mineral Commodity Report 23 – Zeolites," Aug 6 2002.

[107] W. A. Deer, R. A. Howie, W. S. Wise, and J. Zussman, *Rock-Forming Minerals: Framework Silicates: Slica Minerals, Feldspathoids and the Zeolites*, 2 ed., 2004.

[108] D. Karadag, Y. Koc, M. Turan, and M. Ozturk, "A comparative study of linear and non-linear regression analysis for ammonium exchange by clinoptilolite zeolite," *Journal Of Hazardous Materials,* vol. 144, pp. 432-437, 2007.

[109] H. Huang, X. Xiao, B. Yan, and L. Yang, "Ammonium removal from aqueous solutions by using natural Chinese (Chende) zeolite as adsorbent," *Journal Of Hazardous Materials,* 2009.

[110] Y. Wang, F. Lin, and W. Pang, "Ammonium exchange in aqueous solution using Chinese natural clinoptilolite and modified zeolite," *Journal Of Hazardous Materials,* vol. 142, pp. 160-164, 2007.

[111] K. SaltalI, A. Sari, and M. AydIn, "Removal of ammonium ion from aqueous solution by natural Turkish (Yildizeli) zeolite for environmental quality," *Journal Of Hazardous Materials,* vol. 141, pp. 258-263, 2007.

[112] N. KarapInar, "Application of natural zeolite for phosphorus and ammonium removal from aqueous solutions," *Journal Of Hazardous Materials,* vol. 170, pp. 1186-1191, 2009.

[113] X. Guo, L. Zeng, X. LI, and H. Park, "Ammonium and potassium removal for anaerobically digested wastewater using natural clinoptilolite followed by membrane pretreatment," *Journal Of Hazardous Materials,* vol. 151, pp. 125-133, 2008.

[114] P. Antoniou, J. Hamilton, B. Koopman, R. Jain, B. Holloway, G. Lyberatos, and S. Svoronos, "Effect of temperature and pH on the effective maximum specific growth rate of nitrifying bacteria," *Water research,* vol. 24, pp. 97-101, 1990.

[115] G. L. Jones and A. R. Paskins, "Influence of high partial pressure of carbon dioxide and/or oxygen on nitrification," *Journal of chemical technology and biotechnology,* vol. 32, pp. 213-223, 1982.

[116] H. Painter and J. Loveless, "Effect of temperature and pH value on the growth-rate constants of nitrifying bacteria in the activated-sludge process," *Water research,* vol. 17, pp. 237-248, 1983.

[117] M. Rubin, R. Noyes, and K. Smith, "Gas-evolution oscillators. 9. A study of the ammonium nitrite oscillator," *Journal of Physical Chemistry,* vol. 91, pp. 1618-1622, 1987.

[118] L. K. Koopal, "International union of pure and applied chemistry," Sep 5 2001.

[119] V. Vadivelu, J. Keller, and Z. Yuan, "Effect of free ammonia on the respiration and growth processes of an enriched Nitrobacter culture," *Water Research,* vol. 41, pp. 826-834, 2007.

[120] S. Vitzthum von Eckstaedt, G. Ho, W. Charles, and R. Cord-Ruwisch, "A novel way of removing ammonia: Biofilter design and development," *in preparation,* 2011.

[121] Y. Jun and X. Wenfeng, "Ammonia biofiltration and community analysis of ammonia-oxidizing bacteria in biofilters," *Bioresource Technology,* vol. 100, pp. 3869-3876, 2009.

[122] X. J. Guo, J. K. Tak, and R. Johnson, "Ammonia removal from air stream and biogas by a H_2SO_4 impregnated adsorbent originating from waste wood-shavings and biosolids," in *Journal Of Hazardous Materials* vol. 166, ed, 2009, pp. 372-376.

[123] R. Pandey, S. Mudliar, and S. Borgaokar, "Treatment of waste gas containing diethyldisulphide (DEDS) in a bench scale biofilter," *Bioresource Technology,* vol. 100, pp. 131-5, Jan 1 2009.

[124] J. Kim, E. Rene, and H. Park, "Biological oxidation of hydrogen sulfide under steady and transient state conditions in an immobilized cell biofilter," *Bioresource Technology,* vol. 99, pp. 583-588, 2008.

[125] Z. Ji, J. Yuan, and X. Li, "Removal of ammonium from wastewater using calcium form clinoptilolite," *Journal Of Hazardous Materials,* vol. 141, pp. 483-488, 2007.

[126] S. Vitzthum von Eckstaedt, G. Ho, W. Charles, and R. Cord-Ruwisch, "A novel way of removing ammonia: Literature review and proof of concept," *in preparation,* 2011.

[127] C. H. Guo, V. Stabnikov, and V. Ivanov, "The removal of nitrogen and phosphorus from reject water of municipal wastewater treatment plant using ferric and nitrate bioreductions," *Bioresource Technology,* pp. 1-8, Feb 4 2010.

[128] W. Gujer, "Nitrification and me - A subjective review," *Water Research,* vol. 44, pp. 1-19, Jan 1 2010.

[129] T. Ducey, M. Vanotti, A. Shriner, and A. Szogi, "Characterization of a microbial community capable of nitrification at cold temperatures," *Bioresource Technology,* 2010.

[130] A. Mulder, A. van de Graaf, L. Robertson, and J. Kuenen, "Anaerobic ammonium oxidation discovered in a denitrifying fluidized bed reactor," *Fems Microbiology Ecology,* vol. 16, pp. 177-183, Jan 1 1995.

[131] M. Strous, J. Heijnen, J. KUENEN, and M. JETTEN, "The sequencing batch reactor as a powerful tool for the study of slowly growing anaerobic ammonium-oxidizing microorganisms," *Applied Microbiology and Biotechnology,* vol. 50, pp. 589-596, Jan 1 1998.

[132] A. van de Graaf, P. Debruijn, L. Robertson, M. Jetten, and J. Kuenen, "Metabolic pathway of anaerobic ammonium oxidation on the basis of N-15 studies in a fluidized bed reactor," *Microbiol-Uk,* vol. 143, pp. 2415-2421, Jan 1 1997.

[133] A. Van de Graaf, A. MULDER, P. De Bruijn, M. Jetten, L. ROBERTSON, and J. KUENEN, "Anaerobic oxidation of ammonium is a biologically mediated process," *Applied And Environmental Microbiology,* vol. 61, p. 1246, 1995.

[134] M. Waki, T. Yasuda, K. Suzuki, T. Sakai, N. Suzuki, R. Suzuki, K. Matsuba, H. Yokoyama, A. Ogino, Y. Tanaka, S. Ueda, M. Takeuchi, T. Yamagishi, and Y. Suwa, "Rate determination and distribution of anammox activity in activated sludge treating swine wastewater," *Bioresource Technology,* vol. 101, pp. 2685-2690, Jan 1 2010.

[135] S. Ni, P. Lee, A. Fessehaie, B. Gao, and S. Sung, "Enrichment and biofilm formation of Anammox bacteria in a non-woven membrane reactor," *Bioresource Technology,* Jan 1 2010.

[136] C.-C. Wang, P.-H. Lee, M. Kumar, Y.-T. Huang, S. Sung, and J.-G. Lin, "Simultaneous partial nitrification, anaerobic ammonium oxidation and denitrification (SNAD) in a full-scale landfill-leachate treatment plant," *Journal Of Hazardous Materials,* vol. 175, pp. 622-628, Jan 1 2010.

[137] S. Park, W. Bae, B. Rittmann, S. Kim, and J. Chung, "Operation of suspended-growth shortcut biological nitrogen removal (SSBNR) based on the minimum/maximum substrate concentration," *Water Research,* vol. 44, pp. 1419-1428, 2010.

[138] E. Abel, "Kinetik der Stickstotfentwicklung aus Ammoniumnitrit. II," pp. 1-4, Feb 11 1949.

[139] A. Lamb and E. Ohl, "Heats of Adsorption of Gases and Vapors upon Crystallogenetic Adsorbents," *Journal of the American Chemical Society,* Jan 1 1935.

[140] C. Eiserbeck, R. K. Nelson, K. Grice, J. Curiale, and C. M. Reddy, "Robust study of applications and comparison of sophisticated chromatographic techniques including GC´GC for characterising higher

plant biomarkers in Tertiary oils and sediments," *Geochimica et Cosmochimica Acta,* vol. submitted, 2011.

[141] P. Pramanik, "Changes in microbial properties and nutrient dynamics in bagasse and coir during vermicomposting: Quantification of fungal biomass through ergosterol estimation in vermicompost," *Waste Management,* Jan 1 2010.

[142] J. Surmacz-Górska, A. Cichon, and K. Miksch, "Nitrogen removal from wastewater with high ammonia nitrogen concentration via shorter nitrification and denitrification," *Water Science and Technology,* vol. 36, pp. 73-78, 1997.

[143] U. Abeling and C. Seyfried, "Anaerobic-aerobic treatment of high-strength ammonium wastewater--nitrogen removal via nitrite.," *Water Science and Technology,* vol. 26, pp. 1007-1015, Jan 1 1992.

[144] D. Kim, J. Chang, D. Lee, D. Han, I. Yoo, and G. Cha, "Nitrification of high strength ammonia wastewater and nitrite accumulation characteristics," *Water Science and Technology,* pp. 45-51, 2003.

[145] F. Fdz-Polanco, S. Villaverde, and P. Garcia, "Temperature effect on nitrifying bacteria activity in biofilters: activation and free ammonia inhibition," *Water Science and Technology,* vol. 30, pp. 121-130, 1994.

[146] A. Anthonisen, R. Loehr, T. Prakasam, and E. Srinath, "Inhibition of nitrification by ammonia and nitrous acid," *Journal Water Pollution Control Federation,* vol. 48, pp. 835-852, 1976.

[147] V. M. V. Yuan, Jurg Keller, Zhiguo, "Effect of free ammonia and free nitrous acid concentration on the anabolic and catabolic processes of an enriched Nitrosomonas culture," *Biotechnology & Bioengineering,* vol. 95, pp. 830-839, 2006.

[148] J. Pérez, E. Costa, and J. Kreft, "Conditions for partial nitrification in biofilm reactors and a kinetic explanation," *Biotechnology & Bioengineering,* vol. 103, 2009.

[149] J. Almeida, S. Julio, M. Reis, and M. Carrondo, "Nitrite inhibition of denitrification by Pseudomonas fluorescens," *Biotechnology and bioengineering,* vol. 46, pp. 194-201, 1995.

[150] S. Philips, H. J. Laanbroek, and W. Verstraete, "Origin, causes and effects of increased nitrite concentrations in aquatic environments," *Reviews in environmental science and biotechnology,* vol. 1, pp. 115-141, 2002.

[151] C. Glass, "Denitrification kinetics of high nitrate concentration water: pH effect on inhibition and nitrite accumulation," *Water Research,* 1998.

[152] S. Qiao, N. Matsumoto, T. Shinohara, and T. Nishiyama, "High-rate partial nitrification performance of high ammonium containing wastewater under low temperatures," *Bioresource Technology,* vol. 101, pp. 111-117, 2009.

[153] C. Grunditz and G. Dalhammar, "Development of nitrification inhibition assays using pure cultures of Nitrosomonas and Nitrobacter," *Water Research,* vol. 35, pp. 433-440, 2001.

[154] R. L. Snyder, "Humidity Conversion," pp. 1-7, Mar 27 2005.

[155] O. Tetens, "Über einige meteorologische Begriffe," *Zeitschrift Geophysik,* vol. 6, pp. 297-309, 1930.

[156] A. Wexler, "Vapor pressure formulation for water in the range 0° to 100°C," *Journal of Research of the National Bureau of Standards,* vol. 80A, p. 775, 1976.

[157] ISMATEC, "Quality Tubing for Tubing Pumps in Laboratories and Production," pp. 1-18, May 16 2010.

[158] S. Gobain, "Tygon application specific tubing," ed, 2006, pp. 1-42.

[159] HORIBA model VA/ VS 3000, "HORIBA VA/ VS Series," pp. 1-10, Jun 2 2004.

[160] Advantech ADAM 4000 series. (2011). *RS-485 I/O Modules: ADAM-4000*. Available: http://www.advantech.com/products/RS-485-I-O-Modules-ADAM-4000/sub_1-2MLKHT.aspx

[161] Aalborg Instruments and Controls model GFM37. (2011). *Model GFM37*. Available: http://www.aalborg.com/index.php/main_page/product_overview/id_product_overview/20

[162] National Instruments Corporation. (2011). *LabView*. Available: http://www.ni.com/labview

[163] S. Vitzthum von Eckstaedt, G. Ho, W. Chales, and R. Cord-Ruwisch, "A novel way of removing ammonia: Long-Term evaluation of ammonia and total nitrogen removal," *in preparation,* 2011.

[164] D. Gabriel and M. Deshusses, "Technical and economical analysis of the conversion of a full-scale scrubber to a biotrickling filter for odor control," *Water Science and Technology,* vol. 50, pp. 309-18, Jan 1 2004.

[165] S. Chandravathanam and D. Murthy, "Studies in nitrification of municipal sewage in an upflow biofilter," *Bioprocess and Biosystems Engineering,* vol. 21, pp. 117-122, 1999.

[166] M. Galera, E. Cho, E. Tuuguu, S. Park, D. Farnazo, C. Jee, N. Yoo, and W. Chung, "Removal of NH_3, H_2S and Toluene by Biofilters Packed with Rock Wool-Compost Media," *Journal of Industrial and Engineering Chemistry,* vol. 13, pp. 895-902, 2007.

[167] M. Ramírez, J. Gómez, G. Aroca, and D. Cantero, "Removal of ammonia by immobilized Nitrosomonas europaea in a biotrickling filter packed with polyurethane foam," *Chemosphere,* vol. 74, pp. 1385-1390, Jan 1 2009.

[168] H. Kim, Q. Xie, Y. J. Kim, and J. S. Chung, "Biofiltration of Ammonia Gas with Sponge Cubes Coated with Mixtures of Activated Carbon and Zeolite," *Environmental Technology,* vol. 23, pp. 839-847, Aug 1 2002.

[169] A. Rahmani, A. Mahvi, A. Mesdaghinia, and S. Nasseri, "Investigation of ammonia removal from polluted waters by Clinoptilolite zeolite," *International Journal,* vol. 1, pp. 125-133, 2004.

[170] N. Miladinovic, L. Weatherley, and J. López-Ruiz, "Ammonia removal from saline wastewater by ion exchange," *Water, Air and Soil Pollution: Focus,* vol. 4, pp. 169-177, 2004.

[171] C. Cundy and P. Cox, "The hydrothermal synthesis of zeolites: history and development from the earliest days to the present time," *Chemical Reviews,* vol. 103, pp. 663-702, 2003.

[172] K. Hammond, "Quantifying Defects in Zeolites and Zeolite Membranes," *Chemical Engineering,* 2010.

[173] J. Fedeyko, B. Chen, and H. Chen, "Mechanistic study of the low temperature activity of transition metal exchanged zeolite SCR catalysts," *Catalysis Today,* vol. 151, pp. 231-236, 2010.

[174] M. Iwasaki and H. Shinjoh, "NO evolution reaction with NO2 adsorption over Fe/ZSM-5: In situ FT-IR observation and relationships with Fe sites," *Journal of Catalysis,* vol. 273, pp. 29-38, Jul 7 2010.

[175] G. Baquerizo, X. Gamisans, D. Gabriel, and J. Lafuente, "A dynamic model for ammonia abatement by gas-phase biofiltration including pH and leachate modelling," *Biosystems Engineering,* vol. 97, pp. 431-440, 2007.

[176] B. Sheridan, T. Curran, V. Dodd, and J. Colligan, "Biofiltration of Odour and Ammonia from a Pig Unit—Biofiltration of Odour and Ammonia from a Pig Unit—a pilot-scale Study," *Biosystems Engineering,* vol. 82, pp. 441-453, Aug 1 2002.

[177] J. Luo and S. Lindsey, "The use of pine bark and natural zeolite as biofilter media to remove animal rendering process odours," *Bioresource Technology,* vol. 97, pp. 1461-1469, 2006.

[178] M. Sarioglu, "Removal of ammonium from municipal wastewater using natural Turkish (Dogantepe) zeolite," *Separation and purification technology,* vol. 41, pp. 1-11, Jan 1 2005.

[179] M. Laboratorics, "UltraClean Soil DNA Isolation Kit," pp. 1-8, Mar 13 2008.

[180] H. Zipper, H. Brunner, J. Bernhagen, and F. Vitzthum, "Investigations on DNA intercalation and surface binding by SYBR Green I, its structure determination and methodological implications," *Nucleic acids research,* vol. 32, p. e103, 2004.

Additional information to the upcoming Appendix Fig. 7-1

10 mL of 2.5 M NH_4Cl and 1 M $NaNO_2^-$ were added to four serum bottles containing 50 g clean clinoptilolite and closed with a rubber bung. The serum bottles were stored at room temperature and N_2 gas production of two serum bottles were measured via GC analyses (a and b) and two were volumetric (c and d) determined (Appendix Fig. 7-1). That process is described in more detail in chapter 2.2.3.1 and 2.2.3.2. No significant differences in N_2 gas production was observed by using the two different analysis techniques. Based on these results it was concluded that the volumetric gas production measurements were suitable for reliable gas production measurements.

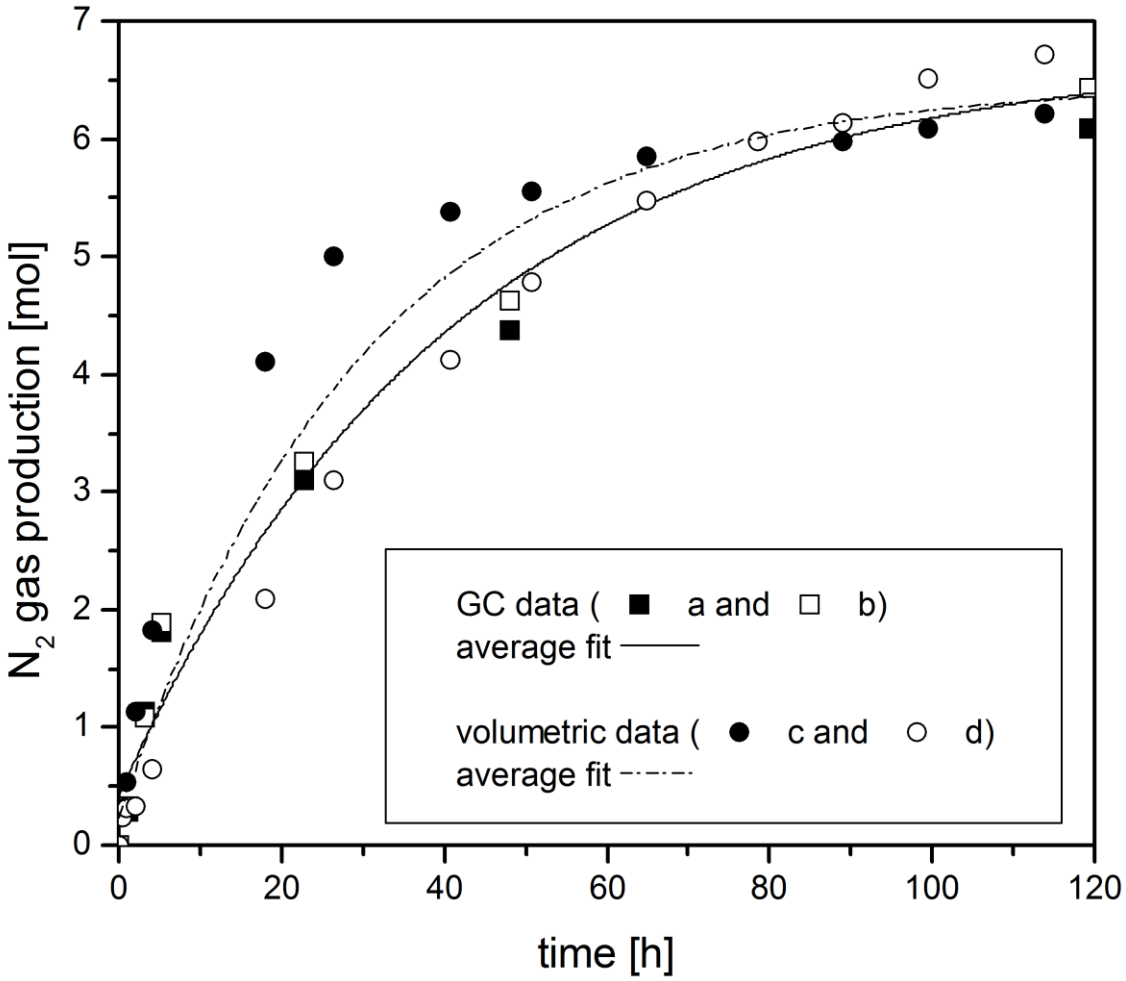

Appendix Fig. 7-1: comparisons of GC (a and b) and volumetric (c and d) N_2 gas production

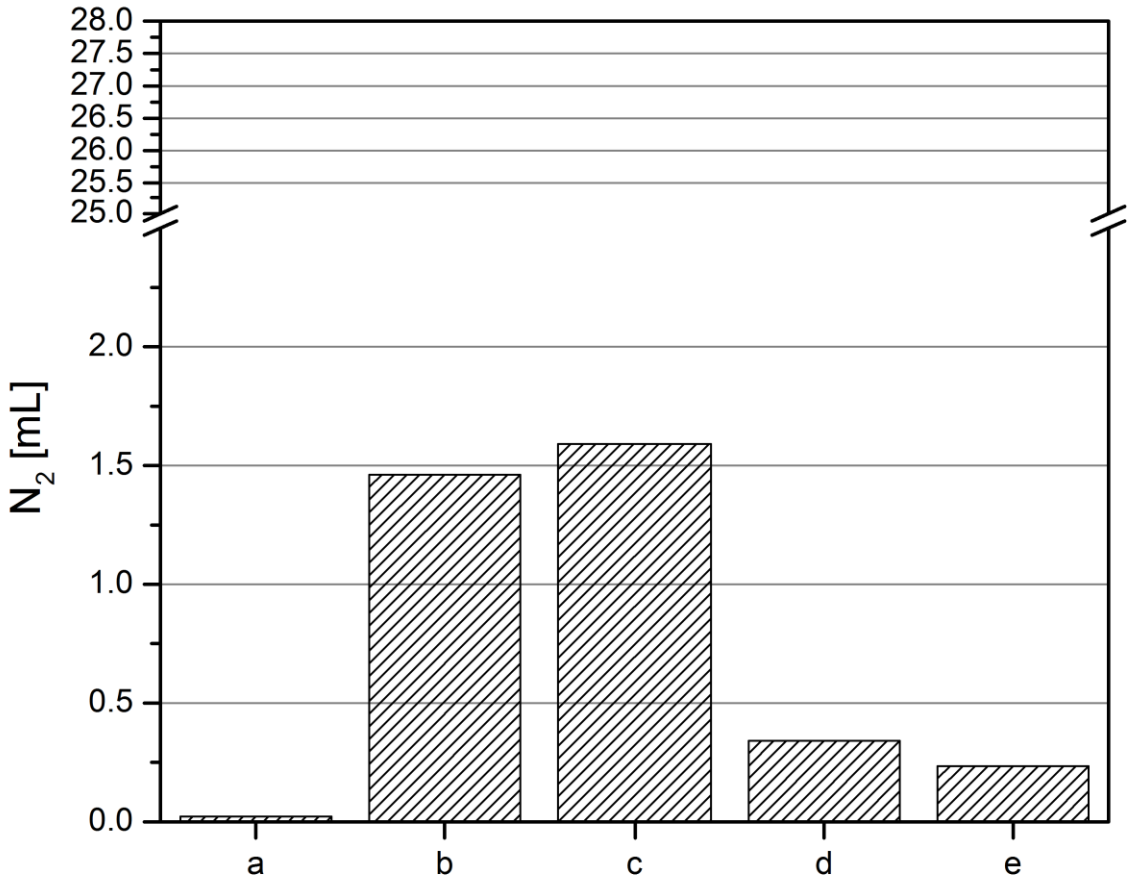

Appendix Fig. 7-2: 10 mL 40 mM NH_4Cl + 300 mM $NaNO_2^-$ @pH 7.85 (a) expected N_2 gas production calculated with Abel equation (Equation 2-1), (b) measured N_2 gas production with 50 g Zeolite, (c) measured N_2 gas production with 5 g Zeolite + 45 g Glass beads, (d) measured N_2 gas production with 0.5 g Zeolite + 49.5 g Glass beads and (e) measured N_2 gas production with 52.5 g Glass beads

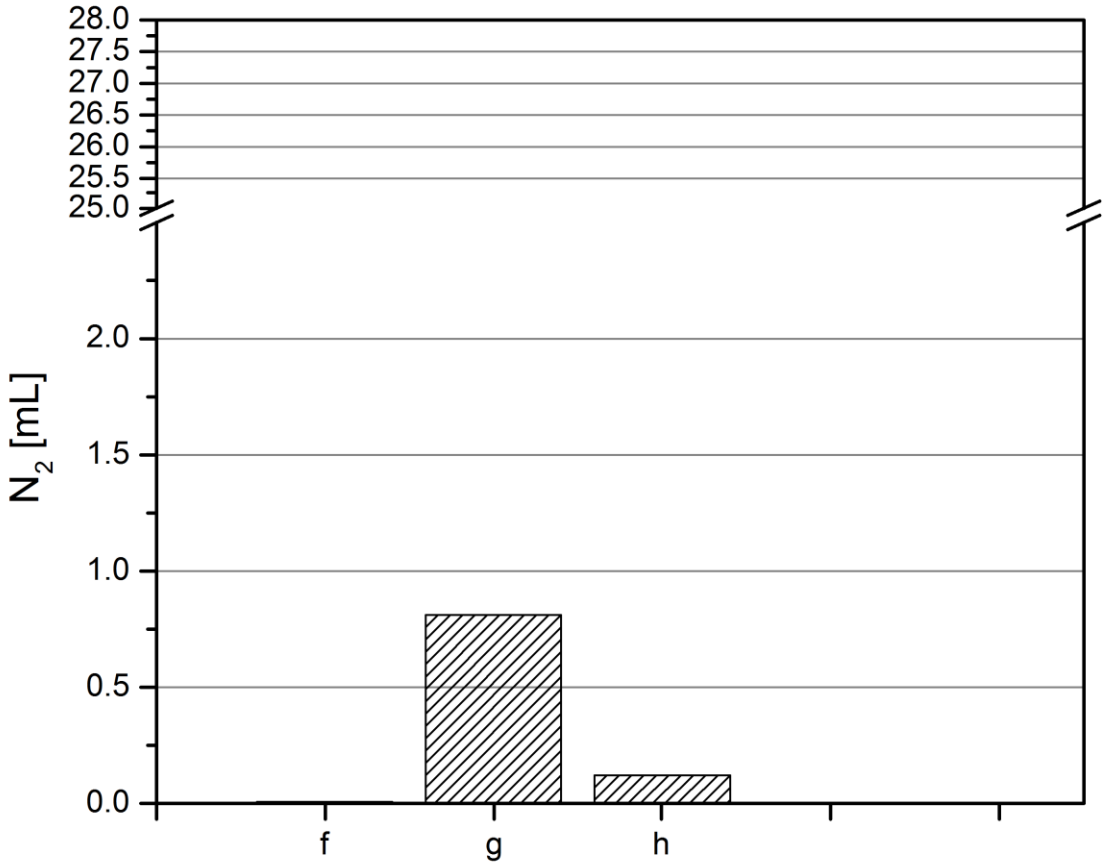

Appendix Fig. 7-3: 10 mL 20 mM NH_4Cl + 150 mM $NaNO_2^-$ @pH 8 (f) expected N_2 gas production calculated with Abel equation (Equation 2-1), (g) measured N_2 gas production with 50 g Zeolite and (h) measured N_2 gas production with 52.5 g Glass beads

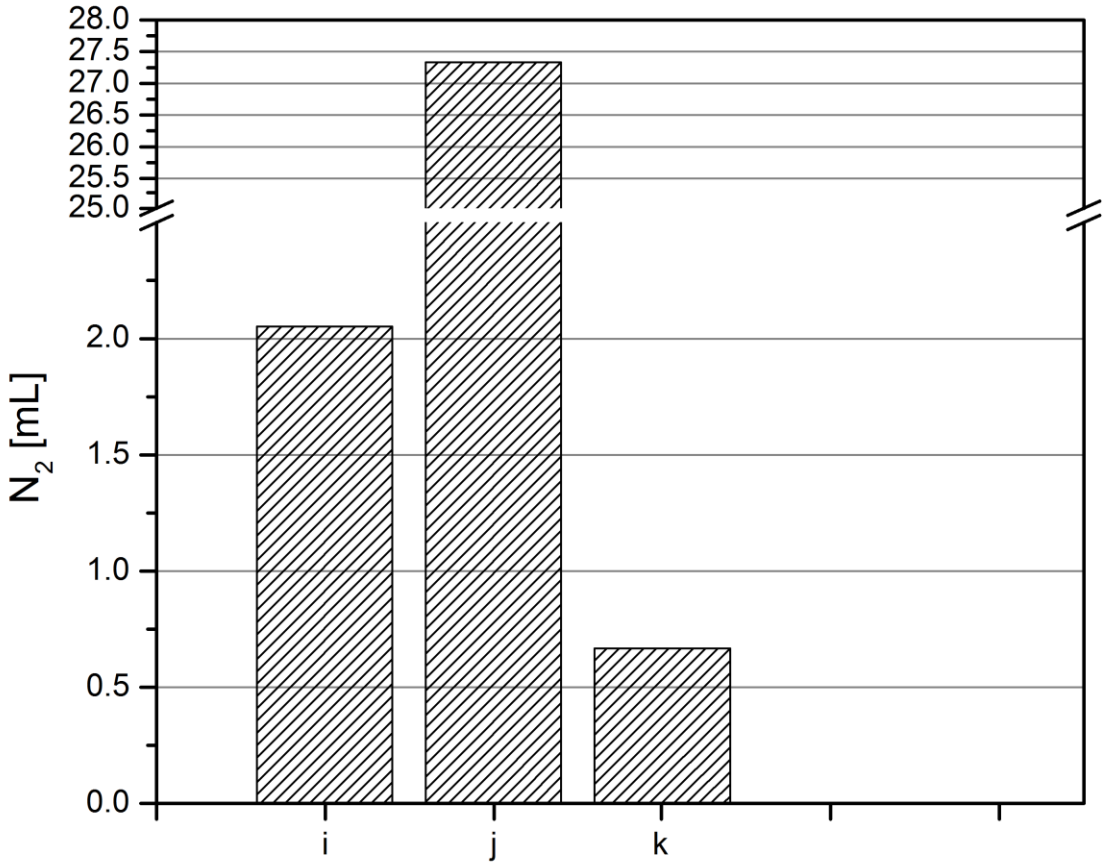

Appendix Fig. 7-4: 10 mL 150 mM NH_4Cl + 1000 mM $NaNO_2^-$ (i) expected N_2 gas production calculated with Abel equation (Equation 2-1), (j) measured N_2 gas production with 50 g Zeolite and (k) measured N_2 gas production with 52.5 g Glass Beads

The content of the attached DVD's is presented in the following three tables (Appendix Table 8-1 to Appendix Table 8-4). The content of the DVD's is divided into subfolders regarding the year of creation. Within the "year" folders the files are further separated into topics such as "experiments", "orders" and "labview" making the search for a particular file logical. Files in the "topic" folders are further subdivided into folders. These folders have either individual names such as "BioLab" referring to the company an order was placed, "cations" indicate the type of analysis or a 6 digit number giving the information on when the experiments were conducted.

Appendix Table 8-2: DVD one

DVD Name	Folder structure			
DVD_1	2008	Experiments	Geotech	
			Murdoch	080417
				080604
				080630
				080716
				NH3
	2009	Clipbord	Order	Biolab
				BOC
				EnviroEquip
				ESC
				Grace
				LOMB
				NarangMedical
				SMC
		Experiments	Info	
			Murdoch	Cations
				ElectronMicro
				graphs
				H2S
				NH3

Appendix Table 8-3: DVD two

DVD Name		Folder structure		
DVD_2	2010	Clipbord	Backup	H2S
				HPLC
				Marvin
			Order	Agilent
				Alltech
				Geneworks
				Grace
				Hinco
				Other
				SigmaAldrich
				ThermoFisher
		Experiments	Murdoch	Cations
				ClosedBottle
				GC
				Graphs
				Marvin
				MolecularWork
				other
				SEM
			SMRC	BioAction
				ChemCenter
				GA2000
				OdourUnit
				SPME
		LabView	Marvin	090605
				100628
				100628_2
				100628_3
				100628_4

Appendix Table 8-4: DVD three

DVD_3	2011	Experiments	Murdoch	ClosedBottle
				GC
			SMRC	Bioaction
				ChemCenter
		Publications	Paper #1	Graphs
				Other
				Powerpoint
				Word
			Paper #2	Excel
				Graphs
				Origin
				Other
				Powerpoint
				Word
			Paper #3	Excel
				Graphs
				Powerpoint
				Word
			Excel	
			Origin	
		Thesis	Excel	
			Forms	
			Graphes	
			Murdoch	
			Powerpoint	